Monoamine oxidase inhibition by novel quinolinones

L Meiring
21069565

Dissertation submitted in fulfillment of the requirements for the degree *Magister Scientiae* in Pharmaceutical Chemistry at the Potchefstroom Campus of the North-West University

Supervisor: Dr A Petzer
Co-Supervisor: Prof JP Petzer

May 2014

This work is based on the research supported in part by the Medical Research Council and National Research Foundation of South Africa (Grant specific unique reference numbers (UID) 85642 and 80647). The Grantholders acknowledge that opinions, findings and conclusions or recommendations expressed in any publication generated by the NRF supported research are that of the authors, and that the NRF accepts no liability whatsoever in this regard.

ACKNOWLEDGEMENTS

I would like to take this opportunity to thank the following people for helping me throughout the completion of this study:

- Dr. A. Petzer for all the guidance, knowledge and patience
- Prof. J.P. Petzer for the advice and inputs
- My parents for their support and love
- North-West University for the financial support and enormous opportunity
- André Joubert for the numerous NMR and MS spectra
- NRF (National Research Foundation of South Africa) for their financial support

TABLE OF CONTENTS

LIST OF ABBREVIATIONS

A	
ADH	Aldehyde dehydrogenase
AD	Alzheimer's disease
ATP	Adenosine triphosphate
B	
BDNF	Brain-derived neurotrophic factor
C	
CINAPS	Committee to identify neuroprotective agents
CNS	Central nervous system
COMT	Catechol-O-methyltransferase
Cys	Cysteine
D	
DA	Dopamine
DDC	Dopamine decarboxylase
DNA	Deoxyribonucleic acid
E	
E	Enzyme
ES	Enzyme-substrate
EtOH	Ethanol
F	
FAD	Flavin adenine dinucleotide
G	
GAPDH	Glyceraldehyde-3-phosphate dehydrogenase
GPO	Glutathione peroxidase
H	
5-HT	Serotonin
I	
IC_{50}	Inhibitor concentration at 50% inhibition
J	
JNK	c-Jun N-terminal kinase
K	
Kd	Dissociation constant
K_i	Inhibitor constant
K_m	Michaelis constant

L

LBs	Lewy bodies

M

MAO	Monoamine oxidase
MAPK	Mitogen-activated protein kinase
mRNA	Messenger ribonucleic acid

N

NA	Noradrenaline
NGF	Nerve growth factor
NMDA	N-Methyl-D-aspartate
NSAIDs	Non-steroidal anti-inflammatory drugs

P

PD	Parkinson's disease

R

ROS	Reactive oxygen species

S

S	Substrate
SD	Standard deviation
SET	Single electron transfer
SN	Substantia nigra
SNpc	Substantia nigra pars compacta
SSRI	Selective serotonin reuptake inhibitor
SV	Synaptic vesicle

T

TH	Tyrosine hydroxylase
TNFα	Tumor necrosis factor

V

v_i	Initial velocity
V_{max}	Maximum velocity

LIST OF FIGURES

ABSTRACT

Keywords: Monoamine oxidase; Reversible inhibition; Selectivity; 3,4-Dihydro-2(1*H*)-quinolinone; Structure-activity relationship.

Parkinson's disease (PD) is an age-related neurodegenerative disorder. The degeneration of the neurons of the substantia nigra in the midbrain leads to the loss of dopamine from the striatum, which is responsible for the motor symptoms of PD. In the brain, the enzyme, monoamine oxidase B (MAO-B), represents a major catabolic pathway of dopamine. Inhibitors of MAO-B conserve the depleted supply of dopamine and are thus used in the therapy of PD. In the present study, a series of 3,4-dihydro-2(1*H*)-quinolinone derivatives were synthesized and evaluated as inhibitors of recombinant human MAO-A and MAO-B. These quinolinone derivatives are structurally related to a series of coumarin (1-benzopyran-2-one) derivatives, which has been reported to act as MAO-B inhibitors. C6- and C7-substituted 3,4-dihydro-2(1*H*)-quinolinone derivatives were synthesized by reacting 6- or 7-hydroxy-3,4-dihydro-2(1*H*)-quinolinone with an appropriately substituted alkyl bromide in the presence of base. To evaluate the MAO inhibitory properties (IC_{50} values) of the quinolinone derivatives the recombinant human MAO-A and MAO-B enzymes were used. The reversibility of inhibition of a representative 3,4-dihydro-2(1*H*)-quinolinone derivative was examined by measuring the recovery of enzyme activity after the dilution of the enzyme-inhibitor complexes, while the mode of MAO inhibition was determined by constructing Lineweaver-Burk plots. To determine the lipophilicity of the 3,4-dihydro-2(1*H*)-quinolinone derivatives, the logP values were measured. The toxicity of the 3,4-dihydro-2(1*H*)-quinolinone derivatives towards cultured cells (cytotoxicity) was also measured.

The results document that the 3,4-dihydro-2(1*H*)-quinolinone derivatives are highly potent and selective MAO-B inhibitors with most homologues exhibiting IC_{50} values in the nanomolar range. The most potent MAO-B inhibitor, 7-(3-bromobenzyloxy)-3,4-dihydro-2(1*H*)-quinolinone, exhibits an IC_{50} value of 2.9 nM with a 2750-fold selectivity for MAO-B over the MAO-A isoform. As a MAO-B inhibitor, this compound is approximately equipotent to the most potent coumarin derivative (IC_{50} = 1.14 nM) reported in literature. Since MAO-B activity could be recovered after dilution of enzyme-inhibitor mixtures, it may be concluded that 7-(3-bromobenzyloxy)-3,4-dihydro-2(1*H*)-quinolinone is a reversible MAO-B inhibitor. The Lineweaver-Burk plots constructed for the inhibition of MAO-B by 7-(3-bromobenzyloxy)-3,4-dihydro-2(1*H*)-quinolinone were linear and intersected on the y-axis. These data indicated that this compound also is a competitive MAO-B inhibitor.

An analysis of the Lineweaver-Burk plots indicated that 7-(3-bromobenzyloxy)-3,4-dihydro-2(1*H*)-quinolinone inhibits MAO-B with a K_i value of 2.7 nM. An analysis of the structure-activity relationships for MAO-B inhibition shows that substitution on the C7 position of the 3,4-dihydro-2(1*H*)-quinolinone moiety leads to significantly more potent inhibition compared to substitution on C6. In this regard, a benzyloxy substituent on C7 is more favourable than phenylethoxy and phenylpropoxy substitution on this position.

In spite of this, C6-substituted 3,4-dihydro-2(1*H*)-quinolinone with potent MAO-B inhibitory activities were also identified. An analyses of selected properties of the 3,4-dihydro-2(1*H*)-quinolinones showed that the compounds are highly lipophilic with logP values in the range of 3.03-4.55. LogP values between 1 and 3 are, however, in the ideal range for bioavailability. The compounds synthesised have logP values higher than 3, which may lead to lower bioavailability. Laboratory data further showed that none of the 3,4-dihydro-2(1*H*)-quinolinones are highly toxic to cultured cells at the concentrations, 1 μM and 10 μM, tested. For example, the most potent MAO-B inhibitor, 7-(3-bromobenzyloxy)-3,4-dihydro-2(1*H*)-quinolinone, reduced cell viability to 88.11% and 86.10% at concentrations of 1 μM and 10 μM, respectively. These concentrations are well above its IC_{50} value for the inhibition of MAO-B. At concentrations required for MAO-B inhibition, the more potent 3,4-dihydro-2(1*H*)-quinolinones are thus unlikely to be cytotoxic.

It may thus be concluded that C7-substituted 3,4-dihydro-2(1*H*)-quinolinones are promising highly potent and selective MAO-B inhibitors, and thus leads for the therapy of Parkinson's disease.

UITTREKSEL

Sleutelwoorde: Monoamienoksidase; Omkeerbare inhibeerders; Selektiwiteit; 3,4-Dihidro-2(1*H*)-kinolinoon; Struktuur-aktiwiteitsverwantskap.

Parkinson se siekte (PS) is ‘n ouderdomsverwante neurodegeneratiewe siekte. Die degenerasie van die neurone van die substantia nigra in die brein lei tot die verlies van dopamien (DA) in die striatum. Hierdie proses is verantwoordelik vir die simptome van PS. Die ensiem, monoamienoksidase (MAO), speel moontlik ‘n rol in die neurodegeneratiewe proses in die brein. MAO-inhibeerders verlaag die katabolisme van DA en word dus gebruik om die siekteverloop van PD te vertraag. In hierdie studie is ‘n reeks van 3,4-dihidro-2(1*H*)-kinolinoonderivate gesintetiseer en geëvalueer as inhibeerders van rekombinante menslike MAO-A en MAO-B. Hierdie kinolinoonderivate is struktureel verwant aan ‘n reeks kumarien- (1-bensopiraan-2-oon-)derivate, wat in vorige studies as potente MAO-B-inhibeerders geïdentifiseer is. C6- en C7-gesubstitueerde 3,4-dihidro-2(1*H*)-kinolinoonderivate is gesintetiseer deur 6- of 7-hidroksie-3,4-dihidro-2(1*H*)-kinolinoon met ‘n toepaslike gesubstitueerde alkielbromied in die teenwoordigheid van ‘n basis te laat reageer. Rekombinante menslike MAO-A en MAO-B is gebruik om die MAO-inhibirende eienskappe (IC_{50}-waardes) van die kinolinoonderivate te evalueer. Die omkeerbaarheid van inhibisie van een 3,4-dihidro-2(1*H*)-kinolinoonderivaat is geëvalueer deur die herstel van ensiemaktiwiteit na die verdunning van die ensiem-inhibeerderkompleks, te meet. Die meganisme van inhibisie is bepaal deur Lineweaver-Burk-grafieke op te stel. Die lipofilisiteit is bepaal deur die logP-waardes van 3,4-dihidro-2(1*H*)-kinolinoonderivate te meet. Die toksisiteit van die 3,4-dihidro-2(1*H*)-kinolinoonderivate teenoor selkulture (sitotoksisiteit) is ook gemeet.

Die resultate toon dat die 3,4-dihidro-2(1*H*)-kinolinoonderivate hoogs potente en selektiewe MAO-B-inhibeerders is. Die mees potente MAO-B-inhibeerder, 7-(3-bromobensieloksie)-3,4-dihidro-2(1*H*)-kinolinoon, het ‘n IC_{50} waarde van 2.9 nM, met ‘n 2750-voudige selektiwiteit vir MAO-B in vergelyking met MAO-A. Vergeleke met die mees potente kumarienderivaat (IC_{50} = 1.14 nM), is dié verbinding ongeveer net so ‘n potente MAO-B-inhibeerder. Aangesien die MAO-B-aktiwiteit herstel het na verdunning van die ensiem-inhibeerderkompleks, is 7-(3-bromobensieloksie)-3,4-dihidro-2(1*H*)-kinolinoon ‘n omkeerbare MAO-B-inhibeerder. Die resultate toon ook dat die Lineweaver-Burk-grafieke op een punt op die y-as sny. Dit dui daarop dat 7-(3-bromobensieloksie)-3,4-dihidro-2(1*H*)-kinolinoon ‘n kompeterende inhibeerder van MAO-B is. Verdere analise van die Lineweaver-Burk-grafieke dui daarop dat 7-(3-bromobensieloksie)-3,4-dihidro-2(1*H*)-kinolinoon, MAO-B met ‘n K_i waarde van 2.7 nM inhibeer. Analise van die struktuur-aktiwiteitsverwantskappe vir MAO-B-inhibisie, dui daarop dat substitusie op C7 van 3,4-dihidro-2(1*H*)-kinolinone aanleiding gee tot meer potente inhibisie in vergelyking met substitusie op C6. In dié geval is substitusie met ‘n bensieloksiegroep op C7 meer gunstig as fenieletoksie- en fenielpropoksiegroepe op dieselfde posisie.

Substitusie op C6 van die 3,4-dihidro-2(1*H*)-kinolinone het ook gelei tot verbindings wat potente MAO-B-inhibeerders is. Die evaluasie van geselekteerde eienskappe van die 3,4-dihidro-2(1*H*)-kinolinoonderivate het aangedui dat die verbindings hoogs lipofiel is, met logP-waardes van 3.03-4.55. LogP-waardes tussen 1 en 3 is egter ideaal vir goeie biobeskikbaarheid. Die logP-waardes vir die gesintetiseerde verbindings is hoër as 3, wat aanleiding tot laer biobeskikbaarheid kan gee. Die resultate van die studie dui verder daarop dat geen van die 3,4-dihidro-2(1*H*)-kinolinoon-derivate hoogs toksies teenoor selkulture, by konsentrasies van 1 µM en 10 µM, is nie. Byvoorbeeld, die mees potente MAO-B-inhibeerder, 7-(3-bromobensieloksie)-3,4-dihidro-2(1*H*)-kinolinoon, verlaag die lewensvatbaarheid van selle tot 88.11% en 86.10% by konsentrasies van 1 µM en 10 µM, onderskeidelik. Hierdie konsentrasies is hoër as die IC_{50}- waarde vir die inhibisie van MAO-B. By die lae konsentrasies wat benodig word vir MAO-B-inhibisie, is sitotoksisiteit dus onwaarskynlik met die meer potente 3,4-dihidro-2(1*H*)-kinolinoon derivate.

Uit hierdie studie kan afgelei word dat C7-gesubstitueerde 3,4-dihidro-2(1*H*)-kinolinone belowende, hoogs potente en selektiewe MAO-B-inhibeerders is wat as moontlike geneesmiddelkandidate vir die behandeling van PS kan dien.

CHAPTER 1
INTRODUCTION

1.1 Parkinson's disease

James Parkinson described the core clinical features of Parkinson's disease (PD) in his monograph "Essay on the Shaking Palsy", as the second most common age-related neurodegenerative disease (Dauer & Przedborski, 2003; Parkinson, 2002). Over one million people in the United States are diagnosed with PD, thus making it one of the most common degenerative diseases, second to Alzheimer's disease (AD) (Bové *et al.*, 2005; Fahn & Przedborski, 2000). The degeneration of the neurons of the substantia nigra (SN) in the midbrain leads to the loss of dopamine (DA) from the striatum (Jenner, 1998), which in turn leads to PD symptoms (Dauer & Przedborski, 2003; Carlsson, 1959). PD is a sporadic condition, although few environmental factors have been identified as contributing to the pathogenesis of PD. The disease progresses with age and the mean duration thereof from diagnoses to death is 15 years, with a median age onset of 60 years (Lees *et al.*, 2009; Bower *et al.*, 1999; De Rijk *et al.*, 1995; Katzenschlager *et al.*, 2008; Korrell & Tanner, 2005). Current research on PD treatment is directed towards prevention of dopaminergic neuron degeneration (Dauer & Przedborski, 2003), but at present very little is known of how this process begins and progresses (Bové *et al.*, 2005). At present the most effective treatment of PD is with levodopa, the metabolic precursor of DA. Levodopa causes a "wearing-off" effect and leads to dyskinesias in about 50% of patients treated with levodopa (Rascol *et al.*, 2002a).

1.2 Monoamine oxidase

The enzyme monoamine oxidase (MAO) was named by Zeller (MAO; EC 1.4.3.4). MAO is a flavo-protein with flavine adenine dinucleotide (FAD) as the cofactor. MAO consists of two isoenzymes, MAO-A and MAO-B, which vary in proportion from tissue to tissue. For example, in the basal ganglia, blood platelets and liver, MAO-B is the main form, while in placenta and gastrointestinal tract, MAO-A is the most represented form. MAO-A and MAO-B also have different substrate affinities, pH optima and sensitivity to heat inactivation, as well as different specificities for inhibitors (Youdim *et al.*, 2006; Youdim *et al.*, 1988; Shih *et al.*, 1999; Nicotra & Parvez, 1999). Both isoenzymes are localised to the mitochondrial outer membrane (Youdim *et al.*, 2006). The oxidative deamination reactions of a range of monoamines including histamine, serotonin (5-HT) and catecholamine neurotransmitters such as dopamine, tyramine, noradrenaline and adrenaline are catalysed by MAO-A and MAO-B. The reaction produces hydrogen peroxide, the corresponding aldehyde and either ammonia or a substituted amine.

Since the oxidative deamination reaction catalyzed by MAO-B is a major catabolic pathway of dopamine in the brain, inhibition of MAO-B in the brain may slow the depletion of dopamine stores and elevate the levels of endogenous dopamine and dopamine produced from exogenously administered levodopa (Finberg *et al*., 1998). MAO-B inhibitors are thus considered to be useful agents for the symptomatic treatment of PD, especially in combination with levodopa.

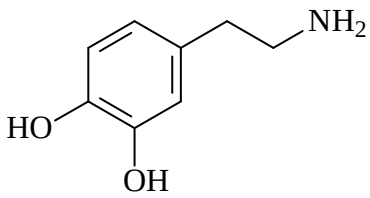

Figure 1.1: The structure of dopamine

As mentioned above, in the brain dopamine is oxidised predominantly by MAO-B to form the corresponding aldehyde, dopaldehyde, and H_2O_2. Elevated levels of aldehydes and H_2O_2 as a result of MAO-B catalysis are thought to contribute to neurotoxicity and reactive oxygen species (ROS) formation, and subsequently neurodegeneration in PD. Considering that MAO-B activity exhibits an age-related increase in the human brain (Nicotra *et al*., 2004; Fowler *et al*., 1997) while MAO-A activity remains constant, inhibition of this enzyme is especially relevant in PD. Thus, MAO-B inhibitors may play an important role in the treatment of PD, by reducing production of potentially neurotoxic aldehydes and H_2O_2. MAO-B inhibitors may thus protect against further neuronal degeneration in PD (Riederer *et al*., 2004).

From the above analysis it is clear that MAO-B inhibitors are useful therapeutic agents for the treatment of PD as they may alleviate the symptoms of the disease by preventing the MAO-B-catalyzed catabolism of DA in the brain. In addition, MAO-B inhibitors may also protect against neuronal degeneration in PD by reducing the formation of aldehydes and H_2O_2 in the catalytic cycle of MAO-B. Several research groups are therefore interested in the discovery of new MAO-B inhibitors for the treatment of PD. This study will attempt to design novel MAO-B inhibitors using quinolinone as scaffold. As shown below the structure of quinolinone is related to coumarin, a well-known scaffold for the design of MAO-B inhibitors.

1.3 Rationale

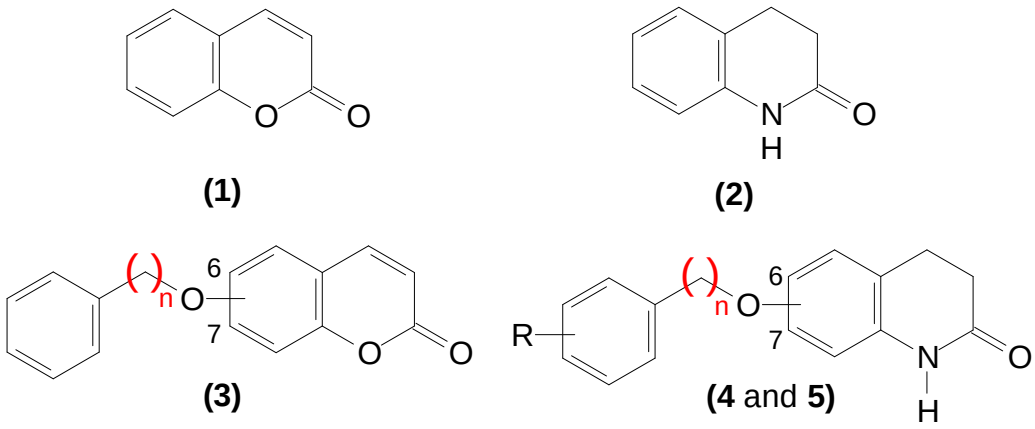

R = H, Cl, Br.

Figure 1.2: The structures of coumarin (**1**), quinolinone (**2**), C6/7-substituted coumarins (**3**) and C6/7-substituted quinolinones (**4** and **5**). The C6- and C7-substituted quinolinones (**4** and **5**) shown here will be synthesised in this study, and evaluated as MAO inhibitors.

Coumarin (benzopyran-2-one) (**1**) has previously been used as scaffold for the design of MAO-A and MAO-B inhibitors. Coumarins have been shown to act as competitive inhibitors and yield particularly potent MAO-B inhibitors with substitution at C6 and C7 (**3**) (Gnerre *et al*., 2000). The current study will attempt to discover novel highly potent MAO-A and MAO-B inhibitors by using quinolinone as scaffold. Quinolinone (**2**) is structurally related to coumarin and may thus, with the appropriate substitution, yield structures with MAO-B inhibitory properties. In this study a series of quinolinones will be synthesized and evaluated *in vitro* as inhibitors of MAO-A and MAO-B. The quinolinones will be substituted on C6 and C7 with a variety of substituents.

The general structure of the quinolinones that will be synthesised is shown in figure 1.2. As shown in table 1.1, quinolinone will firstly be substituted with the benzyloxy side chain at the C6 and C7 positions to yield compounds **4a** and **5a**. The benzyloxy moiety appears to be particularly suitable for MAO-B inhibition since numerous MAO-B inhibitors contain the benzyloxy moiety attached to a heterocyclic scaffold. Examples of such structures are the coumarin derivatives (**3**) and the reference MAO-B inhibitor, safinamide (Figure **1.3**). To explore the structure-activity relationships of MAO inhibition by the quinolinone class of compounds, the benzyloxy phenyl rings will be substituted on the *meta* and *para* positions with chlorine (to yield structures **4b** and **5b**) and bromine (to yield structures **4c** and **5c**). To further explore chemical space the quinolinone derivatives will also contain the phenylethoxy (to yield structures **4d** and **5d**) and phenylpropoxy (to yield structures **4e** and **5e**) moieties at C6 and C7. In total 10 quinolinone derivatives will be synthesised.

Table 1.1: The structures of the C6- and C7-substituted quinolinones (**4** and **5**) that will be synthesised in this study.

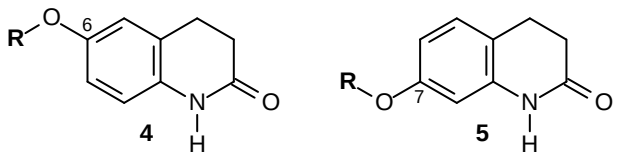

	R
4a	$C_6H_5CH_2$–
4b	3-$ClC_6H_4CH_2$–
4c	3-$BrC_6H_4CH_2$–
4d	$C_6H_5(CH_2)_2$–
4e	$C_6H_5(CH_2)_3$–
5a	$C_6H_5CH_2$–
5b	3-$ClC_6H_4CH_2$–
5c	3-$BrC_6H_4CH_2$–
5d	$C_6H_5(CH_2)_2$–
5e	$C_6H_5(CH_2)_3$–

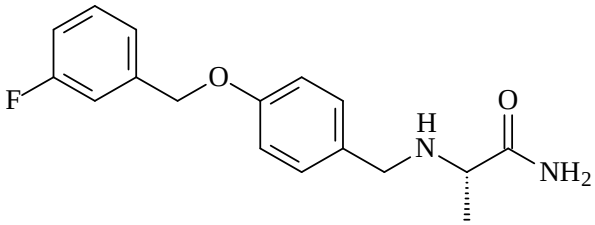

Figure 1.3: The structure of safinamide

Based on the structural similarity with coumarin, it is anticipated that these selected quinolinones will possess MAO-B inhibitory activity. This study is therefore an exploratory study with the aim to discover novel potent inhibitors of MAO-B. Such compounds may have potential in the therapy of PD by prolonging the action of endogenous dopamine. As mentioned above the quinolinones that will be synthesised in this study are expected to act as reversible MAO-B inhibitors since coumarins are reported to interact reversibly with the MAO enzymes. Reversible MAO-B inhibitors have a shorter duration of action, which reduces the possibility of loss of selectivity, and with elimination of the inhibitor from the tissues, enzyme activity is recovered.

In contrast, after treatment with irreversible MAO-B inhibitors, the recovery of enzyme activity is slow and with repeated administration of the drug, loss of isoform selectivity may occur (Tipton *et al.*, 2004). These advantages make reversible inhibitors more desirable than irreversible inhibitors (Binda *et al*., 2003).

1.4 Hypothesis of this study

Based on the report that substituted coumarins (**3**) are highly potent MAO-B inhibitors, it is postulated that quinolinone derived compounds, with the appropriate substitution, may also act as potent MAO-B inhibitors (Gnerre *et al.*, 2000). Quinolinone may thus be a promising scaffold for the design of potent MAO-B inhibitors. It is further postulated that the benzyloxy side chain substituted at C6 and C7 of quinolinone may be particularly suitable for the design of potent MAO-B inhibitors. This assumption is based on the observation that numerous MAO-B inhibitors contain a benzyloxy moiety attached to a heterocyclic scaffold. It is also postulated that simple halogen (Cl and Br) substituents on the phenyl ring of the benzyloxy moiety will significantly enhance the inhibition potency of the quinolinone derivatives.

This study further explores the effect that the phenylethoxy and phenylpropoxy moieties at C6 and C7 of quinolinone have on MAO-B inhibition potency. The inhibition potencies of these homologues will subsequently be compared to those of the quinolinones substituted with the benzyloxy side chain on C6 and C7. Also for comparison, the MAO-A inhibitory properties of the series of quinolinones will be examined.

1.5 Objectives of this study

- A series of quinolinone derivatives (**4a-e** and **5a-e**) will be synthesised. The structures of the target quinolinone derivatives are shown in table 1.1. For the purpose of this study, the quinolinones will be substituted on C6 and C7 of the quinolinone scaffold.
- The synthesised analogues will be investigated as potential MAO-A and MAO-B inhibitors using the recombinant human MAO enzymes. IC_{50} values (concentration of the inhibitor that produces 50% inhibition) will be used to express the inhibition potencies of the analogues.
- To determine the reversibility of inhibition by a selected quinolinone derivative, the recovery of the enzymatic activity after dilution of the enzyme-inhibitor complex will be evaluated.
- Furthermore, a set of Lineweaver-Burk plots will be constructed to determine if a selected inhibitor's mode of inhibition is competitive.
- Finally a limited analysis of selected properties of the quinolinone derivatives will be carried out. For this purpose, the log P values and toxicity to tissue cultures will be examined.

CHAPTER 2
LITERATURE OVERVIEW

2.1 Parkinson's disease

2.1.1 General background

The cause of PD is still uncertain, but it is believed to be caused by aging genetic mutations and various biological and environmental factors (Dauer & Przedborski, 2003). The role of environmental toxins and genetic factors is still not known, but the environmental hypothesis was dominant for much of the 20th century and states that the exposure to dopaminergic neurotoxins may lead to neurodegeneration associated with PD. A final possibility that does not fit the categories above is that endogenous toxins and distortions of normal metabolism may be responsible for neurodegeneration (Dauer & Przedborski, 2003).

The loss of nigrostriatal dopaminergic neurons in the Substantia nigra pars compacta (SNpc), a component of the nigrostriatal dopamine pathway in the brain, and the presence of intraneuronal proteinacious cytoplasmic inclusions called "Lewy Bodies" (LBs), are the principal pathological features of PD. The loss of the cell bodies of the nigrostriatal neurons results in SNpc depigmentation. This is associated with the loss of DA transporter mRNA expression and a deficiency of DA in the striatum, which then leads to PD symptoms (Dauer & Przedborski, 2003).

The principal symptoms of PD are tremors, rigidity, postural instability, slowness or absence of voluntary movement and freezing. Tremors usually occur when patients are at rest, while with movement the tremors decrease. Freezing refers to the inability to begin with a usually voluntary movement such as walking. Depression and dementia are two common characteristics of PD, especially in older patients. In 5% of patients, the disease is inherited, which means that in 95% of patients, there is no definite link to a genetic cause. After 5-10 years, even with treatment, the symptoms often get worse (Dauer & Przedborski, 2003). Only when approximately 60% of the SNpc neurons have died and 70% DA has been lost from the striatum, will the symptoms of PD present itself. There are two major hypotheses regarding the pathogenesis of PD.

Firstly the misfolding and aggregation of proteins may be crucial in the death of SNpc dopaminergic neurons. Abnormal protein conformations may be induced by pathogenic mutations, which are believed to be the case with α-synuclein (α-syn). Secondly, mitochondrial dysfunction and the consequent oxidative stress may lead to neuronal death (Dauer & Przedborski, 2003). These mechanisms will be discussed in the sections below.

2.1.2 Mechanisms of neurodegeneration

As mentioned above, the two principal mechanisms of neurodegeneration in PD are (1) the misfolding and aggregation of proteins and (2) mitochondrial dysfunction and the subsequent oxidative stress. Additional mechanisms that may play a role include neuroinflammation, excitotoxicity, apoptosis and loss of trophic factors.

2.1.2.1 Protein aggregation and misfolding

Aggregates of misfolded proteins have been shown to possess toxic properties. The major aggregating protein in PD is α-syn. This protein is also the major component of LBs and Lewy neurites. It has also been found that gene duplication of α-syn may cause PD. Although it is certain that there is a definite link between α-syn and PD and that the aggregation caused thereby may be a central mechanism in this disease, the mechanism of aggregation is not understood.

Enhancing protein clearance and proteosomal or lysosomal degradation pathways of α-syn might have therapeutic potential (Yacoubain & Standaert, 2009; Athanassiadou *et al.,* 1999; Kruger *et al.,* 1998; Polymeropoulos *et al.,* 1997; Zarranz *et al.,* 2004). Protein aggregates may damage neurons by deforming the cell or interfering with intracellular trafficking. Protein aggregates may also sequester protein in the cell that is required for cell survival (Dauer & Przedborski, 2003).

2.1.2.2 Oxidative stress and mitochondrial dysfunction

Overproduction of reactive oxygen species (ROS) or failure to limit their accumulation through buffering mechanisms may lead to overabundance of reactive free radicals. This leads to oxidative stress. Sources producing ROS are DA metabolism and mitochondrial dysfunction. For each mole of DA metabolized by MAO, one mole of hydrogen peroxide is produced. Hydrogen peroxide may be converted to reactive and damaging species via the Fenton reaction. Mitochondrial dysfunction, in turn, results in the abnormal consumption of oxygen by the respiratory chain and subsequently the generation of superoxide, a reactive species (Kirkinezos & Moraes, 2001).

ROS may damage proteins, lipids and nucleic acids in the SNpc and thus induce neurodegeneration in PD. Glutathione promotors, for example selenium, may be useful in limiting oxidative stress since the antioxidant protein, glutathione, is reduced in post-mortem PD nigra. Other ways of limiting oxidative stress include MAO-A and MAO-B inhibitors, mitochondrial electron transport enhancers (for example Coenzyme Q10), and finally antioxidants such as vitamin E and uric acid. Although all of the above show very good tolerance, there is still not enough clinical evidence for their effectiveness in PD (Yacoubain & Standaert, 2009).

2.1.2.3 Neuroinflammation

Neuroinflammation is believed to be involved in PD. In the SN and striatum from post-mortem PD brains, activated microglia has been observed. Microglial activation may be enhanced by cytokines and α-syn, leading to the release of cytotoxic factors. Several anti-inflammatory drugs have been and are currently reviewed for their potential as neuroprotectants (Yacoubain & Standaert, 2009).

2.1.2.4 Excitotoxicity

In the central nervous system (CNS), glutamate is identified as the main excitatory transmitter and glutamate receptors are present in high levels on dopaminergic neurons in the SN. Glutamate is also believed to be the main driver of the excitotoxic process. Glutamate activates NMDA channels and this leads to increased intracellular calcium levels. The excessive activation of NMDA channels may lead to the activation of cell death pathways. In addition, calcium influx may activate nitric oxide synthase, which leads to the enhancement of peroxynitrite production. Protection against the loss of dopaminergic cell loss may be achieved by NMDA receptor antagonists. Such drugs therefore represent an opportunity for the development of novel neuroprotective agents for the treatment of PD (Yacoubain & Standaert, 2009).

2.1.2.5 Apoptosis

Neural development as well as neural injury is influenced by apoptosis. Evidence of apoptosis and autophagic cell death has been found in the SN of PD brains, but to a low extent. It is hypothesised that oxidative stress, protein aggregation, excitotoxicity or inflammatory processes activate apoptotic and autophagic cell death pathways. Thus, inhibitors of these cell death pathways have been suggested as treatment in PD (Yacoubain & Standaert, 2009).

2.1.2.6 Loss of trophic factors

The death of neuronal cells in PD may be initiated by the loss of neurotrophic factors. Several neurotrophic factors are reduced in the nigra in PD, such as brain-derived neurotrophic factor (BDNF), glial-derived neurotrophic factor (GDNF) and nerve growth factor (NGF). GDNF and other growth factors, such as neurturin, may be successful in the treatment of PD because it has shown protection against neurodegeneration in animal models. Although GDNF shows similar results in humans, neurturin is still being investigated (Yacoubain & Standaert, 2009).

2.1.3 Symptomatic treatment

Treating PD offers relief of symptoms, although the disease is not curable (Lees *et al*., 2009). The primary goal in treating PD is neuroprotection. Although there is no concrete evidence that any of the current treatments provide neuroprotection, levodopa may possess some neuroprotective effects in the short-term (Fernandez & Chen, 2007). The patient should always be encouraged to do both physical and mental exercises during any phase of the disease (Lees *et al*., 2009).

2.1.3.1 Levodopa

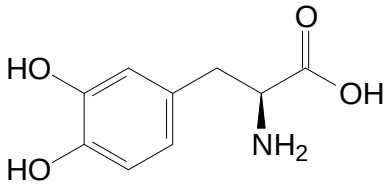

Figure 2.1: The structure of levodopa.

Levodopa's discovery had a profound effect on the treatment of PD and it remains the most effective treatment (Fernandez & Chen, 2007). Levodopa may, however, lead to involuntary movements and dyskinesias after several years of use. This makes daily life difficult for patients (Dauer & Przedborski, 2003; Fernandez & Chen, 2007). Levodopa also has other side effects, including nausea, anorexia, faintness and gastrointestinal effects, but if the drug dose is gradually increased levodopa is very well tolerated (Lees *et al*., 2009, Hardman & Limbird, 2001).

Levodopa is the metabolic precursor of DA and is absorbed very quickly through the active transport system in the small bowel. When administered orally its absorption is influenced by the rate of gastric emptying. After levodopa has been absorbed, it crosses the blood brain barrier through an active process that is mediated by the carrier system of aromatic amino acids. Finally, decarboxylase converts levodopa to DA in the brain (Hardman & Limbird, 2001). The combination of levodopa with a DA decarboxylase inhibitor (benserazide or carbidopa) is usually used as the initial therapy for patients of all ages (Lees *et al*., 2009).

Levodopa can also be combined with a catechol-O-methyltransferase (COMT) inhibitor (entacapone) or a MAO-B inhibitor [(R)-deprenyl or rasagiline] to reduce dyskinesias (Lees *et al*., 2009). As mentioned above, levodopa has serious adverse effects and its efficacy decreases with time. This leads to a narrowing of levodopa's therapeutic window (Fernandez & Chen, 2007). Levodopa is also used in diagnosing PD, as it will relieve the symptoms of PD (Lees *et al*., 2009; Katzenschlager e*t al.*, 2008; Fahn *et al.*, 2004; Hely *et al.*, 2008; Rascol *et al.*, 2002b; Miyasaki, 2006).

2.1.3.2 Dopamine agonists

DA agonists act at striatal DA receptors and this may have several advantages. DA agonists may be more effective than levodopa since it is not dependent on the functional capacity of nigrostriatal neurons (Hardman & Limbird, 2001). DA agonists have a much longer half-life than levodopa and, although it is believed that they may delay the development of motor complications induced by levodopa, they also have adverse effects of their own. These adverse effects include nausea, sedation, neuropsychiatric effects (such as hallucinations and psychosis), orthostatic hypotension and agonist-specific effects (such as ankle edema and erythromelalgia) (Fernandez & Chen, 2007). These effects may necessitate the withdrawal of the drug (Lees *et al*., 2009). DA agonists can be used as an adjunct to levodopa, an alternative to levodopa or as first-line therapy in early PD (Hardman & Limbird, 2001; Fernandez & Chen, 2007). There are four commonly used DA agonists. These include two older compounds, bromocriptine and pergolide, and two newer more selective compounds, ropinirole and pramipexole. (Hardman & Limbird, 2001).

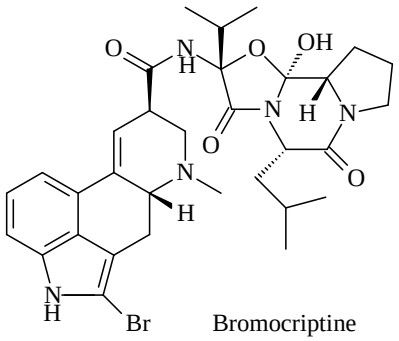

Bromocriptine

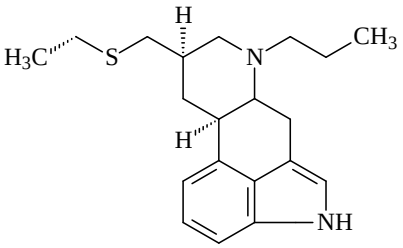

Pergolide

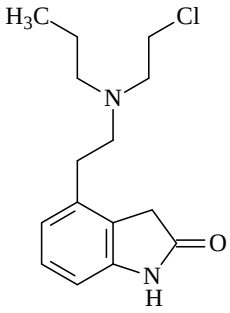

Ropinirole

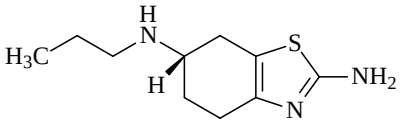

Pramipexole

Figure 2.2: The structures of bromocriptine, pergolide, ropinirole and pramipexole.

2.1.3.3 COMT inhibitors

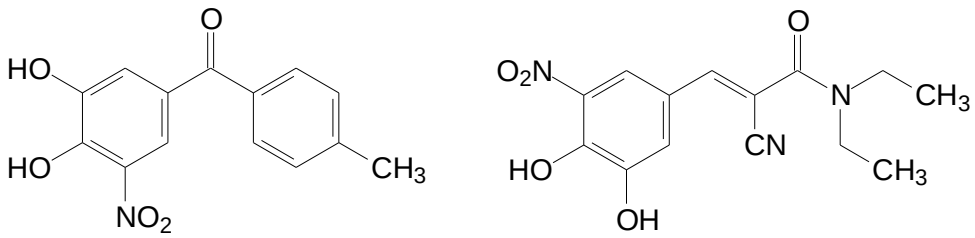

Figure 2.3: Examples of COMT inhibitors, with tolcapone left and entacapone right.

Since COMT and MAO are responsible for the metabolism of levodopa and DA, inhibitors of these enzymes are used in the treatment of PD. Currently there are two COMT inhibitors available for the treatment of PD, tolcapone and entacapone. Both these inhibitors can reduce the so called “wearing off” symptoms in patients that are treated with levodopa.

The two inhibitors have similar properties, with side effects such as nausea, orthostatic hypotension, vivid dreams, confusion and hallucinations. Only tolcapone is associated with serious hepatotoxicity and should now only be used for treating patients who do not successfully respond to other therapies (Hardman & Limbird, 2001).

2.1.3.4 MAO-B inhibitors

MAO-B inhibitors are used in the treatment of PD for two reasons. Firstly, MAO-B inhibitors enhance striatal dopaminergic activity by inhibiting DA metabolism, which leads to an improvement of PD motor symptoms. Secondly, selective MAO-B inhibitors may modify the disease progression by acting as neuroprotective agents (Fernandez & Chen, 2007). This effect may be the result of the inhibition of the formation of toxic metabolic by-products associated with dopamine oxidative metabolism. Selective MAO-B inhibitors are a feasible option for the treatment of PD because, without affecting MAO-A activity, they increase synaptic DA concentrations. Non-selective MAO inhibitors are contraindicated in levodopa-treated patients since the combination of levodopa with MAO-A inhibition may lead to hypertension (Fernandez & Chen, 2007). Selective MAO-B inhibitors are tolerated well by PD patients (Lees *et al*., 2009). Selective irreversible MAO-B inhibitors include (R)-deprenyl (selegiline) and rasagiline.

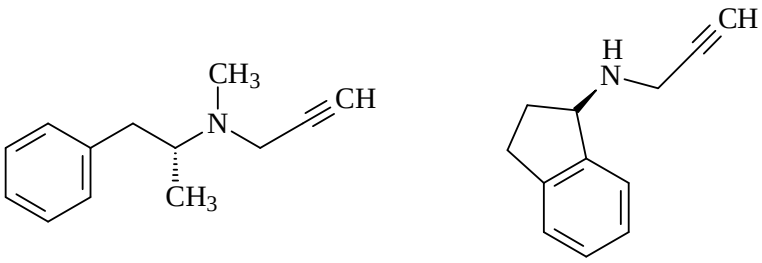

Figure 2.4: The structures of (R)-deprenyl and rasagiline.

2.1.3.5 Anticholinergic drugs

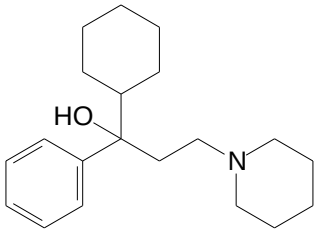

Figure 2.5: The structure of trihexyphenidyl.

Anticholinergic drugs can be useful in treating dystonic pain, especially in early stages and have been used in the treatment of PD long before the discovery of levodopa. It is believed that this drug works within the neostriatum, but its action is not fully understood. Several anticholinergic drugs can be used in the treatment of early PD or as an adjunct to other therapies. Examples of anticholinergic drugs used in PD therapy are trihexyphenidyl, benztropine and diphenhydramine. Side effects associated with anticholinergic drugs include sedation, constipation, mental confusion, urinary retention and blurred vision. These drugs must therefore be used very carefully in elderly patients (Hardman & Limbird, 2001).

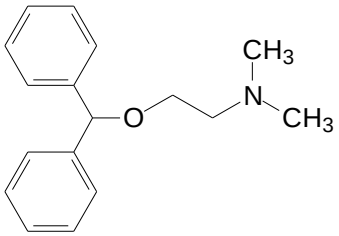

Figure 2.6: The structure of diphenhydramine.

2.1.3.6 Amantadine

Amantadine is an antiviral drug used in the prophylactic treatment of influenza A (Hardman & Limbird, 2001). Amantadine shows activity at the N-methyl-D-aspartate (NMDA) glutamate receptors, acting as an antagonist (Lees *et al*., 2009). Amantadine can be used as initial therapy for PD and is very well tolerated (Lees *et al*., 2009). In some cases it has mild side effects such as dizziness, lethargy, anticholinergic effects, sleep disturbance, nausea and vomiting (Hardman & Limbird, 2001).

2.1.4 Drugs for neuroprotection

As mentioned above, the primary goal of PD treatment is neuroprotection. Neuroprotection refers to the process of preventing, slowing or halting the neurodegenerative processes responsible for PD. To date, no treatment strategy has been proven to exert neuroprotection in PD.

2.1.4.1 MAO-B inhibitors: (R)-Deprenyl, lazabemide and rasagiline

In the 1980s studies were carried out with the aim of preventing or reducing the catabolism of DA by MAO-A and MAO-B by employing inhibitors of these enzymes. The first compound selected for these studies was (R)-deprenyl, also known as selegiline. (R)-Deprenyl is an irreversible selective MAO-B inhibitor. It was found that (R)-deprenyl leads to a significant delay in a patient's need for levodopa treatment, which suggested that this drug may possess a neuroprotective effect in PD. Rasagiline is another highly selective irreversible inhibitor of MAO-B. Similar to (R)-deprenyl, rasagiline has a propargylamine structure and also displays this apparent neuroprotective effect. (R)-deprenyl and rasagiline display several activities, such as enhancement of DA release, retarding the catabolism of DA, functional recovery and antagonising cellular processes that lead to apoptosis, including intranuclear translocation of the glycolytic enzyme glyceraldehyde-3-phosphate dehydrogenase, induction of bcl-2 and activation of mitochondrial permeability transition (LeWitt & Taylor, 2008). All these effects may contribute to the neuroprotective effects of (R)-deprenyl and rasagiline.

2.1.4.2 Dopaminergic drugs: pramipexole

DA receptor agonists can reduce oxidative stress by acting at the D2 autoreceptors, which are located on dopaminergic SN terminals. Based on this, DA agonists may be neuroprotective. Reduction in dopaminergic cell death was found in studies with DA receptor agonists. In a comparative study between pramipexole and levodopa, patients being treated with levodopa showed more of a decline than patients treated with pramipexole. These studies suggest that DA agonists have a neuroprotective effect, with the limitation that it is difficult to establish whether the neuroprotection is long-term (Yacoubain & Standaert, 2009).

2.1.4.3 Antioxidant therapy

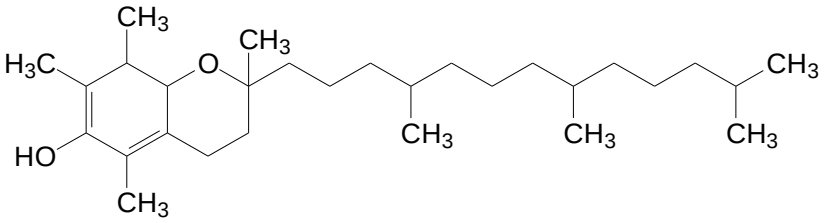

Figure 2.7: The structure of α-tocopherol

An antioxidant that has been tested for a potential neuroprotective effect in PD is α-tocopherol (vitamin E). Oxyradical species are demolished by the chain-breaking antioxidant, α-tocopherol, which enters lipid-soluble cellular regions such as biological membranes. Clinical studies have, however, not been able to proof that α-tocopherol protects against neurodegeneration in PD patients (LeWitt & Taylor, 2008; Yacoubain & Standaert, 2009).

2.1.4.4 Mitochondrial energy enhancement drugs: coenzyme Q10 and creatine

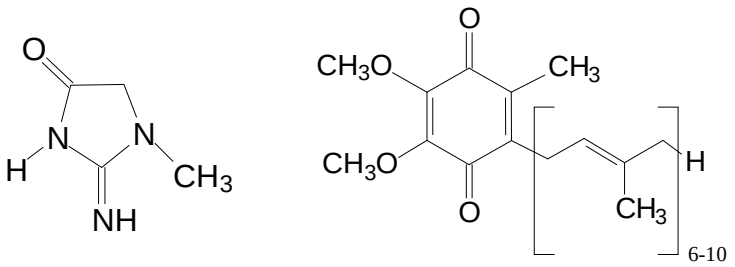

Figure 2.8: Examples of mitochondrial energy enhancement drugs, with creatine left and coenzyme Q10 right.

Two strategies to correct defects of mitochondrial respiration include treatment with coenzyme Q10 and creatine. In the mitochondria, coenzyme Q10 serves as a cofactor in the electron transport chain. Since defective mitochondrial respiration may play a role in the neurodegenerative processes in PD, the enhancement of mitochondrial respiration through supplementation with coenzyme Q10 may represent a neuroprotective strategy. Since the production of ATP in the mitochondria is promoted by creatine, this molecule may also represent a neuroprotective strategy in PD. Phospho-creatine is produced from the precursor, creatine, which transfers phosphoryl groups, leading to the synthesis of ATP. To date, no convincing evidence have shown coenzyme Q10 and creatine to be neuroprotective in PD (LeWitt & Taylor, 2008; Yacoubain & Standaert, 2009).

2.1.4.5 Anti-inflammatory drugs

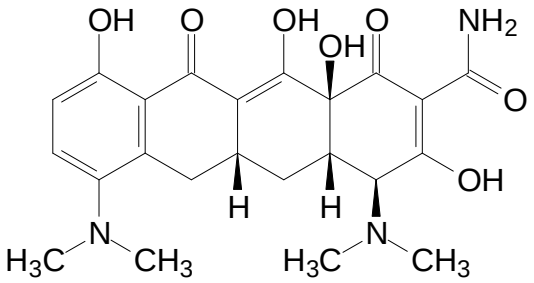

Figure 2.9: The structure of minocycline

Inflammation may contribute to neurodegeneration in PD. Studies have evaluated several anti-inflammatory agents, such as non-steroidal anti-inflammatory drugs (NSAIDs) and minocycline, as potential neuroprotective agents in PD. The results have revealed that aspirin has neuroprotective properties, with uncertainty as to what dose provides the best neuroprotection. The well tolerated minocycline, which was primarily used for its antimicrobial activity, is also an anti-inflammatory agent. Preliminary results suggest that minocycline protects against dopaminergic cell loss (Yacoubain & Standaert, 2009).

2.1.4.6 Antiapoptotic drugs:

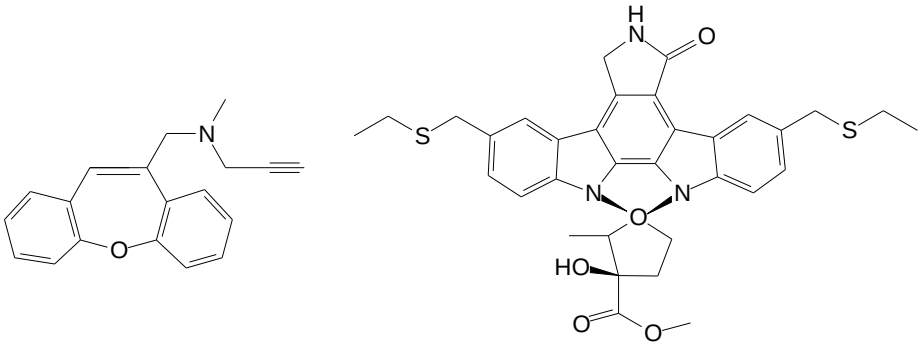

Figure 2.10: Examples of antiapoptotic drugs with TCH 346 left and CEP-1347 right.

It is believed that apoptosis is an end-stage process of neurodegeneration in PD, and antiapoptotic drugs may offer neuroprotection regardless of the initial degenerative mechanism. Antiapoptotic drugs include the propargylamines, TCH346 and CEP-1347. Apoptosis can be inhibited through inhibition of the glycolytic enzyme glyceraldehyde-3-phosphate dehydrogenase (GAPDH) by the propargylamine TCH346 (LeWitt & Taylor, 2008). TCH346 has structural similarities to (R)-deprenyl and has been shown to increase cell survival by inhibiting a key step in age-induced neuronal apoptosis.

CEP-1347 is an inhibitor of mixed lineage kinase-3 (Yacoubain & Standaert, 2009). Although this drug has shown promise in laboratory experiments, its putative neuroprotective effects still have to be examined in the clinical setting. There is still uncertainty as to whether antiapoptotic drugs must be used in combination with other trophic agents or whether it can be used as monotherapy in the late stage of PD (Yacoubain & Standaert, 2009).

2.1.4.7 NMDA antagonists and antiglutamatergic drugs

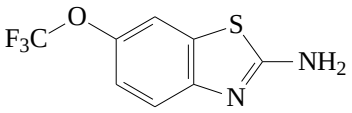

Figure 2.11: The structure of riluzole

Glutamate can cause excitotoxic neuronal damage by acting on NMDA receptors. Drugs acting on glutamate may thus offer neuroprotective effects in PD. Riluzole, an NMDA antagonist, blocks the presynaptic release of glutamate and is very well tolerated, unlike potent glutamate blockers that can cause substantial CNS toxicity. Riluzole has also been FDA-approved for effectively slowing deterioration of amyotrophic lateral sclerosis (LeWitt & Taylor, 2008). This drug may therefore be a promising agent for the neuroprotective treatment of PD.

2.2 Monoamine oxidase

As shown above, a variety of treatment strategies exist for PD. These include both agents for the symptomatic treatment of PD and potential neuroprotective therapies. In this dissertation the focus will be on MAO and the role of MAO inhibitors in PD.

2.2.1 General background

MAO is an enzyme that protects the body by preventing exogenous amines from entering the circulation and by oxidising amines already present in the blood and tissue (Youdim *et al*., 2006). Two isoforms of MAO have been identified: MAO-A and MAO-B. MAO-B is the main form in the human brain (Youdim *et al*., 2006), whilst MAO-A is the main form in the intestinal tract. In the brain, MAO-B is responsible for metabolizing DA to 3,4-dihydroxyphenylacetic acid. MAO-B is also responsible for the deamination of ß-phenylethylamine. ß-Phenylethylamine stimulates the release of DA and inhibits the uptake of DA into neurons. In the intestine, MAO-A is necessary for the deactivation of catecholamines as well as vasopressors such as tyramine ingested in the diet. This prevents these species from entering the systemic circulation (Fernandez & Chen, 2007). In the CNS MAO-A metabolizes serotonin.

2.2.2. Genes and MAO

Although the isoenzymes MAO-A and MAO-B have a ~70% sequence identity they are encoded by separate genes located on the X chromosome (Xp11,23). The MAO-A and MAO-B genes may be expressed differently, a process which is controlled by some hormones, for example, progesterone, testosterone, corticosterone and glucocorticosteroids, which increase MAO-A expression, but has little effect on MAO-B. The expression of MAO-B is regulated by a mitogen-activated protein kinase (MAPK). Personality traits, for example extraversion, and also vulnerability to the abuse of certain substances and smoking, may be linked to low platelet MAO-B activity (Youdim *et al*., 2006).

2.2.3 Biological function of MAO-A

2.2.3.1 The cheese reaction

The cheese reaction is caused by tyramine and other indirectly acting sympathomimetic amines present in food, such as cheeses and fermented drinks. Normally these foods are metabolised by MAO-A in the gut and liver, but in the presence of MAO-A inhibitors, the metabolism is prevented, thus ingested sympathomimetic amines may enter the circulation.

Entering the circulation, the amines have access to the peripheral adrenergic neurons, causing the release of noradrenaline. This leads to a hypertensive response, which can be fatal. The cheese reaction restricts MAO-A inhibitors, selective and non-selective, from being commonly used in the clinical treatment of depression (Youdim & Bakhle, 2006; Youdim *et al.*, 2006; Youdim & Weinstock, 2004; Hasan *et al.*, 1988; Finberg & Tenne, 1982; Chen & Swope, 2005).

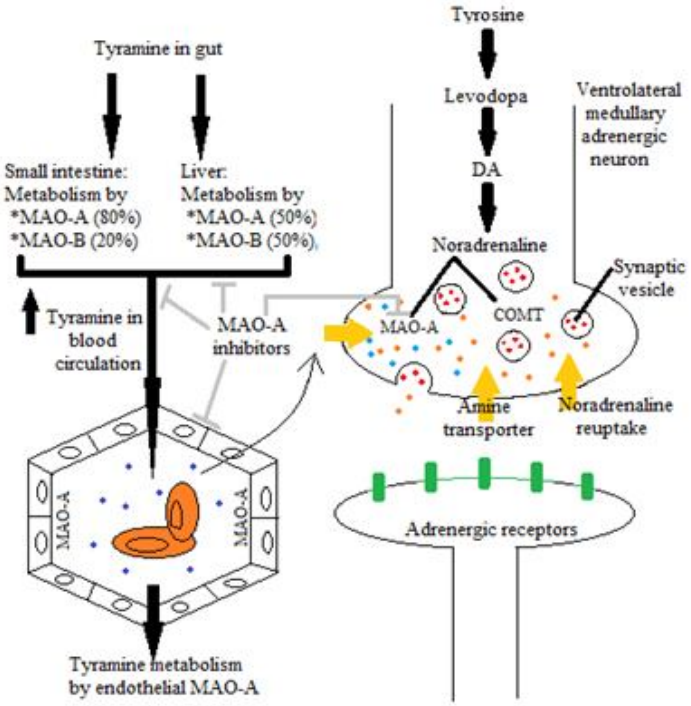

Figure 2.12: The cheese reaction (Youdim *et al.*, 2006).

2.2.3.2 MAO-A in depression

The antidepressant properties of MAO inhibitors is believed to result from the selective inhibition of MAO-A in the CNS. Inhibition of MAO-A in the CNS leads to increased levels of serotonin and noradrenaline in the brain and thus an antidepressive effect. MAO-A inhibitory drugs that are still clinically used for depression include non-selective irreversible inhibitors such as phenelzine and tranylcypromine, as well as reversible MAO inhibitors such as moclobemide, befloxatone and toloxatone (Youdim *et al.*, 2006).

2.2.3.3 The serotonin syndrome

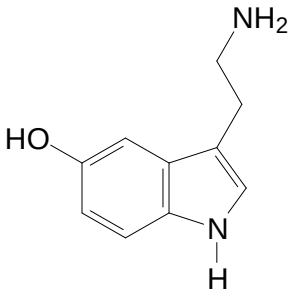

Figure 2.13: The structure of serotonin

Since MAO-A is also responsible for the catabolism of serotonin, the use of MAO-A inhibitors in combination with serotonin-enhancing drugs such as selective serotonin reuptake inhibitors (SSRIs), can cause a serious condition called the serotonin syndrome. Restlessness, hallucinations, loss of coordination, rapid heartbeat, increased body temperature, nausea, vomiting, diarrhoea, overactive reflexes and sudden changes in blood pressure are symptoms related to this syndrome (Fernandez & Chen, 2007; Chen & Swope, 2005). The serotonin syndrome occurs because of an over activity of serotonin in the CNS.

2.2.4 The role of MAO-B in Parkinson's disease

2.2.4.1 Synthesis and metabolism of dopamine

Tyrosine passes through the blood brain barrier where it is hydroxylated by tyrosine hydroxylase (TH) to yield levodopa. Levodopa is subsequently decarboxylated in the neuron by DOPA decarboxylase (DDC) to yield DA. DA is either metabolised by MAO-A (at the neuronal mitochondria) or taken up by synaptic vesicles (SV). DA is then released from the terminal after which it is cleared by uptake into astrocytes and glia (Youdim & Bakhle, 2006). In glia, DA is metabolized by MAO-B.

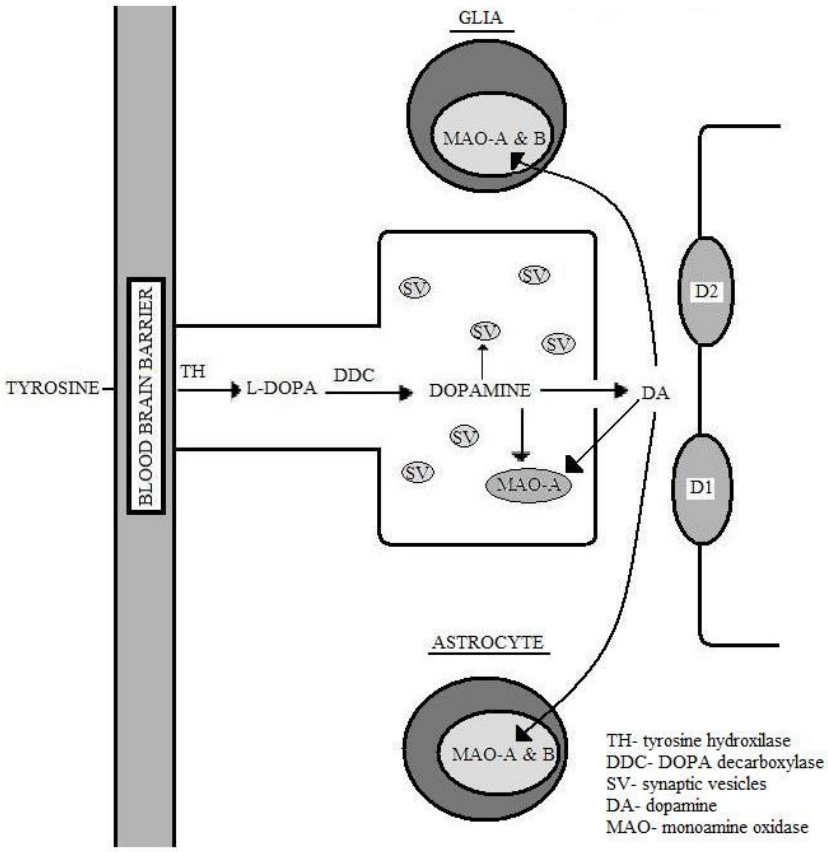

Figure 2.14: The biosynthesis and metabolism of dopamine

2.2.4.2 MAO-B levels in the brain and aging

Studies have shown that MAO-B levels in the brain increase with age as well as in certain neurodegenerative diseases. It was found that the increase of MAO-B with age is consistent with its localisation within the cell bodies of the serotonergic neurons and in glial cells. Reports have shown that glial cells increase in the brain with age and as a result of neurodegeneration. Since MAO-B is localised in glial cells, this leads to an increase of MAO-B activity and density. The sensitivity of the brain DA system to degenerate with age may be enhanced by oxidative stress, which increases with the increase of MAO-B in the brain (Fowler *et al*., 1997).

2.2.4.3 The role of aldehyde dehydrogenase and glutathione peroxidase

The reaction catalysed by MAO (Figure 2.15) ultimately results in the formation of acidic metabolites such as the carboxylic acid (RCOOH) derived from dopamine metabolism. These metabolites are commonly used for measuring MAO activity *in vitro* or *in vivo*. Hydrogen peroxide is also formed in the MAO catalytic cycle. During the Fenton reaction (Figure 2.16) a highly active free radical, the hydroxyl radical, is generated from hydrogen peroxide by iron. When cellular anti-oxidants are depleted, lipids, proteins and DNA are damaged by the hydroxyl radical.

With an increase in age hydroxyl radical generation also increases, due to the increase in brain iron and brain MAO. When an amine is oxidised by MAO, the direct product is an aldehyde. Aldehydes may be neurotoxic if not rapidly metabolised to yield the acidic metabolites. The enzyme responsible for this process is aldehyde dehydrogenase (ADH). In PD, ADH may be reduced and this may lead to an increase in neurotoxic aldehydes derived from dopamine by MAO. In PD, glutathione peroxidase (GPO) activity may also be reduced due to low GSH levels and this may lead to accumulation of hydrogen peroxide. Hydrogen peroxide is then available as substrate for the Fenton reaction.

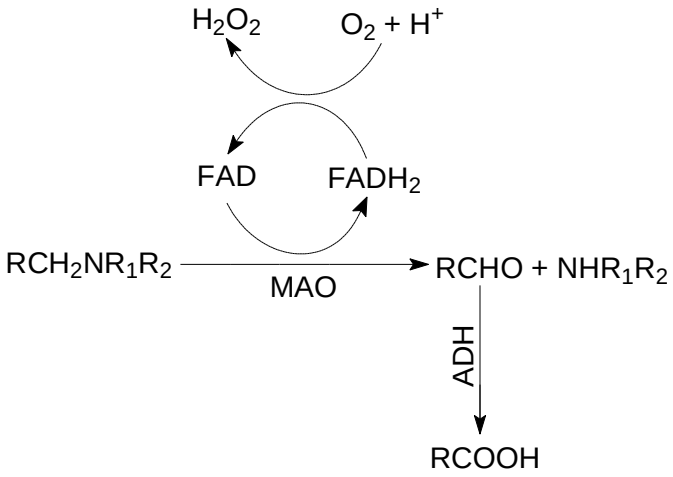

Figure 2.15: The reaction pathway of monoamine metabolism. An aldehyde is the primary product of MAO acting on a monoamine. The aldehyde (RCHO) is oxidised by aldehyde dehydrogenase (ADH), releasing the final excreted metabolite, a carboxylic acid (RCOOH) (Youdim & Bakhle, 2006).

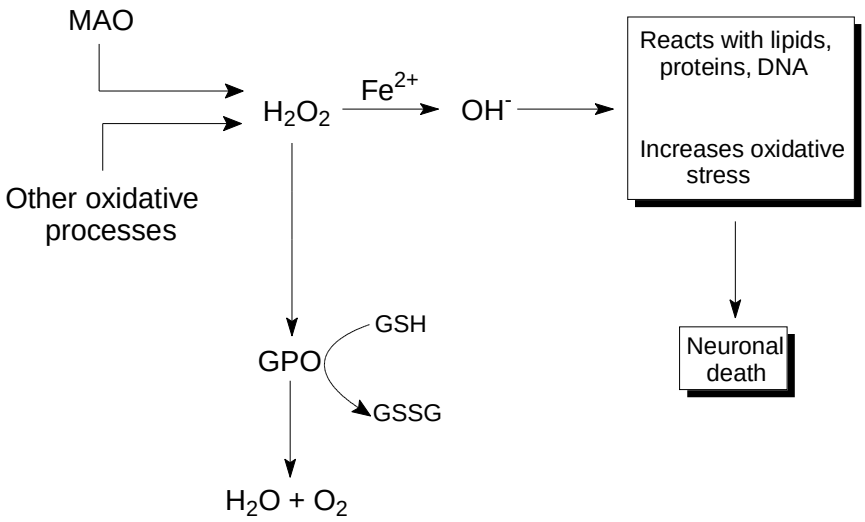

Figure 2.16: Hydrogen peroxide (H_2O_2) is produced with the metabolism of monoamines by MAO. H_2O_2 can either be converted into the hydroxyl radical or inactivated by glutathione peroxidase (GPO) (Youdim & Bakhle, 2006).

2.2.5 Irreversible inhibitors of MAO-B

Irreversible inhibitors bind to the enzyme, after which they are oxidised to the active inhibitor. The active inhibitor then binds covalently to the active site of the enzyme by reacting with the FAD cofactor (Abeles & Maycock, 1976). Irreversible inhibitors include (R)-deprenyl and rasagiline.

2.2.5.1 (R)-Deprenyl

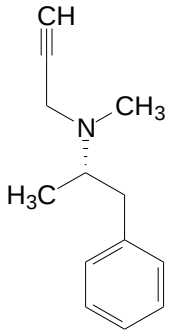

Figure 2.17: The structure of (R)-Deprenyl

(R)-Deprenyl is a propargyl amphetamine derivative with a low absolute bioavailability. The metabolism of (R)-deprenyl results in the following metabolites: desmethylselegiline, L-methamphetamine and L-amphetamine. Amphetamine metabolites of (R)-deprenyl are associated with adverse cardiovascular and psychiatric effects and potential neurotoxicity (Fernandez & Chen, 2007).

2.2.5.2 Rasagiline

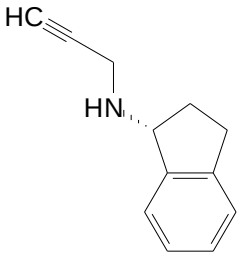

Figure 2.18: The structure of rasagiline

Rasagiline is a nonamphetamine propargylamine with a 36% bioavailability, thus greater than (R)-deprenyl. The metabolism of rasagiline results in the inactive metabolite aminoindan. Rasagiline can be used in combination with levodopa, but is also effective as monotherapy in PD (Fernandez & Chen, 2007).

2.2.6 Reversible inhibitors of MAO-B

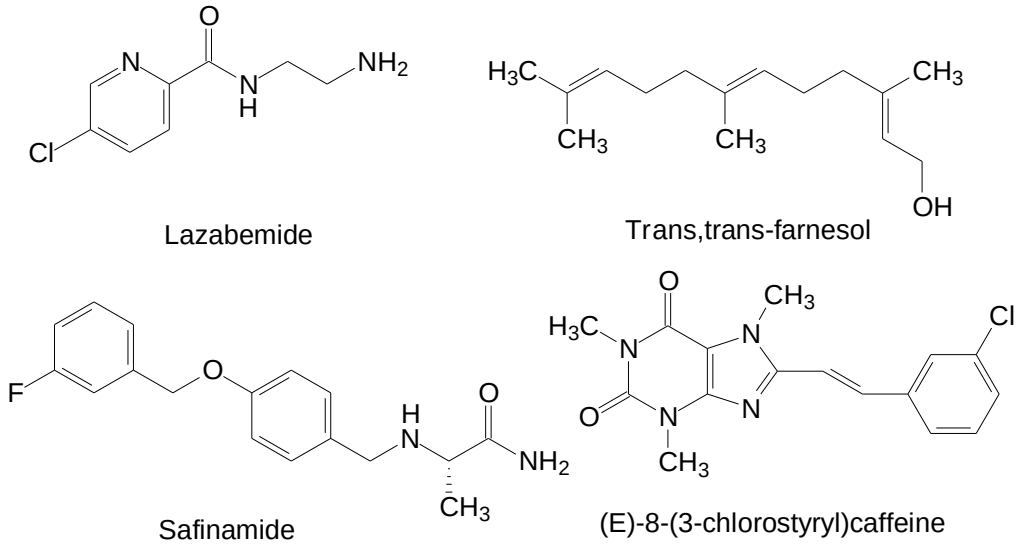

Figure 2.19: Examples of reversible inhibitors of MAO-B, lazabemide, trans,trans-farnesol, safinamide, (E)-8-(3-chlorostyryl)caffeine.

Reversible inhibitors bind non-covalently to the active sites of MAO-A and MAO-B (Binda *et al*., 2003). Lazabemide has an IC_{50} value of 0.03 µM for MAO-B and >100 µM for MAO-A. Trans,trans-farnesol is a component of tobacco smoke and a reversible inhibitor of MAO-B with a K_i value of 0.676 µM (Khalil *et al*., 2006; Hubálek *et al*., 2005). Safinamide is an α-aminoamide derivative. Along with its MAO-B inhibition activity, safinamide also inhibits the uptake of DA.

In addition to its motor benefits in PD, cognitive function is also improved by the use of safinamide (Fernandez & Chen, 2007). (E)-8-(3-Chlorostyryl)caffeine, a known A_{2A} adenosine receptor antagonist, has also been shown to act as a highly potent MAO-B inhibitor with a K_i value of 0.07 μM (Chen *et al.*, 2002; Petzer *et al.*, 2013).

2.2.7 Inhibitors of MAO-A

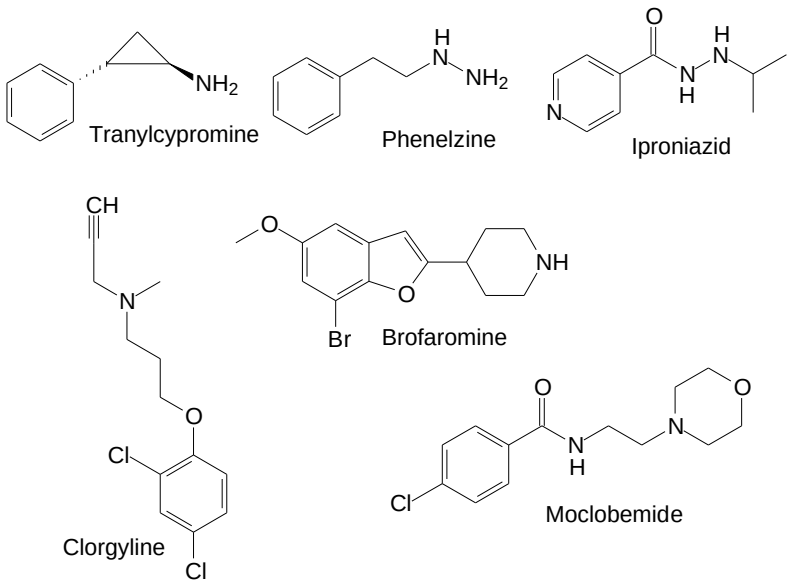

Figure 2.20: Examples of MAO-A inhibitors, tranylcypromine, phenelzine, iproniazid, clorgyline, brofaromine, moclobemide.

MAO-A inhibitors were clinically used in the 1950s as antidepressants, with iproniazid as the first non-selective MAO inhibitor to be used. Iproniazid was found to cause severe liver toxicity as well as hypertensive crises. Other inhibitors of MAO-A include clorgyline, tranylcypromine, phenelzine, moclobemide and brofaromine. Clorgyline is a selective irreversible inhibitor of MAO-A. Depressive disorders are effectively treated with clorgyline but it is not clinically used as an antidepressant due to the 'cheese reaction' which is induced by clorgyline. Tranylcypromine, also an irreversible inhibitor, is a non-hydrazine derivative of MAO which is also known to cause the 'cheese reaction' (Youdim *et al.*, 2006). Phenelzine is a hydrazine derivative of MAO and may cause liver toxicity and hypertensive crises (Youdim *et al.*, 2006). Moclobemide, a reversible MAO-A inhibitor, was developed to overcome the hypertensive crisis caused by tranylcypromine and other irreversible MAO-A inhibitors (Da Prada *et al.*, 1990). In contrast to irreversible inhibitors, reversible MAO-A inhibitors are not associated with the 'cheese reaction'.

2.2.8 Mechanism of action of MAO-B

2.2.8.1 The FAD cofactor and flavin adducts

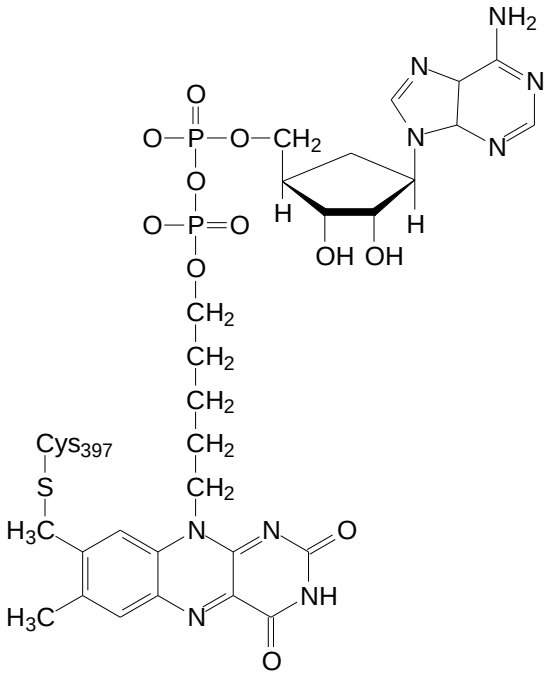

Figure 2.21: Structure of the FAD cofactor in MAO.

The FAD cofactor is present in both MAO-A and MAO-B and covalently binds to a cysteine (Cys) amino acid through a 8α-thioether linkage. The binding is between the cysteinyl residue, Cys397, for MAO-B and Cys406 for MAO-A, and the 8α-methylene of the isoalloxazine ring. The N(5) and C(4a) atoms are the reactive sites of the isoalloxazine ring (Edmondson *et al*., 2004a). Interestingly, the usually planar structure of the flavin ring in free FAD is bent 30° from planar, when bound to MAO-B (Binda *et al*,. 2003).

2.2.8.2 The SET and polar nucleophillic mechanistic pathways

MAO catalysis is dependent on the nature of the substrate. For interaction with the flavin, the amine substrate must bind to the MAO enzyme. Transferring the electron from the amine to the flavin can be done by two mechanisms:

- Single electron transfer (SET) mechanism
- Polar nucleophilic mechanism

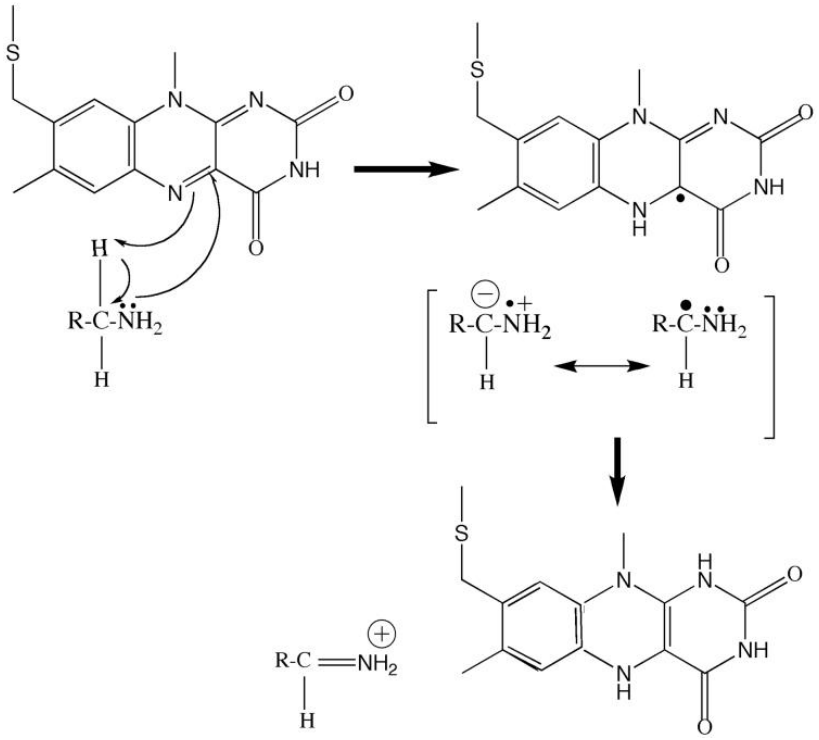

Figure 2.22: Single electron transfer (SET) mechanism for MAO catalysis (Edmondson *et al*., 2007).

The single electron transfer (SET) mechanism (Figure 2.22) was proposed by Silverman and co-workers in 1980. The rationale of this mechanism is the acidification of the α-CH bond through the oxidation of the substrate amine nitrogen, allowing abstraction. The mechanism consists of two one-electron transfers from the substrate to the flavin. An amine radical cation and a flavin radical are formed in the first step of the mechanism. One-electron oxidation of the lone pair on the amine nitrogen causes the α-protons of the amine to be more acidic. An active site base is proposed to abstract one of these α-protons. The second one-electron transfer takes place forming the iminium ion and the reduced flavin (Silverman *et al*., 1980).

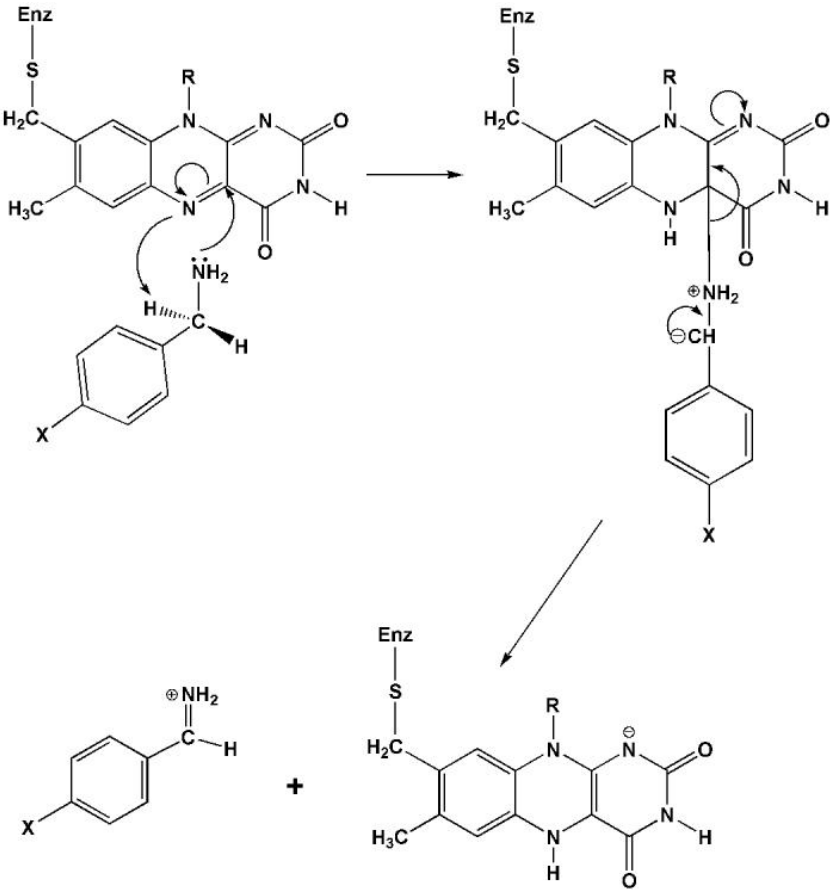

Figure 2.23: Polar nucleophilic mechanism for MAO catalysis. The products of amine oxidation are the protonated imine and the flavin hydroquinone (Edmondson *et al*., 2007).

The polar nucleophilic mechanism (Figure 2.23) was first proposed by Miller & Edmondson (1999). In this mechanism the deprotonated amine nucleophilically attacks the flavin at the C(4a)-position resulting in a flavin-substrate adduct. With formation of the flavin-substrate adduct, the N(5)-position of the flavin becomes a very strong base, with a pKa in the range of 25-27, thus exhibiting sufficient basicity for the α-pro-R-H abstraction from the substrate (Edmondson *et al*., 2004b). In the last step, the imine product is released with the formation of the reduced flavin.

2.2.9 Three dimensional structure of MAO-B

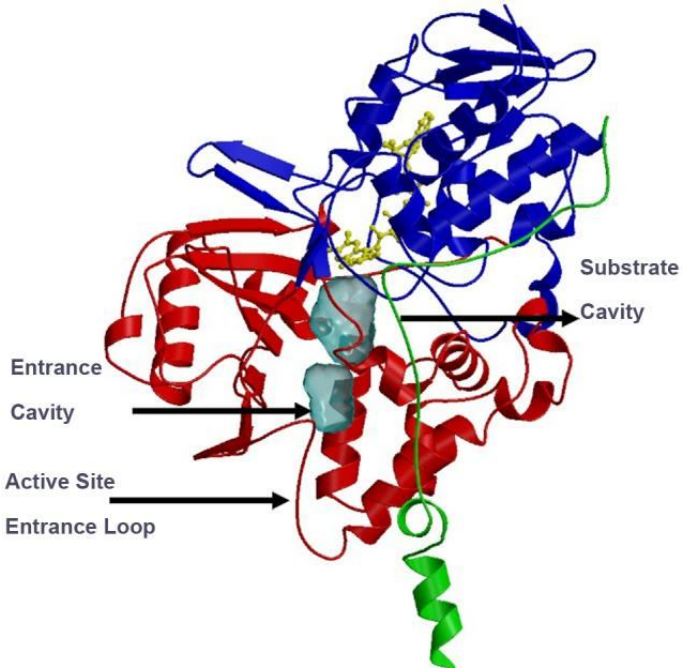

Figure 2.24: Three dimensional structure of human MAO-B. The ball and stick model in yellow represents the covalent flavin moiety. The blue represents the flavin binding domain. The red is the substrate domain. The green represents the membrane binding domain (Edmondson *et al*., 2007).

Human MAO-B crystallises as a dimer. A substrate molecule must first negotiate a protein loop at the entrance to one of two cavities before it will reach the flavin coenzyme. The two cavities include the "entrance cavity" and the "substrate/active site cavity" and they are separated by the side chain of Ile199. This residue thus serves as a "gate" between the two cavities. The "entrance cavity" is hydrophobic with a volume of 290 $Å^3$. The "substrate cavity" is similarly hydrophobic with a volume of 390 $Å^3$. The FAD coenzyme is covalently bound via an 8α-thioether linkage to Cys397 at the end of the substrate cavity (Edmondson *et al*., 2007). The *re*-face of the FAD coenzyme is approached by the amine functional group of the substrate molecule through an "aromatic cage". The aromatic cage consists of two tyrosine residues which are perpendicular to the plane of the flavin ring. The "aromatic cage" is formed by Tyr398 and Tyr435 (Binda *et al*., 2003).

2.2.10 Three dimensional structure of MAO-A

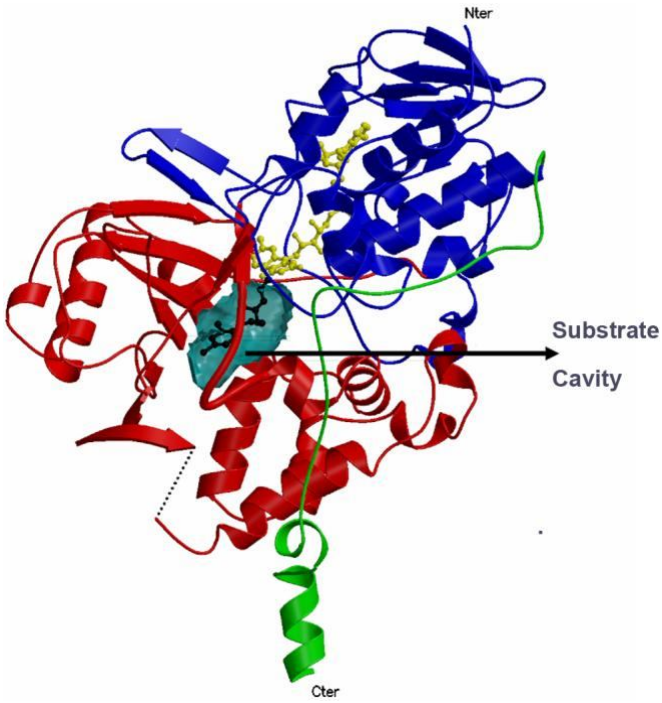

Figure 2.25: Three dimensional structure of human MAO-A. The colouring is similar to those in figure 2.24 (Edmondson *et al*., 2007).

Human MAO-A crystallises as a monomer. In contrast to human MAO-B, both human and rat MAO-A only have single substrate binding cavities with protein loops at the entrances of either cavities. Similar to MAO-B, human MAO-A is also hydrophobic, with a volume of 550 $Å^3$. The covalent attachment of the FAD cofactor in MAO-A and the tyrosines which forms the "aromatic cage" in the active sites, are identical to those of MAO-B (Edmondson *et al*., 2007; De Colibus *et al*., 2005).

2.2.11 *In vitro* measurements of MAO activity

Measuring MAO activity may be done by several methods. Determining MAO activity is important for pharmacological studies. Below are given some examples of methods used to determine MAO activity.

- Use an oxygen sensitive electrode to detect oxygen consumption by MAO (Averill-Bates *et al*., 1993).
- Measure the absorbance of H_2O_2 at a wavelength of 230 nm to detect H_2O_2 formed during catalysis (Stevanato *et al*., 1995).
- The detection of absorbance or fluorescence of the oxidised monoamine product (Zhou *et al*., 1996).

- The MAO enzyme generates H_2O_2, which may be detected with a horseradish peroxidase coupled reaction system. H_2O_2-sensitive probes are used to detect the H_2O_2 (Morpurgo *et al*., 1989). N-Acetyl-3,7-dihydroxyphenoxazine (Amplex Red), which is a highly sensitive H_2O_2 probe, is used to measure H_2O_2 in a horseradish peroxidase-coupled reaction. H_2O_2 oxidises Amplex Red to a fluorescent dye, resorufin. Resorufin has an absorption and emission wavelength maximum of >560 nm (Zhou & Panchuk-Voloshina, 1997)
- Kynuramine will undergo oxidative deamination by MAO to yield 4-hydroxyquinoline. A spectrofluorometer is used to determine the concentration of 4-hydroxyquinoline, at an excitation wavelength of 310 nm and an emission wavelength of 400 nm (Weissbach *et al*., 1960). In this study, this method will be used to measure MAO catalytic activities.

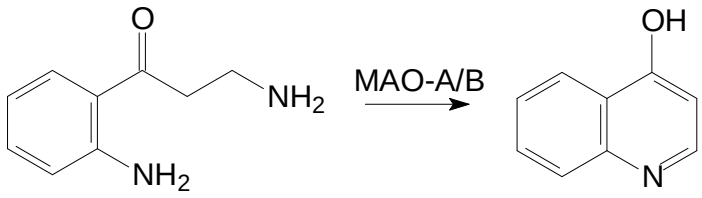

Figure 2.26: Kynuramine is oxidatively deaminated by MAO to yield 4-hydroxyquinoline

2.2.12 Enzyme kinetics

In this study novel synthetic compounds will be evaluated as potential MAO inhibitors. In order to interpret the inhibitory potencies of the compounds, a short overview of the basics of enzyme kinetics will be provided below.

$$E + S \leftrightarrow ES \leftrightarrow EP \rightarrow P + E$$

Equation 1

Equation 1 illustrates the theory that the reaction between an enzyme (E) and its substrate (S) will reach equilibrium. The ES complex will then give rise to the formation of an enzyme-product complex before the product is released (Lineweaver & Burk, 1934). Enzyme kinetics is crucial in determining the potency of inhibitors.

$$K_d = \frac{k_{-1}}{k_1}$$

Equation 2

Equation 2 illustrates the dissociation constant $K_{d,}$ for the dissociation of the ES product. The inverse of K_d is the affinity of an enzyme for its substrate. The dissociation constant, under certain conditions, approximates the Michaelis constant (K_m).

$$v_i = \frac{(V_{max} \times S)}{(K_m + S)}$$

Equation 3: Michaelis-Menten equation.

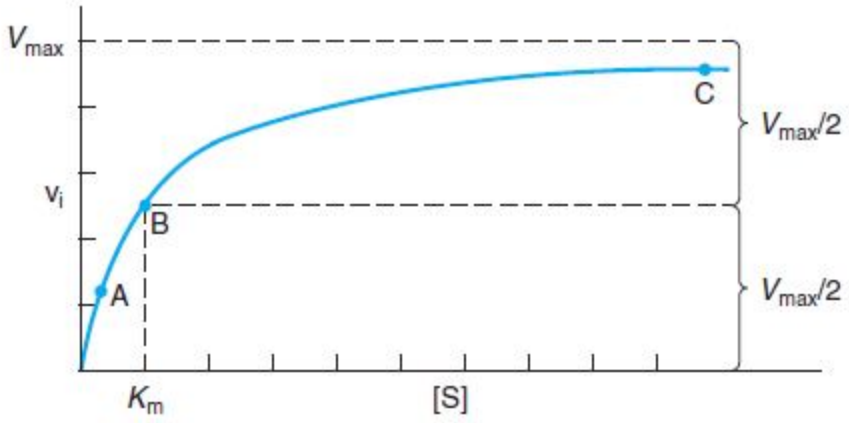

Figure 2.27: Illustration of a Michaelis-Menton graph.

Equation 3 illustrates the initial reaction velocity. When the initial velocity (v_i) is at half maximum velocity (V_{max}) the Michaelis constant (K_m) is defined as the substrate concentration. Equation 3 may be manipulated into the equation of a straight line (y = mx + c) resulting in equation 4.

$$\frac{1}{v_i} = \left(\frac{K_m}{V_{max}}\right)\frac{1}{[S]} + \frac{1}{V_{max}}$$

Equation 4

The calculation of K_m and V_{max} may be difficult as it requires an extremely high concentration of substrate and achieving saturating conditions. Manipulation of the Michaelis-Menten equation to a linear form could resolve this difficulty, according to Lineweaver and Burk (1934). The plot illustrated in figure 2.28 may be used to determine V_{max} and K_m, this can be done by setting the y term to 0 and solving the x (Murray *et al.*, 2003)

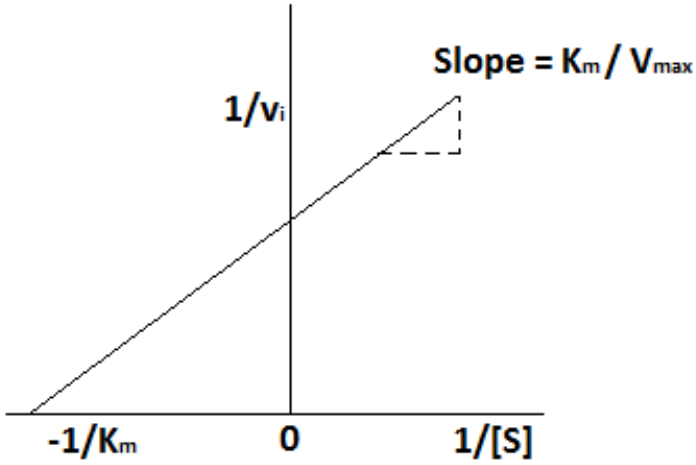

Figure 2.28: A Lineweaver-Burk plot. The Y-axis is equal to $1/v_i$, the X-axis is equal to 1/[S] and the x intercept is equal to $-1/K_m$.

Competitive and non-competitive inhibitors can be distinguished by Lineweaver-Burk plots. Lineweaver-Burk plots may also be used to evaluate the inhibitor constant K_i. By using the K_i values the potencies of inhibitors for the same enzyme can be determined. A lower K_i value illustrates a more potent inhibitor.

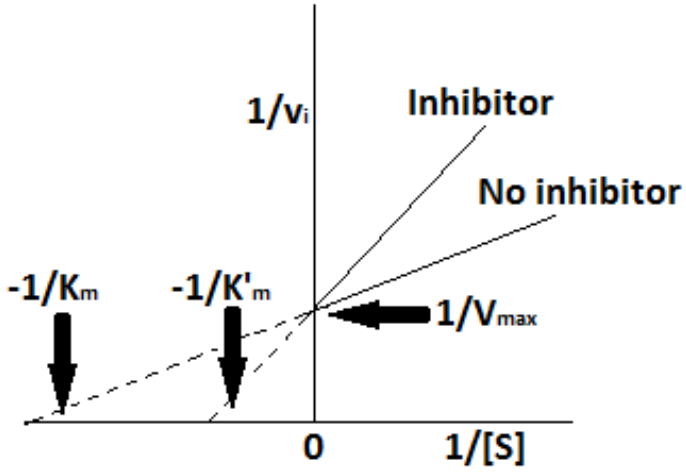

Figure 2.29: A Lineweaver-Burk plot of competitive inhibition. The y intercept is equal to $1/V_{max}$ and the x intercept is equal to $-1/K_m$ and $-1/K'_m$, for no inhibitor and inhibitor, respectively.

For competitive inhibition (Figure 2.29) V_{max} is independent of inhibitor presence whereas the x intercept varies with inhibitor concentrations. For non-competitive inhibition (Figure 2.30) the Lineweaver-Burk plots show a constant apparent K_m value, while V_{max} is decreased (Murray *et al.*, 2003). The equation illustrated in equation 5 can be used to calculate the x intercept as well as the K_i value of the inhibitor for figure 2.29.

$$x = \frac{-1}{K_m}\left(1 + \frac{[I]}{K_i}\right)$$

Equation 5

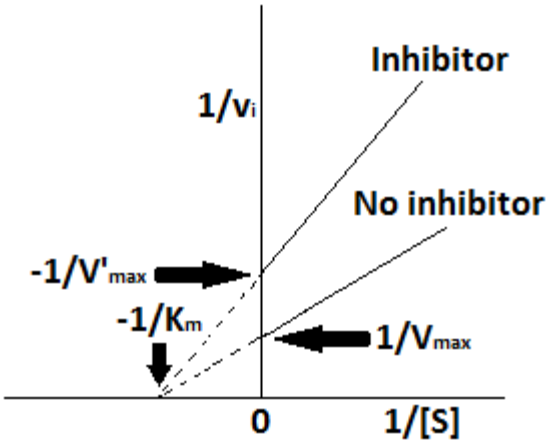

Figure 2.30: A Lineweaver-Burk plot of noncompetitive inhibition. The x intercept is constant and equal to -1/K_m and the y intercept are equal to 1/V'$_{max}$ and 1/V_{max} for no inhibitor and inhibitor, respectively.

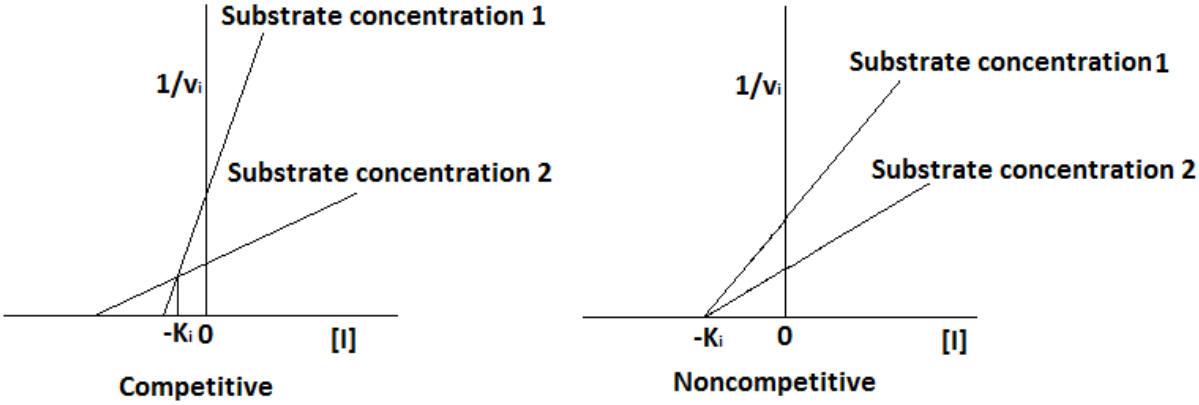

Figure 2.31: Dixon's method for determining the K_i values for competitive inhibition (left) and non-competitive inhibition (right).

In 1953 an article was published by Dixon, describing a more convenient way to determine the K_i value of an inhibitor. As illustrated in figure 2.31, $1/v_i$ is plotted versus the inhibitor concentration at constant substrate concentration. Two substrate concentrations are used, thus two straight lines will cross to the left of the y axis. The x value at the cross point is equal to K_i.

Another way of expressing inhibitor potency is the IC_{50} value. The IC_{50} value is the concentration of an inhibitor that is required for 50% inhibition of the substrate *in vitro*. Figure 2.32 shows how the IC_{50} value may be obtained from a plot of enzyme activity versus the logarithm of the inhibitor concentration. The relationship between the K_i value and the IC_{50} value (Equation 6) was described by Cheng & Prusoff (1973).

$$IC_{50} = K_i(1 + \frac{[S]}{K_m})$$

Equation 6

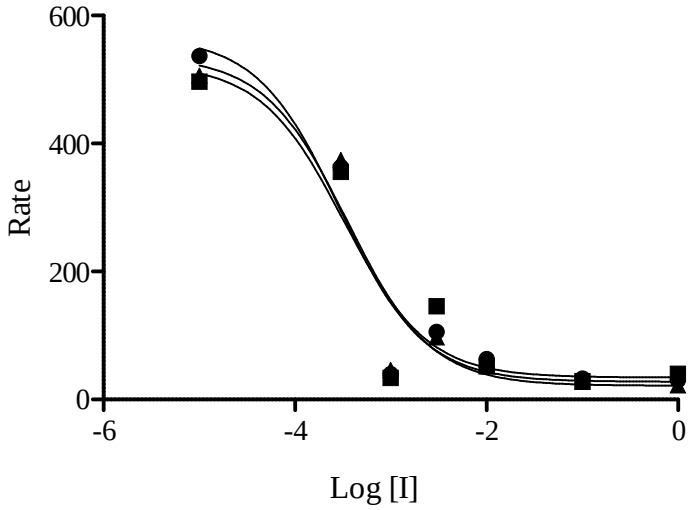

Figure 2.32: The sigmoidal concentration-inhibition curve that may be used to estimate IC_{50} values.

2.2.13 Conclusion

In this chapter, the neurodegenerative disorder, PD, is discussed including the mechanisms of neurodegeneration associated with PD and symptomatic treatment strategies. Although PD is an incurable disease, the symptoms may be treated following a variety of pharmacological approaches. One strategy for treating the symptoms of PD is with MAO-B inhibitors. MAO-B catalyses the oxidative deamination of DA in the brain and this is thought to enhance the depletion of DA stores in PD. MAO-B inhibitors are considered to be a useful treatment strategy of PD since these drugs prevent the central degradation of dopamine and thus may conserve the dopamine supply in the brain. In addition, MAO-B inhibitors may also elevate dopamine levels which are derived from administered levodapa. For this reason, MAO-B inhibitors may be used in conjunction with levodopa therapy. As shown in the next chapter, it is anticipated that the quinolinone derivatives that will be synthesised in this study, will possess MAO-B inhibitory activity, based on the structural similarity with coumarin derived MAO inhibitors.

CHAPTER 3
SYNTHESIS

3.1 Introduction

In this study, a series of 3,4-dihydro-2(1*H*)-quinolinone derivatives will be synthesized and investigated as MAO-A and MAO-B inhibitors. The structures of the quinolinones that will be synthesised are shown in Table 3.1. As shown in the table, 3,4-dihydro-2(1*H*)-quinolinones will firstly be substituted with the benzyloxy side chain on the C6 and C7 positions (to yield compounds **4a** and **5a)**. The benzyloxy phenyl rings will further be substituted on the meta positions with chlorine (to yield structures **4b** and **5b**) and bromine (to yield structures **4c** and **5c**). The quinolinone derivatives will also contain the phenylethoxy substituent (to yield structures **4d** and **5d**) and phenylpropoxy substituent (to yield structures **4e** and **5e**) on the C6 and C7 positions. In total 10 quinolinone derivatives will be synthesized. It is anticipated that the following structure-activity relationships may be determined:

- The effect that halogen (Cl and Br) substituents on the phenyl ring of the benzyloxy moiety will have on the MAO inhibition potencies of the 3,4-dihydro-2(1*H*)-quinolinone derivatives.

- The effect that benzyloxy, phenylethoxy and phenylpropoxy moieties at C6 and C7 of 3,4-dihydro-2(1*H*)-quinolinones will have on the inhibition potencies of the quinolinone derivatives. For this purpose, 6-hydroxy-3,4-dihydro-2(1H)-quinolinone and 7-hydroxy-3,4-dihydro-2(1H)-quinolinone will also be evaluated as MAO inhibitors.

- The inhibition potencies of the phenylethoxy and phenylpropoxy substituted 3,4-dihydro-2(1*H*)-quinolinones will be compared to those of the 3,4-dihydro-2(1*H*)-quinolinones substituted with the benzyloxy side chain on C6 and C7.

- The MAO inhibitory potencies of the 3,4-dihydro-2(1*H*)-quinolinones substituted on C6 will be compared to the MAO inhibitory potencies of the quinolinones substituted on C7.

The current study will thus attempt to discover novel highly potent MAO-A and MAO-B inhibitors by using the 3,4-dihydro-2(1*H*)-quinolinone structure as scaffold.

Table 3.1: The series of C6- and C7-substituted 3,4-dihydro-2(1*H*)-quinolinones that will be synthesized in this study.

4a 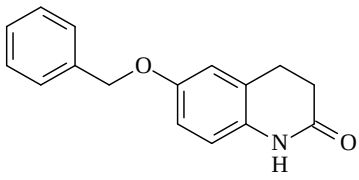	**5a** 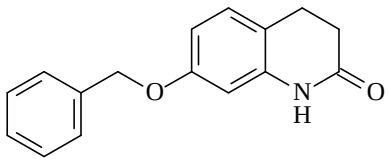
4b 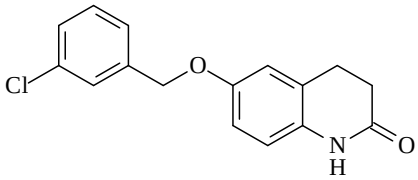	**5b** 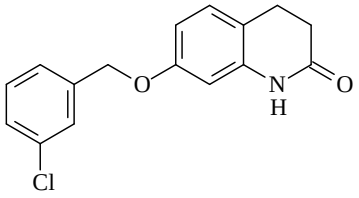
4c 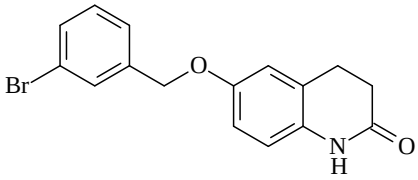	**5c** 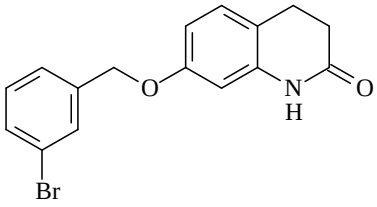
4d 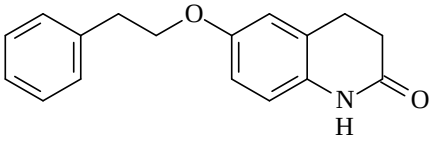	**5d** 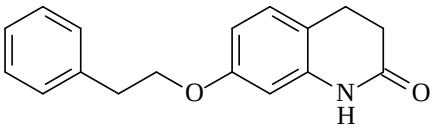
4e 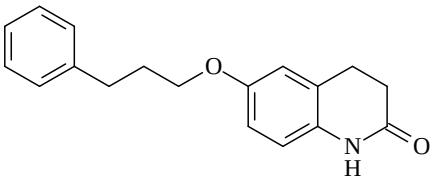	**5e** 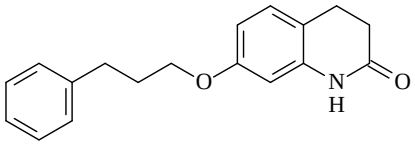

3.2 General approach for the synthesis of the 3,4-dihydro-2(1*H*)-quinolinone derivatives

The C6- and C7-substituted 3,4-dihydro-2(1*H*)-quinolinone derivatives **4** and **5** will be synthesized according to the literature procedure (Figure 3.1) (Shigematsu, 1961). Commercially available 6-hydroxy-3,4-dihydro-2(1*H*)-quinolinone (**6**) and 7-hydroxy-3,4-dihydro-2(1*H*)-quinolinone (**7**) will be suspended in ethanol, and will be treated with an appropriately substituted alkyl bromide in the presence of KOH. After heating the mixture at reflux for 5 h, the reaction mixture will be poured into aqueous NaOH (1%). The crude thus obtained will be purified by recrystallization and the structures of the target compounds will be verified by ^{1}H NMR, ^{13}C NMR and mass spectrometry.

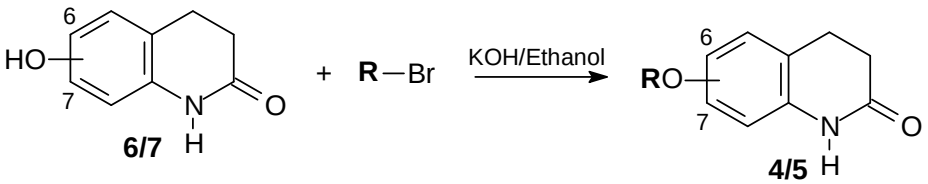

Figure 3.1: The general synthetic route to C6- and C7-substituted 3,4-dihydro-2(1*H*)-quinolinone derivatives.

3.3 Materials and instrumentation

Materials: All the reagents and solvents used in this study were obtained from Sigma-Aldrich.

Thin layer chromatography (TLC): TLC was used to determine whether the reactions were complete, before terminating the synthesis. Silica gel 60 (Merck) TLC sheets with UV254 fluorescent indicator were employed with a mobile phase consisting of 100% ethyl acetate. Using an UV-lamp the developed TLC sheets were observed at a wavelength of 254 nm.

Melting points: A Buchi M-545 melting point apparatus was used to determine the melting points of all the synthesised compounds. All melting points are uncorrected.

Mass spectra: High resolution mass spectra (HRMS) were recorded on a Bruker micrOTOF-Q II mass spectrometer in atmospheric-pressure chemical ionization (APCI) mode.

Nuclear magnetic resonance (NMR): Proton (^{1}H) and carbon (^{13}C) NMR spectra were recorded on a Bruker Avance III 600 spectrometer. ^{1}H NMR spectra were recorded at 600 MHz and ^{13}C NMR at 150 MHz. The chemical shifts are reported in parts per million (δ) downfield from the signal of tetramethylsilane added to the deuterated solvent. Spin multiplicities are given as s (singlet), d (doublet), dd (doublet of doublets), t (triplet), qn (quintet) or m (multiplet). The coupling constants (J) are expressed in Hertz (Hz).

3.4 Synthesis of 3,4-dihydro-2(1*H*)-quinolinone derivatives (4 and 5)

Commercially available 6-hydroxy-3,4-dihydro-2(1*H*)-quinolinone (**6**) or 7-hydroxy-3,4-dihydro-2(1*H*)-quinolinone (**7**) (1.50 mmol) was suspended in ethanol (6 ml) containing KOH (1.66 mmol). The reaction was treated with an appropriately substituted alkyl bromide (1.50 mmol) and heated at reflux for 5 h. The reaction progress was monitored using silica gel TLC with ethyl acetate as mobile phase. Upon completion, the reaction was poured into aqueous NaOH (1%) and the resulting precipitate was collected by filtration. The crude thus obtained was purified by recrystallization from ethanol.

3.5 Results

The NMR spectra of the synthesised 3,4-dihydro-2(1*H*)-quinolinone derivatives are given in appendix A. The structures of the 3,4-dihydro-2(1*H*)-quinolinones synthesized are given below and correlated with the ^{1}H NMR and ^{13}C NMR data. As shown below, the appropriate ^{1}H NMR and ^{13}C NMR signals were observed for each compound. Based on the NMR data, it may thus be concluded that the structures of the target C6- and C7-substituted 3,4-dihydro-2(1*H*)-quinolinone derivatives are those proposed in this dissertation.

4a. 6-(Benzyloxy)-3,4-dihydro-2(*1H*)-quinolinone

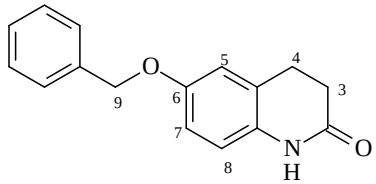

The title compound was prepared in a yield of 32%: mp 161.5–164.6 °C (ethanol). ^{1}H NMR (Bruker Avance III 600, $CDCl_3$) δ 2.60 (t, 2H, J = 7.9 Hz), 2.91 (t, 2H, J = 7.9 Hz), 5.01 (s, 2H), 6.77–6.79 (m, 3H), 7.31 (t, 1H, J = 7.1 Hz), 7.37 (t, 2H, J = 7.2 Hz), 7.40–7.41 (m, 2H), 9.43 (s, 1H); ^{13}C NMR (Bruker Avance III 600, $CDCl_3$) δ 25.6, 30.5, 70.3, 113.4, 114.7, 116.3, 124.9, 127.4, 127.9, 128.5, 131.1, 136.9, 154.6, 171.9; APCI-HRMS *m*/*z*: calcd for $C_{16}H_{16}NO_2$ (MH^+), 254.1181, found 254.1174.

^{1}H NMR:

- The NH proton corresponds to the singlet at 9.43 ppm (The signal integrates for 1 proton).
- The ethylene protons at C3 and C4 correspond to the triplets at 2.60 ppm and 2.91 ppm (The signals integrate for 2 protons each).
- The CH_2 protons at C9 correspond to the singlet at 5.01 ppm (The signal integrates for 2 protons).
- The 8 aromatic protons correspond to the signals at 6.77–6.79 ppm (m), 7.31 ppm (t), 7.37 ppm (t) and 7.40–7.41ppm (m) (These signals integrate for 8 protons).

^{13}C NMR:

- The aliphatic carbons at C3, C4 and C9 are represented by the signals at 25.6 ppm, 30.5 ppm and 70.3 ppm.
- The carbonyl carbon at C2 is represented by the signal at 171.9 ppm.
- The aromatic carbons are represented by the signals at 113.4, 114.7, 116.3, 124.9, 127.4, 127.9, 128.5, 131.1, 136.9 and 154.6 ppm.

4b. 6-(3-Chlorobenzyloxy)-3,4-dihydro-2(1*H*)-quinolinone

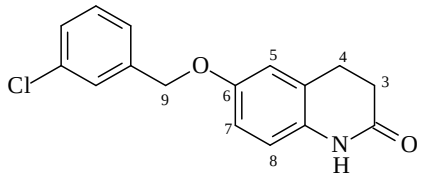

The title compound was prepared in a yield of 42%: mp 156.1–161.4 °C (ethanol). ^{1}H NMR (Bruker Avance III 600, $CDCl_3$) δ 2.59 (t, 2H, J = 7.9 Hz), 2.91 (t, 2H, J = 7.9 Hz), 4.97 (s, 2H), 6.73–6.77 (m, 3H), 7.26–7.30 (m, 3H), 7.40 (s, 1H), 9.33 (s, 1H); ^{13}C NMR (Bruker Avance III 600, $CDCl_3$) δ 25.6, 30.5, 69.5, 113.4, 114.8, 116.3, 125.0, 125.3, 127.3, 128.0, 129.8, 131.3, 134.4, 139.0, 154.3, 171.9; APCI-HRMS *m*/*z*: calcd for $C_{16}H_{15}ClNO_2$ (MH^+), 288.0791, found 288.0765.

^{1}H NMR:

- The NH proton corresponds to the singlet at 9.33 ppm (The signal integrates for 1 proton).
- The ethylene protons at C3 and C4 correspond to the triplets at 2.59 ppm and 2.91 ppm (The signals integrate for 2 protons each).
- The CH_2 protons at C9 correspond to the singlet at 4.97 ppm (The signal integrates for 2 protons).
- The 7 aromatic protons correspond to the signals at 6.73–6.77 ppm (m), 7.26–7.30 ppm (m) and 7.40 ppm (s) (These signals integrate for 7 protons).

^{13}C NMR:

- The aliphatic carbons at C3, C4 and C9 are represented by the signals at 25.6 ppm, 30.5 ppm and 69.5 ppm.
- The carbonyl carbon at C2 is represented by the signal at 171.9 ppm.
- The aromatic carbons are represented by the signals at 113.4, 114.8, 116.3, 125.0, 125.3, 127.3, 128.0, 129.8, 131.3, 134.4, 139.0 and 154.3 ppm.

4c. 6-(3-Bromobenzyloxy)-3,4-dihydro-2(1*H*)-quinolinone

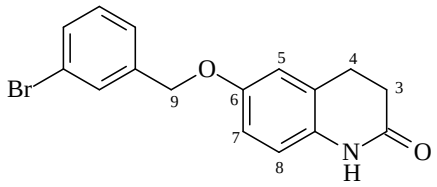

The title compound was prepared in a yield of 98%: mp 104.3–132.8 °C (ethanol). ^{1}H NMR (Bruker Avance III 600, DMSO-d6) δ 2.38 (t, 2H, J = 7.9 Hz), 2.81 (t, 2H, J = 7.9 Hz), 5.03 (s, 2H), 6.75–6.80 (m, 2H), 6.86 (s, 1H), 7.33 (t, 1H, J = 7.9 Hz), 7.41 (d, 1H, J = 7.9 Hz), 7.50 (d, 1H, J = 7.9 Hz), 7.61 (s, 1H), 9.93 (s, 1H); ^{13}C NMR (Bruker Avance III 600, DMSO-d6) δ 25.1, 30.3, 68.5, 113.3, 114.5, 115.8, 121.7, 125.0, 126.5, 130.1, 130.6, 130.7, 132.1, 140.2, 153.3, 169.9; APCI-HRMS *m*/*z*: calcd for $C_{16}H_{15}BrNO_2$ (MH^+), 332.0286, found 332.0250.

^{1}H NMR:

- The NH proton corresponds to the singlet at 9.93 ppm (The signal integrates for 1 proton).
- The ethylene protons at C3 and C4 correspond to the triplets at 2.38 ppm and 2.81 ppm (The signals integrate for 2 protons each).
- The CH_2 protons at C9 correspond to the singlet at 5.03 ppm (The signal integrates for 2 protons).
- The 7 aromatic protons correspond to the signals at 6.75–6.80 ppm (m), 6.86 ppm (s), 7.33 ppm (t), 7.41 ppm (d). 7.50 ppm (d) and 7.61 ppm (s) (These signals integrate for 7 protons).

^{13}C NMR:

- The aliphatic carbons at C3, C4 and C9 are represented by the signals at 25.1 ppm, 30.3 ppm and 68.5 ppm.
- The carbonyl carbon at C2 is represented by the signal at 169.9 ppm.
- The aromatic carbons are represented by the signals at 113.3, 114.5, 115.8, 121.7, 125.0, 126.5, 130.1, 130.6, 130.7, 132.1, 140.2 and 153.3 ppm.

4d. 6-(2-Phenylethoxy)-3,4-dihydro-2(1*H*)-quinolinone

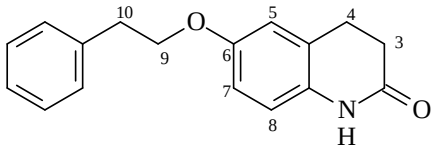

The title compound was prepared in a yield of 21%: mp 119.5 °C (ethanol). ^{1}H NMR (Bruker Avance III 600, $CDCl_3$) δ 2.52 (t, 2H, J = 7.9 Hz), 2.83 (t, 2H, J = 7.9 Hz), 3.00 (t, 2H, J = 7.2 Hz), 4.05 (t, 2H, J = 7.2 Hz), 6.62–6.63 (m, 2H), 6.67 (d, 1H, J = 7.9 Hz), 7.16 (t, 1H, J = 7.2 Hz), 7.20 (d, 2H, J = 7.5 Hz), 7.24 (t, 2H, J = 7.5 Hz), 9.16 (s, 1H); ^{13}C NMR (Bruker Avance III 600, $CDCl_3$) δ 25.6, 30.5, 35.8, 69.1, 113.1, 114.5, 116.3, 124.9, 126.5, 128.4, 128.9, 130.9, 138.1, 154.7, 171.8; APCI-HRMS *m*/*z*: calcd for $C_{17}H_{18}NO_2$ (MH^+), 268.1338, found 268.1322.

^{1}H NMR:

- The NH proton corresponds to the singlet at 9.16 ppm (The signal integrates for 1 proton).
- The ethylene protons at C3 and C4 correspond to the triplets at 2.52 ppm and 2.83 ppm (The signals integrate for 2 protons each).
- The CH_2 protons at C9 correspond to the triplet at 4.05 ppm (The signal integrates for 2 protons).
- The CH_2 protons at C10 correspond to the triplet at 3.00 ppm (The signal integrates for 2 protons)
- The 8 aromatic protons correspond to the signals at 6.62–6.63 ppm (m), 6.67 ppm (d), 7.16 ppm (t), 7.20 ppm (d) and 7.24 ppm (t) (These signals integrate for 8 protons).

^{13}C NMR:

- The aliphatic carbons at C3, C4, C9 and C10 are represented by the signals at 25.6 ppm, 30.5 ppm, 35.8 ppm and 69.1 ppm.
- The carbonyl carbon at C2 is represented by the signal at 171.8 ppm.
- The aromatic carbons are represented by the signals at 113.1, 114.5, 116.3, 124.9, 126.5, 128.4, 128.9, 130.9, 138.1 and 154.7 ppm.

4e. 6-(3-Phenylpropoxy)-3,4-dihydro-2(1*H*)-quinolinone

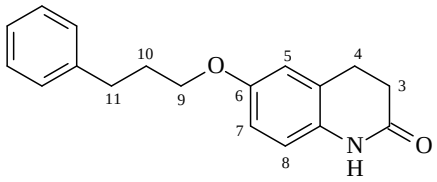

The title compound was prepared in a yield of 58%: mp 123.0–127.4 °C (ethanol). ^{1}H NMR (Bruker Avance III 600, $CDCl_3$) δ 2.07 (qn, 2H, J = 6.40 Hz), 2.60 (t, 2H, J = 7.5 Hz), 2.79 (t, 2H, J = 7.5 Hz), 2.90 (t, 2H, J = 7.9 Hz), 3.90 (t, 2H, J = 6.4 Hz), 6.68–6.70 (m, 2H), 6.76 (d, 1H, J = 8.6 Hz), 7.17–7.20 (m, 3H), 7.28 (t, 2H, J = 7.5 Hz), 9.28 (s, 1H); ^{13}C NMR (Bruker Avance III 600, $CDCl_3$) δ 25.6, 30.5, 30.8, 32.0, 67.2, 113.1, 114.4, 116.3, 124.9, 125.9, 128.4, 128.5, 130.7, 141.4, 154.9, 171.9; APCI-HRMS *m*/*z*: calcd for $C_{18}H_{20}NO_2$ (MH^+), 282.1494, found 282.1479.

^{1}H NMR:

- The NH proton corresponds to the singlet at 9.28 ppm (The signal integrates for 1 proton).
- The ethylene protons at C3 and C4 correspond to the triplets at 2.60 ppm and 2.79 ppm (The signals integrate for 2 protons each).
- The CH_2 protons at C9 and C11 correspond to the triplets at 2.90 ppm and 3.90 ppm (The signals integrate for 2 protons each).
- The CH_2 protons at C10 correspond to the quintet at 2.07 ppm (The signal integrates for 2 protons)
- The 8 aromatic protons correspond to the signals at 6.68–6.70 ppm (m), 6.76 ppm (d), 7.17–7.20 ppm (m) and 7.28 ppm (t) (These signals integrate for 8 protons).

^{13}C NMR:

- The aliphatic carbons at C3, C4, C9, C10 and C11 are represented by the signals at 25.6 ppm, 30.5 ppm, 30.8 ppm, 32.0 ppm and 67.2 ppm.
- The carbonyl carbon at C2 is represented by the signal at 171.9 ppm.
- The aromatic carbons are represented by the signals at 113.1, 114.4, 116.3, 124.9, 125.9, 128.4, 128.5, 130.7, 141.4 and 154.9 ppm.

5a. 7-(Benzyloxy)-3,4-dihydro-2(1*H*)-quinolinone

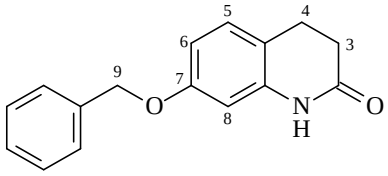

The title compound was prepared in a yield of 57%: mp 153.3–153.6 °C (ethanol). ^{1}H NMR (Bruker Avance III 600, $CDCl_3$) δ 2.61 (t, 2H, J = 7.2 Hz), 2.87 (t, 2H, J = 7.2 Hz), 5.01 (s, 2H), 6.50 (d, 1H, J = 2.3 Hz), 6.58 (dd, 1H, J = 2.3, 8.3 Hz), 7.02 (d, 1H, J = 8.3 Hz), 7.30–7.31 (m, 1H), 7.37 (t, 2H, J = 7.5 Hz), 7.40–7.41 (m, 2H), 9.22 (s, 1H); ^{13}C NMR (Bruker Avance III 600, $CDCl_3$) δ 24.5, 30.9, 70.1, 102.6, 109.0, 116.0, 127.4, 127.9, 128.5, 128.5, 136.7, 138.2, 158.3, 172.4; APCI-HRMS *m*/*z*: calcd for $C_{16}H_{16}NO_2$ (MH^+), 254.1181, found 254.1177.

^{1}H NMR:

- The NH proton corresponds to the singlet at 9.22 ppm (The signal integrates for 1 proton).
- The ethylene protons at C3 and C4 correspond to the triplets at 2.61 ppm and 2.87 ppm (The signals integrate for 2 protons each).
- The CH_2 protons at C9 correspond to the singlet at 5.01 ppm (The signal integrates for 2 protons).
- The 8 aromatic protons correspond to the signals at 6.50 ppm (d), 6.58 ppm (dd), 7.02 ppm (d), 7.30–7.31 ppm (m), 7.37 ppm (t) and 7.40–7.41 ppm (m) (These signals integrate for 8 protons).
- Based on the coupling constants, the doublet at 6.50 ppm represents the proton at C8, the doublet of doublets at 6.58 ppm represents the proton at C6 and the doublet at 7.02 ppm represents the proton at C5.

^{13}C NMR:

- The aliphatic carbons at C3, C4 and C9 are represented by the signals at 24.5 ppm, 30.9 ppm and 70.1 ppm.
- The carbonyl carbon at C2 is represented by the signal at 172.4 ppm.
- The aromatic carbons are represented by the signals at 102.6, 109.0, 116.0, 127.4, 127.9, 128.5, 128.5, 136.7, 138.2 and 158.3 ppm.

5b. 7-(3-Chlorobenzyloxy)-3,4-dihydro-2(1*H*)-quinolinone

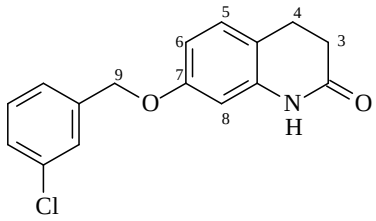

The title compound was prepared in a yield of 32%: mp 149.4–151.6 °C (ethanol). ^{1}H NMR (Bruker Avance III 600, $CDCl_3$) δ 2.65 (t, 2H, J = 7.5 Hz), 2.92 (t, 2H, J = 7.5 Hz), 5.02 (s, 2H), 6.53 (d, 1H, J = 2.6 Hz), 6.60 (dd, 1H, J = 2.6, 8.3 Hz), 7.07 (d, 1H, J = 8.3 Hz), 7.32 (m, 3H), 7.45 (s, 1H), 9.36 (s, 1H); ^{13}C NMR (Bruker Avance III 600, $CDCl_3$) δ 24.5, 30.9, 69.2, 102.6, 108.9, 116.2, 125.3, 127.4, 128.1, 128.6, 129.8, 134.4, 138.3, 138.8, 158.0, 172.5; APCI-HRMS *m*/*z*: calcd for $C_{16}H_{15}ClNO_2$ (MH^+), 288.0791, found 288.0765.

^{1}H NMR:

- The NH proton corresponds to the singlet at 9.36 ppm (The signal integrates for 1 proton).
- The ethylene protons at C3 and C4 correspond to the triplets at 2.65 ppm and 2.92 ppm (The signals integrate for 2 protons each).
- The CH_2 protons at C9 correspond to the singlet at 5.02 ppm (The signal integrates for 2 protons).
- The 7 aromatic protons correspond to the signals at 6.53 ppm (d), 6.60 ppm (dd), 7.07 ppm (d), 7.32 ppm (m) and 7.45 ppm (s) (These signals integrate for 7 protons).
- Based on the coupling constants, the doublet at 6.53 ppm represents the proton at C8, the doublet of doublets at 6.60 ppm represents the proton at C6 and the doublet at 7.07 ppm represents the proton at C5.

^{13}C NMR:

- The aliphatic carbons at C3, C4 and C9 are represented by the signals at 24.5 ppm, 30.9 ppm and 69.2 ppm.
- The carbonyl carbon at C2 is represented by the signal at 172.5 ppm.
- The aromatic carbons are represented by the signals at 102.6, 108.9, 116.2, 125.3, 127.4, 128.1, 128.6, 129.8, 134.4, 138.3, 138.8 and 158.0 ppm.

5c. 7-(3-Bromobenzyloxy)-3,4-dihydro-2(1*H*)-quinolinone

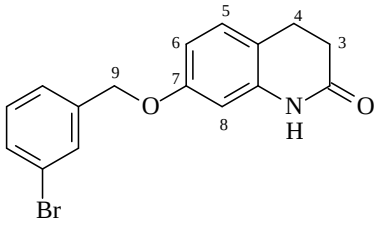

The title compound was prepared in a yield of 76%: mp 145.9–146.5 °C (ethanol). ^{1}H NMR (Bruker Avance III 600, $CDCl_3$) δ 2.54 (t, 2H, J = 7.9 Hz), 2.81 (t, 2H, J = 7.9 Hz), 4.91 (s, 2H), 6.41 (d, 1H, J = 2.6 Hz), 6.49 (dd, 1H, J = 2.3, 8.3 Hz), 6.96 (d, 1H, J = 8.3 Hz), 7.16 (t, 1H, J = 7.9 Hz), 7.25 (d, 1H, J = 7.9 Hz), 7.36 (d, 1H, J = 7.9 Hz), 7.50 (s, 1H), 9.19 (s, 1H); ^{13}C NMR (Bruker Avance III 600, $CDCl_3$) δ 24.5, 30.9, 69.1, 102.6, 108.9, 116.3, 122.6, 125.8, 128.6, 130.1, 130.3, 131.0, 138.3, 139.1, 158.0, 172.4; APCI-HRMS *m*/*z*: calcd for $C_{16}H_{15}BrNO_2$ (MH^+), 332.0286, found 332.0254.

^{1}H NMR:

- The NH proton corresponds to the singlet at 9.19 ppm (The signal integrates for 1 proton).
- The ethylene protons at C3 and C4 correspond to the triplets at 2.54 ppm and 2.81 ppm (The signals integrate for 2 protons each).
- The CH_2 protons at C9 correspond to the singlet at 4.91 ppm (The signal integrates for 2 protons).
- The 7 aromatic protons correspond to the signals at 6.41 ppm (d), 6.49 ppm (dd), 6.96 ppm (d), 7.16 ppm (t), 7.25 ppm (d), 7.36 ppm (d) and 7.50 ppm (s) (These signals integrate for 7 protons).
- Based on the coupling constants, the doublet at 6.41 ppm represents the proton at C8, the doublet of doublets at 6.49 ppm represents the proton at C6 and the doublet at 6.96 ppm represents the proton at C5.

^{13}C NMR:

- The aliphatic carbons at C3, C4 and C9 are represented by the signals at 24.5 ppm, 30.9 ppm and 69.1 ppm.
- The carbonyl carbon at C2 is represented by the signal at 172.4 ppm.
- The aromatic carbons are represented by the signals at 102.6, 108.9, 116.3, 122.6, 125.8, 128.6, 130.1, 130.3, 131.0, 138.3, 139.1 and 158.0 ppm.

5d. 7-(2-Phenylethoxy)-3,4-dihydro-2(1*H*)-quinolinone

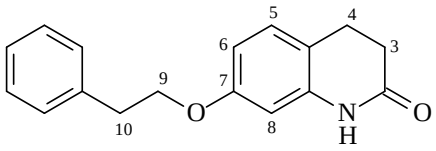

The title compound was prepared in a yield of 22%: mp 111.3–136.9 °C (ethanol). ^{1}H NMR (Bruker Avance III 600, $CDCl_3$) δ 2.52 (t, 2H, J = 7.2 Hz), 2.79 (t, 2H, J = 7.2 Hz), 2.99 (t, 2H, J = 7.2 Hz), 4.05 (t, 2H, J = 7.2 Hz), 6.32 (d, 1H, J = 2.3 Hz), 6.43 (dd, 1H, J = 2.3, 8.3 Hz), 6.93 (d, 1H, J = 8.3 Hz), 7.15 (m, 1H), 7.20 (m, 2H), 7.22–7.25 (m, 2H), 9.11 (s, 1H); ^{13}C NMR (Bruker Avance III 600, $CDCl_3$) δ 24.5, 31.0, 35.7, 68.8, 102.3, 108.7, 115.7, 126.5, 128.4, 128.5, 129.0, 138.1, 138.2, 158.4, 172.4; APCI-HRMS *m*/*z*: calcd for $C_{17}H_{18}NO_2$ (MH^+), 268.1338, found 268.1324.

^{1}H NMR:

- The NH proton corresponds to the singlet at 9.11 ppm (The signal integrates for 1 proton).
- The ethylene protons at C3 and C4 correspond to the triplets at 2.52 ppm and 2.79 ppm (The signals integrate for 2 protons each).
- The CH_2 protons at C9 correspond to the triplet at 4.05 ppm (The signal integrates for 2 protons).
- The CH_2 protons at C10 correspond to the triplet at 2.99 ppm (The signal integrates for 2 protons)
- The 8 aromatic protons correspond to the signals at 6.32 ppm (d), 6.43 ppm (dd), 6.93 ppm (d), 7.15 ppm (m), 7.20 ppm (m) and 7.22–7.25 ppm (m) (These signals integrate for 8 protons).
- Based on the coupling constants, the doublet at 6.32 ppm represents the proton at C8, the doublet of doublets at 6.43 ppm represents the proton at C6 and the doublet at 6.93 ppm represents the proton at C5.

^{13}C NMR:

- The aliphatic carbons at C3, C4, C9 and C10 are represented by the signals at 24.5 ppm, 31.0 ppm, 35.7 ppm and 68.8 ppm.
- The carbonyl carbon at C2 is represented by the signal at 172.4 ppm.
- The aromatic carbons are represented by the signals at 102.3, 108.7, 115.7, 126.5, 128.4, 128.5, 129.0, 138.1, 138.2 and 158.4 ppm.

5e. 7-(3-Phenylpropoxy)-3,4-dihydro-2(1*H*)-quinolinone

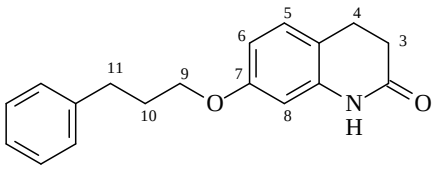

The title compound was prepared in a yield of 62%: mp 137.2–139.9 °C (ethanol). ^{1}H NMR (Bruker Avance III 600, $CDCl_3$) δ 2.07 (qn, 2H, J = 6.4 Hz), 2.61 (t, 2H, J = 7.5 Hz), 2.79 (t, 2H, J = 7.5 Hz), 2.88 (t, 2H, J = 7.9 Hz), 3.92 (t, 2H, J = 6.4 Hz), 6.39 (d, 1H, J = 2.3 Hz), 6.50 (dd, 1H, J = 2.3, 8.3 Hz), 7.02 (d, 1H, J = 8.3 Hz), 7.18–7.21 (m, 3H), 7.28 (t, 2H, J = 7.5 Hz), 9.09 (s, 1H); ^{13}C NMR (Bruker Avance III 600, $CDCl_3$) δ 24.5, 30.8, 31.0, 32.1, 67.0, 102.3, 108.7, 115.6, 125.9, 128.4, 128.5, 128.5, 138.2, 141.4, 158.6, 172.4; APCI-HRMS *m/z*: calcd for $C_{18}H_{20}NO_2$ (MH^+), 282.1494, found 282.1475.

^{1}H NMR:

- The NH proton corresponds to the singlet at 9.09 ppm (The signal integrates for 1 proton).
- The ethylene protons at C3 and C4 correspond to the triplets at 2.61 ppm and 2.79 ppm (The signals integrate for 2 protons each).
- The CH_2 protons at C9 and C11 correspond to the triplets at 2.88 ppm and 3.92 ppm (The signals integrate for 2 protons each).
- The CH_2 protons at C10 correspond to the quintet at 2.07 ppm (The signal integrates for 2 protons)
- The 8 aromatic protons correspond to the signals at 6.39 ppm (d), 6.50 ppm (dd), 7.02 ppm (d), 7.18–7.21 ppm (m) and 7.28 (t) (These signals integrate for 8 protons).
- Based on the coupling constants, the doublet at 6.39 ppm represents the proton at C8, the doublet of doublets at 6.50 ppm represents the proton at C6 and the doublet at 7.02 ppm represents the proton at C5.

^{13}C NMR:

- The aliphatic carbons at C3, C4, C9, C10 and C11 are represented by the signals at 24.5 ppm, 30.8 ppm, 31.0 ppm, 32.1 ppm and 67.0 ppm.
- The carbonyl carbon at C2 is represented by the signal at 172.4 ppm.
- The aromatic carbons are represented by the signals at 102.3, 108.7, 115.6, 125.9, 128.4, 128.5, 128.5, 138.2, 141.4 and 158.6 ppm.

3.6 Interpretation of the mass spectra

The ten 3,4-dihydro-2(1*H*)-quinolinone derivatives synthesized were characterized by mass spectrometry. The calculated and experimentally determined masses are given in table 3.2. The small differences between these masses indicate that the structures of the compounds correspond to those given in table 3.1.

The ppm was determined as follow:

$$\text{ppm} = \left[\frac{(found - calcd.)}{calcd}\right] \times 1000000$$

Equation 3.1

Table 3.2: The calculated and experimentally determined masses of the synthesized compounds:

	Calculated	Found	Formula	ppm
4a	254.1181	254.1174	$C_{16}H_{16}NO_2$	-2.8
4b	288.0791	288.0765	$C_{16}H_{15}ClNO_2$	-9.0
4c	332.0286	332.0250	$C_{16}H_{15}BrNO_2$	-10.8
4d	268.1338	268.1322	$C_{17}H_{18}NO_2$	-6.0
4e	282.1494	282.1479	$C_{18}H_{20}NO_2$	-5.3
5a	254.1181	254.1177	$C_{16}H_{16}NO_2$	-1.6
5b	288.0791	288.0765	$C_{16}H_{15}ClNO_2$	-9.0
5c	332.0286	332.0254	$C_{16}H_{15}BrNO_2$	-9.6
5d	268.1338	268.1324	$C_{17}H_{18}NO_2$	-5.2
5e	282.1494	282.1475	$C_{18}H_{20}NO_2$	-6.7

All masses are given as MH^+.

3.7 Conclusion

In total ten 3,4-dihydro-2(1*H*)-quinolinone derivatives were successfully synthesized from 6-hydroxy-3,4-dihydro-2(1*H*)-quinolinone and 7-hydroxy-3,4-dihydro-2(1*H*)-quinolinone. The 3,4-dihydro-2(1*H*)-quinolinones were substituted on C6 and C7 of the side chain phenyl ring to yield structures **4a**–**e** and **5a**–**e**, respectively. The substituents that were selected for this study were the benzyloxy, phenylethoxy and phenylpropoxy moieties. The benzyloxy phenyl rings were further substituted on the *meta* position with chlorine and bromine. All of the synthesised compounds were characterized by MS and NMR. There were good correlations between the NMR spectra and the structures of the compounds, as well as their experimentally determined masses and the calculated masses. Thus, it can be concluded that the proposed structures correspond with the synthesised compounds. In the next chapter, the MAO inhibitory properties of the ten 3,4-dihydro-2(*1H*)-quinolinone derivatives will be examined.

CHAPTER 4
ENZYMOLOGY

4.1 Introduction

The series of 3,4-dihydro-2(1*H*)-quinolinone derivatives, **4** and **5**, that were synthesized in chapter 3 was evaluated as inhibitors of human MAO-A and MAO-B. To measure the MAO-A and MAO-B inhibition potencies of the test compounds, the IC_{50} values were determined. Compounds which act as inhibitors of MAO-B may be considered as potential lead compounds for the development of therapy for PD. Compounds that are found to be MAO-A inhibitors may act as leads for the design of antidepressive drugs. These studies should establish if the goal of this study was achieved, namely the design of new potent, reversible and competitive inhibitors of the MAOs. The objectives of this chapter were as follows:

- As mentioned above, the 3,4-dihydro-2(1*H*)-quinolinone derivatives, **4** and **5**, that were synthesized in the previous chapter were evaluated as inhibitors of MAO-A and MAO-B. The inhibition potencies were expressed as the IC_{50} values for the inhibition of the MAOs. For this purpose, the recombinant human enzymes (which are commercially available) were employed. A fluorometric assay was used to measure the enzyme activities with kynuramine as substrate. Kynuramine is the substrate for both MAO-A and MAO-B and is oxidized to 4-hydroxyquinoline as shown in figure 4.1. The concentrations of the generated 4-hydroxyquinoline were measured with a fluorescent spectrophotometer at an excitation wavelength of 310 nm and an emission wavelength of 400 nm. Fluorescence decreases as 4-hydroxyquinoline production is reduced by the MAO inhibitors, such as the compounds (**4** and **5**) that were synthesized in this study.
- In order to determine if the inhibitors interact reversibly or irreversibly with MAO-A and MAO-B, the recovery of enzyme activity after dilution of enzyme-inhibitor complexes was examined. For this purpose an inhibitor, compound **5c** was selected as representative compound.
- To examine the mode of MAO inhibition by the 3,4-dihydro-2(1*H*)-quinolinone derivatives, a set of Lineweaver-Burk plots for the inhibition of MAO-B by **5c**, the representative compound, was constructed.
- To evaluate the importance of the C6 and C7 substituent for the inhibition of the MAOs by the 3,4-dihydro-2(1*H*)-quinolinone derivatives, 6-hydroxy-3,4-dihydro-2(1*H*)-quinolinone (**6**) and 7-hydroxy-3,4-dihydro-2(1*H*)-quinolinone (**7**) were also evaluated as human MAO inhibitors.

- The lipophilicities (LogP values) for the 3,4-dihydro-2(1*H*)-quinolinone derivatives were measured, in order to give an indication whether the compounds may gain entry into the brain.
- The effects of the 3,4-dihydro-2(1*H*)-quinolinone derivatives on cell viability of cultured cells were measured. This experiment will provide an estimate of the cytotoxicity of the compounds.

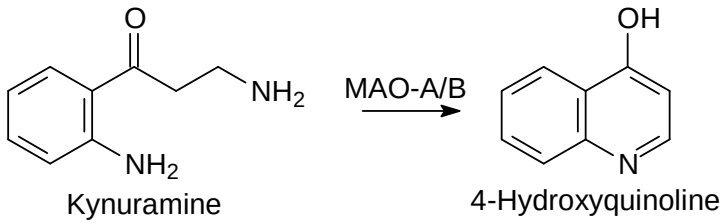

Figure 4.1. The oxidation of kynuramine by MAO-A or MAO-B to yield 4-hydroxyquinoline.

4.2 Chemicals and instrumentation

- For fluorescence spectrophotometry, a Varian Cary Eclipse fluorescence spectrophotometer was employed. Microsomes from insect cells containing recombinant human MAO-A and MAO-B (5 mg/ml) and kynuramine.2HBr were obtained from Sigma-Aldrich.

- HPLC analyses were performed with an Agilent 1100 HPLC system equipped with a quaternary pump and an Agilent 1100 series diode array detector. A Venusil XBP C18 column (4.60 × 150 mm, 5 μm) was used and the mobile phase consisted of 75% acetonitrile and 25% MilliQ water at a flow rate of 1 ml/min.

- n-Octanol (analytical reagent) was obtained from Sigma-Aldrich.

- For UV-VIS spectrophotometry, a Shimadzu MultiSpec-1501 UV-VIS photodiode array spectrophotometer was used.

- MTT [3-(4,5-dimethylthiazol-2-yl)-2,5-diphenyltetrazolium bromide] and phosphate-buffered saline (PBS) were obtained from Sigma-Aldrich.

- Cell culture media (Dulbecco's Modified Eagle Medium; DMEM), fetal bovine serum, penicillin (10 000 units/ml)/streptomycin (10 mg/ml), fungizone (250 µg/ml) and trypsin/EDTA (0.25%/0.02%) were from Gibco.

- A Multiscan RC UV/Vis platereader (from Labsystems) was used to measure the absorbances in 96-well microplates.

- 24-Well and 96-well plates were from Corning.

- Sterile syringe filters (0.22 µM) were obtained from Pall Corporation Life Sciences.

4.3 The determination of IC_{50} values for the 3,4-dihydro-2(1*H*)-quinolinone derivatives, 4 and 5

To determine the potencies by which the 3,4-dihydro-2(1*H*)-quinolinone derivatives, **4** and **5** inhibit MAO-A and MAO-B, the concentration (IC_{50}) that produces 50% inhibition (compared to the activity recorded in the absence of inhibitor) was measured.

4.3.1 Method – IC_{50} value determination

Enzymatic reactions: Recombinant human MAO-A (5 mg/ml) and MAO-B (5 mg/ml) were stored at -70 °C. The incubations were prepared in 500 µl potassium phosphate buffer and contained MAO-A (0.0075 mg/ml) or MAO-B (0.0075 mg/ml), various concentrations of the test inhibitor (0-100 µM) and 4% DMSO (co-solvent). Kynuramine was also added to each incubation, at concentrations of 30 µM and 45 µM for MAO-B and MAO-A, respectively. The reactions were incubated for 20 min at 37 °C and 400 µl NaOH (2 N) was added to terminate the reactions. Finally 1000 µl distilled water was added to each reaction. Centrifugation followed for 10 minutes at 16000g. Concentration measurements of 4-hydroxyquinoline in each incubation were carried out spectrofluorometrically. This was done by measuring the fluorescence of the supernatant at an excitation wavelength of 310 nm and an emission wavelength of 400 nm. For this purpose, the PMT voltage of the fluorescence spectrophotometer was set to medium and the excitation and emission slit widths were set to 5 mm.

Calibration curve: Using a linear calibration curve, constructed with known amounts of 4-hydroxyquinoline dissolved in 500 µl potassium phosphate buffer, quantitative estimations of 4-hydroxyquinoline in the incubations were made. 400 µl NaOH (2 N) and 1000 µl water were added to each calibration standard. To confirm that the fluorescence of 4-hydroquinoline is not quenched by the test inhibitors, control samples were included.

Sigmoidal dose-response curves: Plotting the initial rate of oxidation against the logarithm of the inhibitor concentration, the IC_{50} values were determined from the sigmoidal dose-response curves. Six different inhibitor concentrations spanning at least 3 orders of magnitude were used for each sigmoidal curve. The inhibition data were fitted to the one site competition model incorporated in the Prism (Graphpad) software package. The IC_{50} values were determined in triplicate and are expressed as mean ± standard deviation (SD).

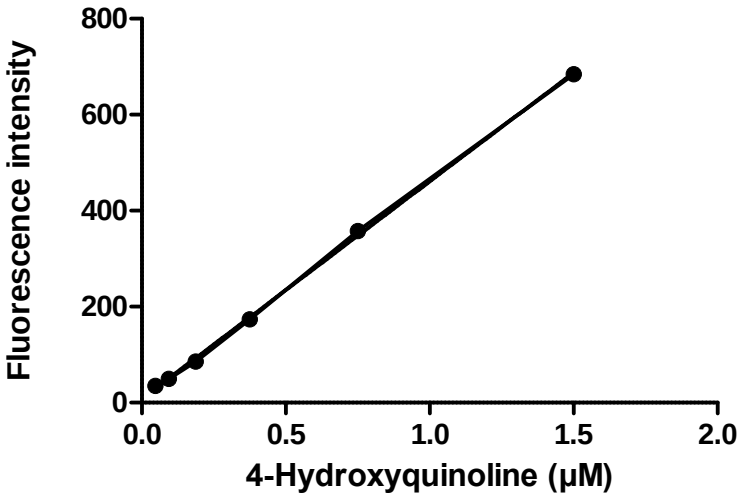

Figure 4.2. An example of a linear calibration curve, constructed with known amounts of 4-hydroxyquinoline.

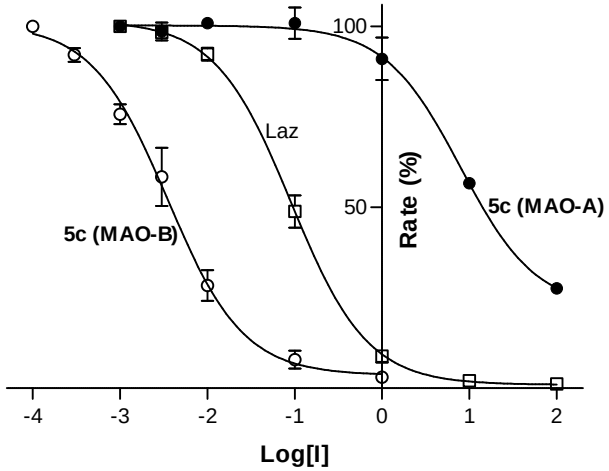

Figure 4.3. An example of a sigmoidal dose-response curve employed for the determination of the IC_{50} value for the inhibition of MAO-A (filled circles) and MAO-B (open circles) by compound **5c**. For comparison, the dose-response curve for the inhibition of MAO-B by lazabemide (squares) is also given. The sigmoidal dose-response curve is that of the initial rates of oxidation of kynuramine by recombinant human MAO-B vs. the logarithm of concentration of inhibitor **5c** (expressed in µM). The determinations were carried out in triplicate and the values are expressed as the mean ± standard deviation.

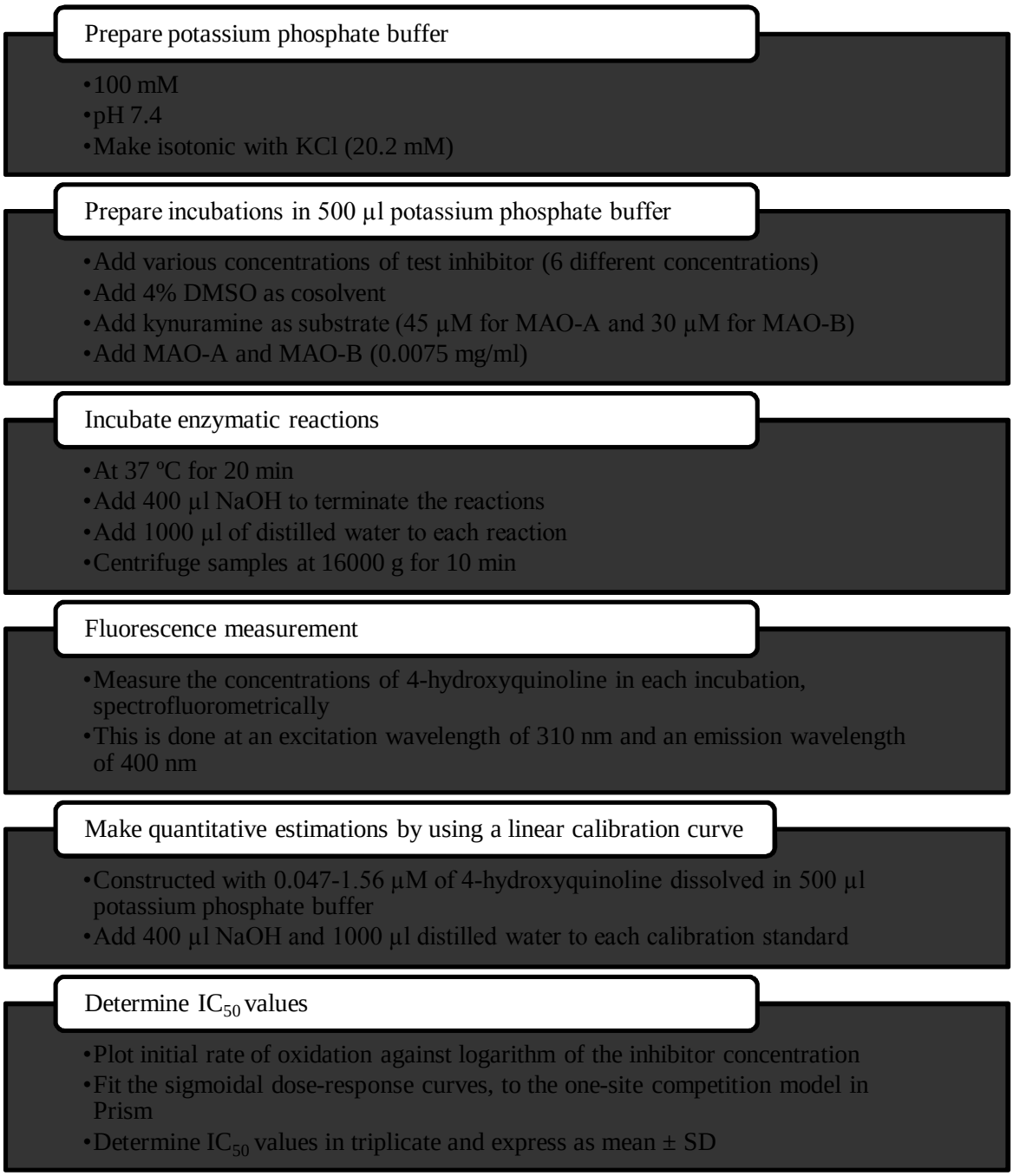

Figure 4.4 Workflow for the determination of IC_{50} values for the inhibition of MAO-A and MAO-B by 3,4-dihydro-2(1*H*)-quinolinone derivatives, **4** and **5**.

4.3.2 **Results:**

*The IC_{50} values for the inhibition of MAO-A and MAO-B by 3,4-dihydro-2(1H)-quinolinone derivatives, **4** and **5**.*

The IC_{50} values for the inhibition of human MAO-A and MAO-B by the 3,4-dihydro-2(1*H*)-quinolinone derivatives, **4** and **5**, are given in table 4.1. From the results, the following observations and conclusions may be made:

- The 3,4-dihydro-2(1*H*)-quinolinone derivatives are potent inhibitors of MAO-B with most homologues (8 of 10) exhibiting IC_{50} values in the nanomolar range.
- The results demonstrate that all of the 3,4-dihydro-2(1*H*)-quinolinone derivatives are selective MAO-B inhibitors. The selectivity index (SI) values, the selectivities of the test compounds for the MAO-B isoform is given as the ratio of IC_{50}(MAO-A)/IC_{50}(MAO-B) in table 4.1. For all of the 3,4-dihydro-2(1*H*)-quinolinone derivatives, these SI values are in excess of 1 which shows that these compounds are selective MAO-B inhibitors. Compound **5b** did not exhibit any inhibitory activity towards MAO-A.
- The most potent MAO-B inhibitor, 7-(3-bromobenzyloxy)-3,4-dihydro-2(1*H*)-quinolinone (**5c**), is an exceptionally potent MAO-B inhibitor with an IC_{50} value of 0.0029 μM. Even though **5c** (IC_{50} = 7.98 μM) also was the most potent MAO-A inhibitor of the series, this compound is a highly selective inhibitor with a ~2750-fold selectivity for MAO-B over the MAO-A isoform.
- Another highly potent MAO-B inhibitor among the compounds evaluated is compound **5b** (IC_{50} = 0.0062 μM). Since compound **5b** did not exhibit any inhibitory activity towards MAO-A (up to a maximal tested concentration of 100 μM) it may also be considered as highly selective for MAO-B.
- Compared to the reversible MAO-B selective inhibitor, lazabemide (IC_{50} = 0.091 μM), compounds **5b** and **5c** are approximately 14- and 31-fold, respectively, more potent as MAO-B inhibitors under identical conditions (Petzer *et al.*, 2013).
- An analysis of the structure-activity relationships (SARs) for MAO-B inhibition reveals interesting trends. Substitution on the C7 position of the 3,4-dihydro-2(1*H*)-quinolinone moiety leads to significantly more potent MAO-B inhibition compared to substitution on C6. For example, **5a** (IC_{50} = 0.038 μM) substituted with the benzyloxy moiety on C7 is approximately 100-fold more potent than **4a** (IC_{50} = 4.01 μM), the homologue containing the benzyloxy moiety on C6. In fact compounds **5a**–**e** were in each instance more potent MAO-B inhibitors than their corresponding C6 substituted homologues **4a**–**e**.

It may thus be concluded that C7-substituted 3,4-dihydro-2(1*H*)-quinolinones are, in general, more suitable for the design of exceptionally potent MAO-B inhibitors than C6-substituted 3,4-dihydro-2(1*H*)-quinolinones.

- In spite of the observation that C7-substituted 3,4-dihydro-2(1*H*)-quinolinones are more potent MAO-B inhibitors, with the appropriate substitution certain C6-substituted 3,4-dihydro-2(1*H*)-quinolinones such as **4c** (IC_{50} = 0.086 μM) may still be viewed as potent MAO-B inhibitors.
- Another interesting SAR is the finding that a benzyloxy substituent on C7 of the 3,4-dihydro-2(1*H*)-quinolinone moiety is more favourable for MAO-B inhibition than phenylethoxy and phenylpropoxy substitution on this position. For example, the C7 benzyloxy substituted homologue **5a** (IC_{50} = 0.038 μM) is at least 3-fold more potent than the phenylethoxy [(**5d**); IC_{50} = 0.191 μM] and phenylpropoxy [(**5e**); IC_{50} = 0.130 μM] substituted homologues.
- Interestingly, for the C6-substituted 3,4-dihydro-2(1*H*)-quinolinones, the benzyloxy substituted homologue **4a** (IC_{50} = 4.01 μM) was a weaker MAO-B inhibitor than the C6 phenylethoxy (**4d**) and phenylpropoxy (**4e**) substituted homologues. Reasons for the different trends observed with the C7- and C6-substituted 3,4-dihydro-2(1*H*)-quinolinones are not apparent.
- From a design point of view, it is noteworthy that, for the C7 benzyloxy substituted 3,4-dihydro-2(1*H*)-quinolinones, halogen (Cl, Br) substitution on the benzyloxy phenyl ring further enhances MAO-B inhibition potency. In this regard, the chlorine and bromine substituted homologues **5b** (IC_{50} = 0.0062 μM) and **5c** (IC_{50} = 0.0029 μM) are 6–13 fold more potent than the unsubstituted 7-benzyloxy-3,4-dihydro-2(1*H*)-quinolinone **5a** (IC_{50} = 0.038 μM). For those compounds with benzyloxy substituents on C6 of the 3,4-dihydro-2(1*H*)-quinolinone moiety, a similar trend was observed with the chlorine and bromine substituted homologues **4b** (IC_{50} = 0.620 μM) and **4c** (IC_{50} = 0.086 μM) exhibiting more potent MAO-B inhibition than the unsubstituted 6-benzyloxy-3,4-dihydro-2(1*H*)-quinolinone **4a** (IC_{50} = 4.01 μM). From these data it is apparent that bromine substitution yields more potent MAO-B inhibitors compared to chlorine substitution. Further investigation is necessary to evaluate the effects on MAO-B inhibition of other halogen and alkyl substituents on the benzyloxy phenyl ring.
- For the inhibition of MAO-A, no clear SARs are apparent. As noted above, the most potent MAO-B inhibitor of the series **5c** also was the most potent MAO-A inhibitor. Also, since **5c** as well as **4c**, the second most potent MAO-A inhibitor of the series, contain bromine on the benzyloxy phenyl ring, substitution with this halogen also enhances MAO-A inhibitory potency.

Table 4.1: The IC_{50} values for the inhibition of recombinant human MAO-A and MAO-B by compounds **4** and **5**.

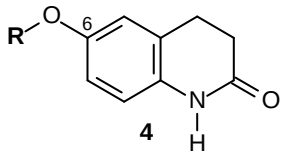

4

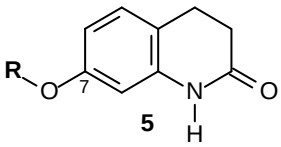

5

		IC_{50} (μM)[a]		
	R	MAO-A	MAO-B	SI[b]
4a	$C_6H_5CH_2$–	25.3 ± 15.2	4.01 ± 1.196	6
4b	3-$ClC_6H_4CH_2$–	50.6 ± 10.3	0.620 ± 0.148	82
4c	3-$BrC_6H_4CH_2$–	12.4 ± 1.93	0.086 ± 0.029	144
4d	$C_6H_5(CH_2)_2$–	22.5 ± 9.69	2.33 ± 1.33	10
4e	$C_6H_5(CH_2)_3$–	19.7 ± 12.8	0.284 ± 0.049	69
5a	$C_6H_5CH_2$–	90.4 ± 47.1	0.038 ± 0.013	2379
5b	3-$ClC_6H_4CH_2$–	No Inh[c]	0.0062 ± 0.00063	–
5c	3-$BrC_6H_4CH_2$–	7.98 ± 1.09	0.0029 ± 0.0009	2751
5d	$C_6H_5(CH_2)_2$–	53.7 ± 12.0	0.191 ± 0.041	281
5e	$C_6H_5(CH_2)_3$–	22.5 ± 4.08	0.130 ± 0.010	173

[a] All values are expressed as the mean ± SD of triplicate determinations.

[b] The selectivity index is the selectivity for the MAO-B isoform and is given as the ratio of IC_{50}(MAO-A)/IC_{50}(MAO-B).

[c] No inhibition at a maximum tested concentration of 100 μM.

*The IC_{50} values for the inhibition of MAO-A and MAO-B by 7-hydroxy-3,4-dihydro-2(1H)-quinolinone derivatives **6** and **7**.*

To evaluate the importance of the C6 and C7 substituent for the inhibition of the MAOs by the the 3,4-dihydro-2(1*H*)-quinolinone derivatives, 6-hydroxy-3,4-dihydro-2(1*H*)-quinolinone (**6**) and 7-hydroxy-3,4-dihydro-2(1*H*)-quinolinone (**7**) were also evaluated as human MAO inhibitors. The results are given in table 4.2 and show that **6** and **7** are weak MAO inhibitors with IC_{50} values >161 μM. This result demonstrates that appropriate C6 and C7 substitution is a requirement for the MAO inhibitory activities of 3,4-dihydro-2(1*H*)-quinolinone derivatives.

Table 4.2: The IC_{50} values for the inhibition of recombinant human MAO-A and MAO-B by 6- and 7-hydroxy-3,4-dihydro-2(1*H*)-quinolinone derivatives **6** and **7**.

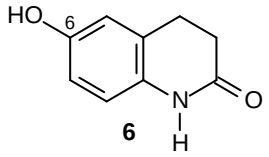

6

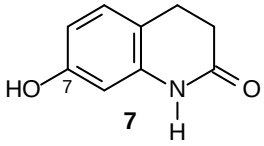

7

	IC_{50} (μM)[a]		
	MAO-A	MAO-B	SI[b]
6	161 ± 16.1	201 ± 31.3	0.8
7	183 ± 2.48	No Inh[c]	–

[a] All values are expressed as the mean ± SD of triplicate determinations.

[b] The selectivity index is the selectivity for the MAO-B isoform and is given as the ratio of IC_{50}(MAO-A)/IC_{50}(MAO-B).

[c] No inhibition at a maximum tested concentration of 100 μM.

4.4 Reversibility of inhibition

The most potent MAO inhibitor, compound **5c**, was selected to determine if the MAO inhibition observed by the 3,4-dihydro-2(1H)-quinolinone derivatives is reversible or irreversible. For the purpose of this study, only the reversibility of MAO-B inhibition was examined since the 3,4-dihydro-2(1H)-quinolinone derivatives were highly potent and selective MAO-B inhibitors. MAO-B inhibitors with a reversible mode of action may possess certain advantages over irreversible MAO-B inhibitors, which are currently used in Parkinson's disease therapy. The most notable advantage is an immediate recovery of enzyme activity when the inhibitor has been eliminated from the tissues. In contrast, after termination of treatment with irreversible inhibitors, the rates of recovery of enzyme activity are slow and variable, in part because the turnover rate for the biosynthesis of MAO-B in the human brain may be as much as 40 days (Tipton *et al*., 2004; Fowler *et al*., 1994).

4.4.1 Method - Recovery of enzyme activity after dilution

Preincubation: The test MAO-B inhibitor, **5c** [IC_{50}(MAO-B) = 0.0029 μM], at concentrations equal to 10 × IC_{50} and 100 × IC_{50}, was preincubated with recombinant human MAO-B (0.75 mg/ml) for 30 min at 37 ºC (K_2HPO_4/KH_2PO_4, pH 7.4, 100 mM, made isotonic with KCl). These preincubations contained DMSO (4%) as co-solvent.

Dilution: The reactions were subsequently diluted 100-fold with the addition of a solution of kynuramine (in K_2HPO_4/KH_2PO_4, pH 7.4, 100 mM) to yield final concentrations of the test inhibitor equal to 1 × IC_{50} and 0.1 × IC_{50}. After dilution, the final concentration of kynuramine was 30 µM and the final concentration of MAO-B was 0.0075 mg/ml. The volumes of these diluted reactions were 500 µl each.

Incubation: The reactions were incubated for a further 20 min at 37 °C, terminated and the residual rates of 4-hydroxyquinoline formation were measured. This was accomplished by adding 400 µl NaOH and 1000 µl of distilled water to each reaction. Centrifugation followed for 10 minutes at 16000g. Concentration measurements of the 4-hydroxyquinoline in each incubation was carried out spectrofluorometrically. This was done by measuring the fluorescence of the supernatant at an excitation wavelength of 310 nm and an emission wavelength of 400 nm. For this purpose, the PMT voltage of the fluorescence spectrophotometer was set to medium and the excitation and emission slit widths were set to 5 mm.

Calibration curve: Using a linear calibration curve, constructed with known amounts of 4-hydroxyquinoline dissolved in 500 µl potassium phosphate buffer, quantitative estimations of 4-hydroxyquinoline in the incubations were made. 400 µl NaOH (2N) and 1000 µl water were added to each calibration standard.

Control reactions: For comparison, (R)-deprenyl (IC_{50} = 0.079 µM), at a concentration of 10 × IC_{50} was similarly preincubated with MAO-B, diluted to 0.1 × IC_{50} and the residual MAO-B catalytic activity was measured as above. Similar reactions, which served as controls, were also conducted in the absence of inhibitor (Petzer *et al*., 2012).

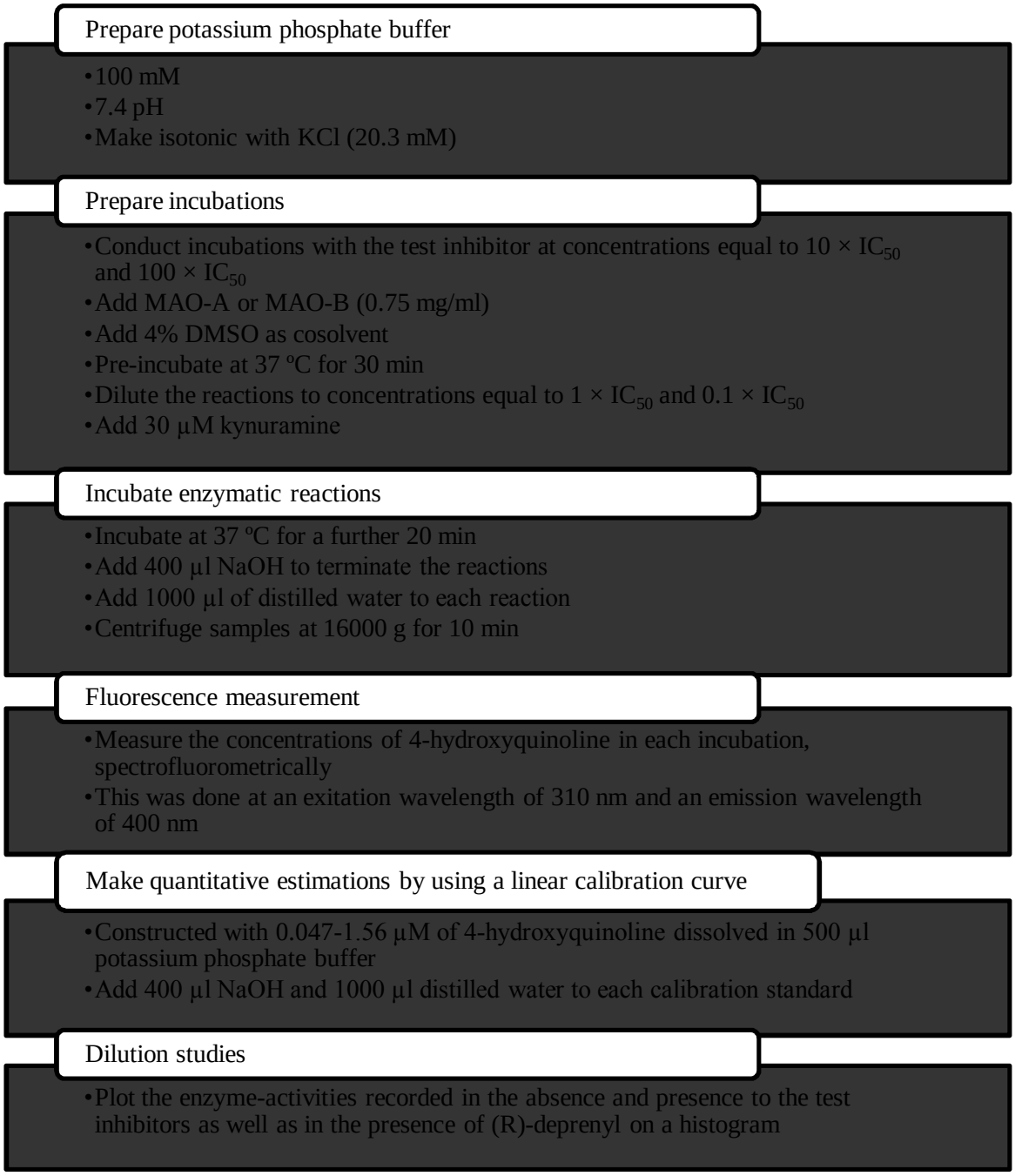

Figure 4.5 Workflow for the measurement of recovery of enzyme activity after dilution.

4.4.2 **Results:**

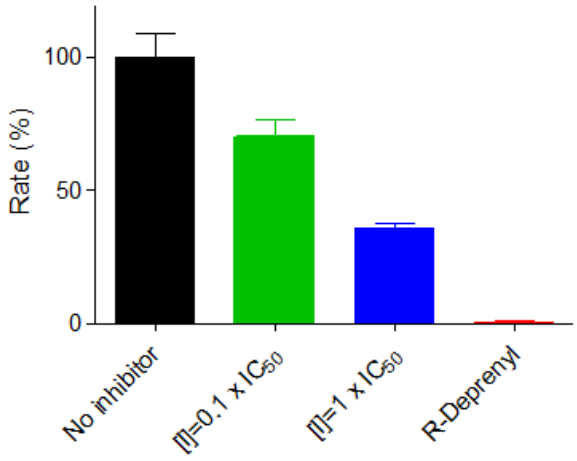

Figure 4.6 The reversibility of inhibition of MAO-B by compound **5c**. MAO-B was preincubated with **5c** at 10 × IC_{50} and 100 × IC_{50} for 30 min and then diluted to 0.1 × IC_{50} and 1 × IC_{50}, respectively. For comparison, the irreversible MAO-B inhibitor, (R)-deprenyl, at 10 × IC_{50}, was similarly incubated with MAO-B and diluted to 0.1 × IC_{50}. The residual activities of MAO-B was subsequently measured.

Since compound **5c** was found to be the most potent MAO-B inhibitor of the series, the reversibility of MAO-B inhibition by this compound was evaluated. None of the 3,4-dihydro-2(1*H*)-quinolinone derivatives were potent MAO-A inhibitors, and the reversibility of MAO-A inhibition therefore was not examined. To evaluate the reversibility of inhibition, the recovery of enzyme activities after the dilution of the enzyme-inhibitor complexes was examined (Petzer *et al.*, 2012). For this purpose, MAO-B and **5c** were combined and preincubated for 30 min at inhibitor concentrations equal to 10 x IC_{50} and 100 x IC_{50}. The reactions were subsequently diluted 100-fold to yield concentrations of **5c** of 0.1 x IC_{50} and 1 x IC_{50}, and the residual enzyme activities were measured. Control reactions conducted in the absence of inhibitor were included in the study. The results are given in Fig. 4.6 and show that, after dilution of **5c** to concentrations of 0.1 x IC_{50} and 1 x IC_{50}, the catalytic activities of MAO-B are recovered to levels of 70% and 36% of the control levels, respectively. This result suggests that **5c** acts as a reversible MAO-B inhibitor since, after similar treatment of MAO-B with the irreversible inhibitor (R)-deprenyl at concentrations equal to 10 × IC_{50}, and dilution of the resulting reactions to 0.1 x IC_{50}, the MAO-B activities are not recovered (0.7% of control). Interestingly, after dilution of **5c** to concentrations of 0.1 × IC_{50} and 1 × IC_{50}, the MAO-B catalytic activities are not recovered to 90% and 50%, respectively, as would be expected for reversible inhibition. This result suggests that **5c** may possess a quasi-reversible interaction or tight-binding component.

4.5 Lineweaver-Burk plots

Using a set of Lineweaver–Burk plots, the mode of inhibition may be examined. For this purpose, an experiment with the same principles as the experiment used for IC_{50} value determinations was employed. For the purpose of this study compound **5c** was selected as representative inhibitor. Since **5c** is a highly potent MAO-B inhibitor, the mode of MAO-B inhibition by **5c** was further investigated with the aid of Lineweaver-Burk plots. The MAO-B catalytic rates were recorded at 8 different kynuramine concentrations (15–250 µM) in the absence of inhibitor, and presence of five different concentrations (¼ × IC_{50}, ½ × IC_{50}, ¾ × IC_{50}, 1 × IC_{50} and 1¼ × IC_{50}) of **5c**.

4.5.1 Method - The construction of Lineweaver-Burk plots and K_i value calculations

Inhibitor concentrations: The mode of MAO-B inhibition was examined by constructing a set of six Lineweaver-Burk plots. The first plot was constructed in the absence of inhibitor while the remaining five plots were constructed in the presence of different concentrations (0.725–3.6 nM) of inhibitor **5c**. These inhibitor concentrations were ¼ × IC_{50}, ½ × IC_{50}, ¾ × IC_{50}, 1 × IC_{50} and 1¼ × IC_{50}.

Incubations: Recombinant human MAO-B (5 mg/ml) was stored at -70 °C. The enzymatic reactions were prepared in 500 µl potassium phosphate buffer (K_2HPO_4/KH_2PO_4, pH 7.4, 100 mM, made isotonic with KCl). All incubations contained DMSO (4%) as co-solvent, compound **5c** and the MAO substrate kynuramine. As mentioned above, five Lineweaver-Burk plots were constructed in the presence of different concentrations of inhibitor **5c**, while one plot was constructed in the absence of inhibitor. Eight different concentrations of kynuramine, at concentrations of 15–250 µM, were used to construct each Lineweaver-Burk plot. Recombinant human MAO-B at a concentration of 0.015 mg/ml was subsequently added to each enzymatic reaction. The reactions were incubated for 20 min at 37 °C, 400 µl NaOH was added to terminate the reactions after which 1000 µl of distilled water was added. Centrifugation followed for 10 minutes at 16000g.

Fluorometric measurements: Concentration measurements of the 4-hydroxyquinoline in each incubation were carried out spectrofluorometrically. This was done by measuring the fluorescence of the supernatant at an excitation wavelength of 310 nm and an emission wavelength of 400 nm. For this purpose, the PMT voltage of the fluorescence spectrophotometer was set to medium and the excitation and emission slit widths were set to 5 mm.

Calibration curve: Using a linear calibration curve, constructed with known amounts of 4-hydroxyquinoline dissolved in 500 µl potassium phosphate buffer, quantitative estimations of 4-hydroxyquinoline in the incubations were made. 400 µl NaOH (2N) and 1000 µl water were added to each calibration standard.

K_i value: The slopes of the six Lineweaver-Burk plots were graphed versus the concentration of **5c**, and the K_i value was estimated from the x-axis intercept of this plot, which is equal to $-K_i$.

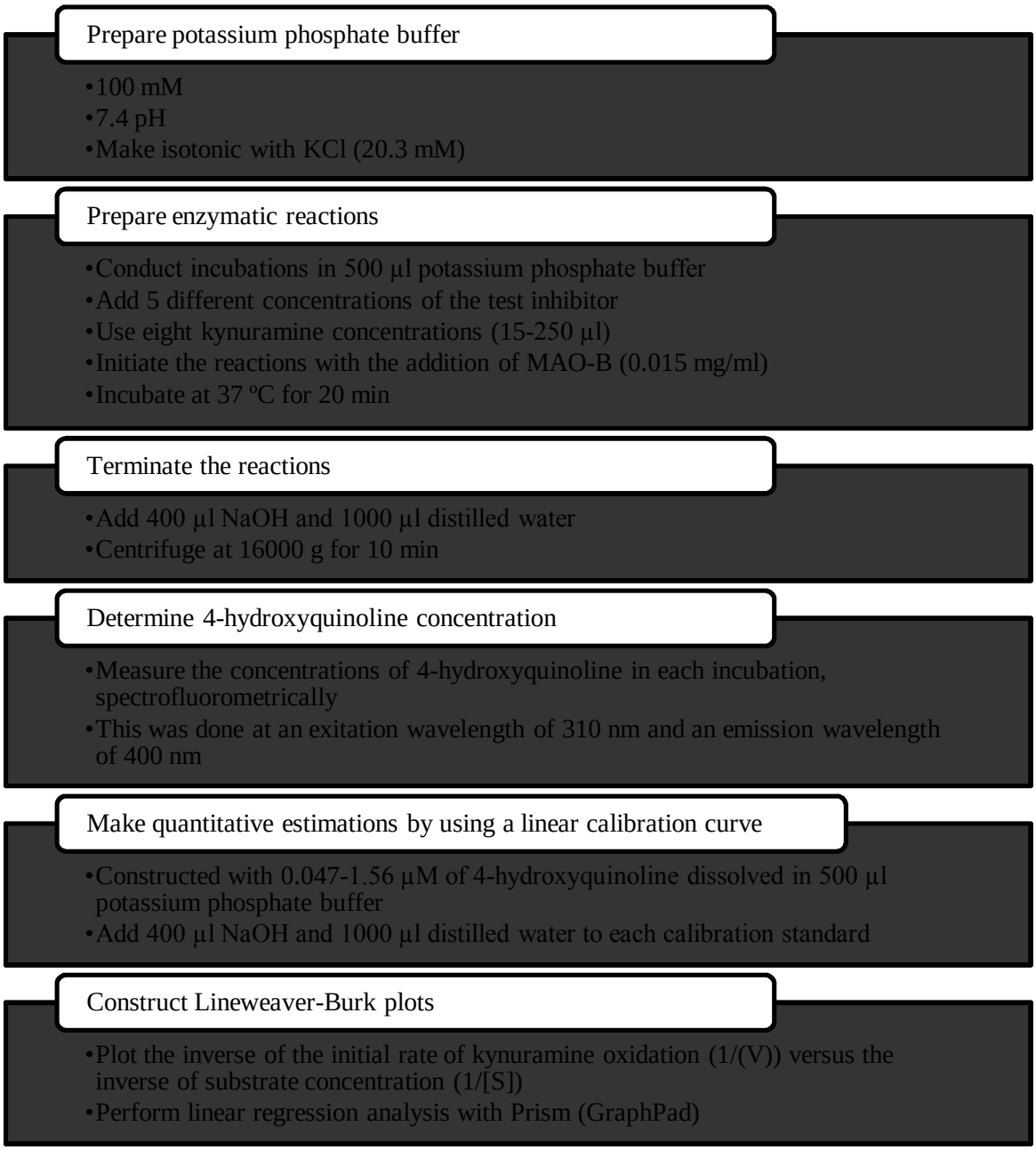

Figure 4.7 Protocol used for the construction of Lineweaver-Burk plots.

4.5.2 Results:

To examine the mode of MAO-B inhibition by the 3,4-dihydro-2(1*H*)-quinolinone derivatives, a set of Lineweaver-Burk plots for the inhibition of MAO-B by **5c** was constructed. For this purpose, the MAO-B catalytic rates were recorded at 8 different kynuramine concentrations (15–250 μM) in the absence of inhibitor, and presence of five different concentrations (¼ × IC_{50}, ½ × IC_{50}, ¾ × IC_{50}, 1 × IC_{50} and 1¼ × IC_{50}) of **5c**. The set of Lineweaver-Burk plots is given in Fig. 4.8. The observation that the lines are linear and intersect on the y-axis suggests that **5c** is a competitive inhibitor of human MAO-B. This is further evidence that the interaction of **5c** with MAO-B is reversible. From a replot of the slopes of the Lineweaver-Burk plots versus the concentration of **5c**, a K_i value of 0.0027 μM for the inhibition of MAO-B is estimated.

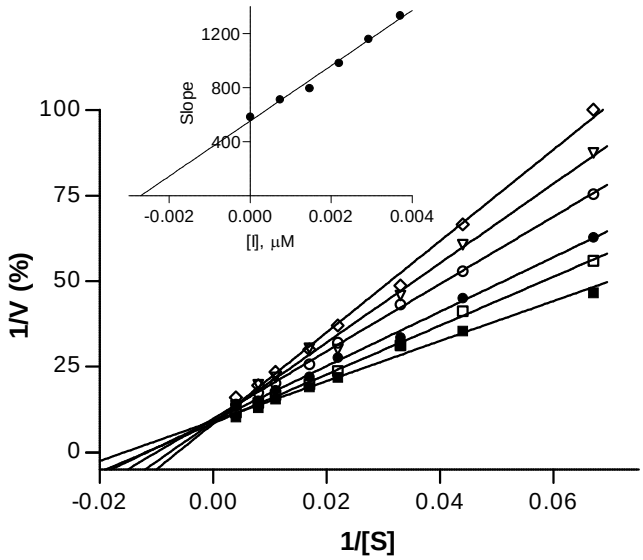

Figure 4.8. Lineweaver-Burk plots for the inhibition of human MAO-B by **5c**. The plots were constructed in the absence (filled squares) and presence of various concentrations of **5c**. The inset is a plot of the slopes of the Lineweaver-Burk plots versus inhibitor concentration.

4.6 LogP values

LogP is the logarithm of the partition coefficient (P) and is used to express the lipophilicity of a compound. A partition coefficient is the ratio of concentrations of a compound in the two phases of a mixture of two liquids at equilibrium. In this case the immiscible solvents selected were water and octanol, with water being the hydrophilic phase and octanol being the hydrophobic phase. Hence the partition coefficient is a measure of how hydrophilic or hydrophobic the compound is. Lipophilicity has a major effect on the permeability of a compound through biological membranes, and may thus be used to determine whether a compound will penetrate the blood-brain barrier.

4.6.1 Method

Shake flask method for LogP determination

n-Octanol (analytical reagent from Sigma-Aldrich) and deionised water (MilliQ) were mutually saturated in a separatory funnel. In a 10 ml glass vessel, 4 ml of water was placed followed by 4 ml of n-octanol containing 2 mM of the 3,4-dihydro-2(1*H*)-quinolinone derivatives. The vessels were shaken by hand for 5 min and centrifuged at 4,000 g for 10 min. The n-octanol phase was diluted 30-fold into neat n-octanol and the absorbance of the resulting solution was recorded at an absorbance maximum of 254 nm. The concentrations of the test compounds in the n-octanol phase were determined by employing the molar extinction coefficients recorded in n-octanol for each of the compounds. The molar extinction coefficients are given in Table 4.3.

The water phases were placed in HPLC vials and analyzed by HPLC. For this purpose, a Venusil XBP C18 column (4.60 × 150 mm, 5 μm) was used and the mobile phase consisted of 75% acetonitrile and 25% MilliQ water at a flow rate of 1 ml/min. A volume of 20 μl of the water phases were injected into the HPLC system and the eluent was monitored at a wavelength of 254 nm. To quantify the analytes, linear calibration curves were constructed by similarly analyzing known amounts of the test compounds (0.05–10 μM) dissolved in 50% acetonitrile in water. The logP value is equal to the logarithm of the octanol/water partition coefficients (P). The partition coefficient is the ratio of the concentration of the test compound in the n-octanol phase to the water phase. These studies were carried out in triplicate for each analyte and the logP values are expressed as mean ± SD.

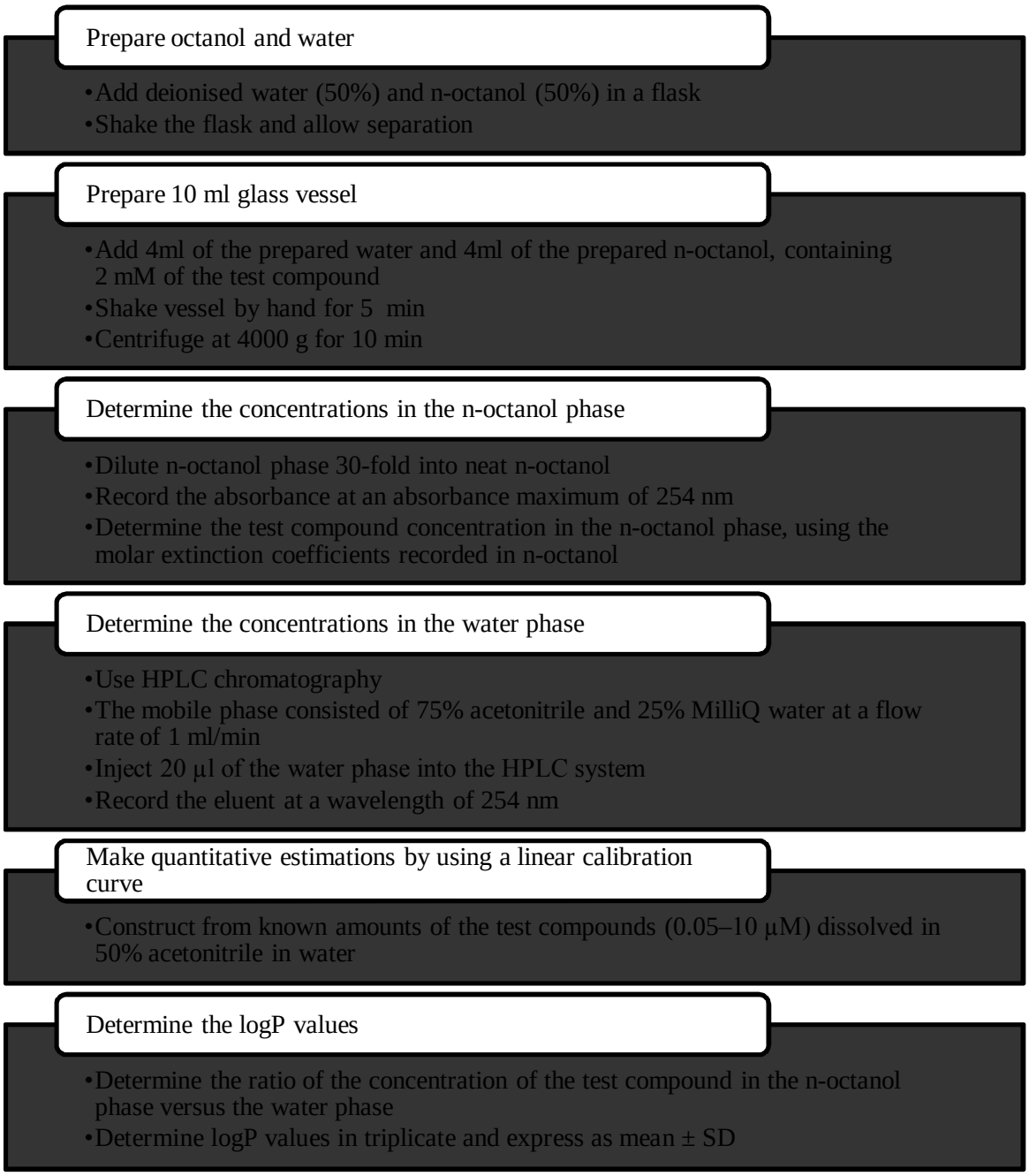

Figure 4.9 Workflow for the determination of LogP values.

4.6.2 Results – LogP values:

Table 4.3: The LogP values of the 3,4-dihydro-2(1*H*)-quinolinone derivatives as estimated by the shake flask method. The extinction coefficients at λ_{max} in n-octanol are also given.

	LogP value[a]	Extinction coefficients(M^{-1})	λ_{max} (nm)
4a	3.03 ± 0.037	15409	259
4b	4.18 ± 0.291	15023	259
4c	3.63 ± 0.058	18687	259
4d	3.74 ± 0.110	15989	259
4e	4.08 ± 0.191	12035	259
5a	3.09 ± 0.015	8234	254
5c	4.38 ± 0.142	7865	254
5d	3.95 ± 0.127	10106	254
5e	4.55 ± 0.279	8125	254

[a] All values are expressed as the mean ± SD of triplicate determinations.

To examine the potential of 3,4-dihydro-2(1*H*)-quinolinone derivatives for the treatment of CNS disorders, the octanol/water partition coefficients (P) were measured. The partition coefficient is a measure of the lipophilicity of a compound, a property which has a major effect on the permeability of a compound through biological membranes. Lipophilicity estimates may thus be used to predict the likelihood of a compound to penetrate the blood-brain barrier. As shown in Table 4.3, all of the evaluated compounds may be viewed as lipophilic since they display LogP values in excess of 3.00. As a general guide, LogP values ranging from 0–3 are optimal for passive diffusion permeability and such compounds are expected to display good oral bioavailability and blood-brain barrier permeation (Kerns & Di, 2008). While the measurement of additional properties such as solubility, permeability, metabolism and protein binding will provide a clearer picture, these preliminary results suggest that the 3,4-dihydro-2(1*H*)-quinolinone derivatives may possess suitable properties to freely permeate biological membranes and to gain access in the central nervous system. Their high LogP values, however, suggest that they possess a low degree of aqueous solubility, a property which may reduce oral bioabailability. Even though the LogP values recorded for certain compounds (compounds **4a**, **4d** and **5a**) are relatively close to the general guideline of 0–3, this dissertation recommends that the structures of the 3,4-dihydro-2(1*H*)-quinolinone derivatives be modified to reduce LogP. Approaches that may be followed are the inclusion of an ionisable functional group or groups with hydrogen bond donating and accepting potentials.

4.7 Cytotoxicity

Toxicity refers to the degree of damage that can be caused by a compound, either on the organism itself or substructures thereof, such as cells. To successfully develop a new drug, attention and priority must be given to the toxicity of the drug. One method used to estimate the toxicity of a compound is to determine the toxicity of the compound to human cells. To estimate the toxicity of the 3,4-dihydro-2(1*H*)-quinolinone derivatives, their effects on the viability of cultured cells were examined. For this purpose, the MTT cell viability assay was used (Mosmann, 1983). The MTT assay is a standard cell viability assay, measuring mitochondrial activity in live (metabolically viable) cells. Metabolically active mitochondria in viable cells have the ability to reduce MTT to coloured formazan crystals that can be quantified spectrophotometrically. The presence of a toxic agent will reduce cell viability and the reduction of MTT to the formazan product. For this study HeLa cells were selected. This selection was based on the high growth rate of HeLa cells and on the observation that these cells are frequently used to measure cell viability in the presence of toxic agents (Rahbari *et al*., 2009).

4.7.1 Method - cell viability determination

For the cell viability assay, three types of experiments with triplicate observations of each condition are recommended. Two types of controls are needed, namely the negative control (100% cell viability with no drug treatment) and positive control (100% cell death, induced by 0.03% formic acid). The third type is the test experiments where the viability of cells treated with the test compound is measured.

HeLa cells were maintained in 1 litre flasks in 30 ml DMEM containing, 10% fetal bovine serum, 1% penicillin (10 000 units/ml)/streptomycin (10 mg/ml) and 0.1% fungizone (250 µg/ml). The cells were incubated at 37 °C in an atmosphere of 10% CO_2. Once confluent, the cells were seeded at 500 000 cells/well in 24-well plates and incubated for 24 hours. A volume of 3 ml trypsin/EDTA (0.25%/0.02%) was used to facilitate cell detachment and the counting of cells was done with a haemocytometer. The wells were subsequently rinsed with 0.5 ml DMEM containing no fetal bovine serum. A volume of 0.99 ml DMEM (containing no fetal bovine serum) was subsequently added to each well followed by 10 ul of the test compound. Stock solutions of the test drugs were prepared in DMSO and sterilized through a 0.22 µm syringe filter (Pallman). In each 24-well plate, wells were reserved as positive controls (100% cell death via lyses with 0.33% formic acid) and negative controls (0% cell death as a result of no treatment). The well-plates were incubated for a further 24 h after which the culture medium was aspirated from the cells. The wells were washed twice with 0.5 ml/well phosphate-buffered saline (PBS) and 200 µl of 0.5% MTT reagent dissolved in PBS was added to each well.

The well-plates were incubated at 37 °C for 2 hours in the dark, the MTT-reagent was aspirated from the wells and 250 µl isopropanol was added to each well. The well-plates were then incubated at room temperature for 5 minutes to dissolve the purple formazan crystals, where after 100 µl of the isopropanol phase was transferred to a 96-well plate. The absorbance of each isopropanol phase was measured spectrophotometrically at 560 nm. The effect on cell viability of each test compound was evaluated in triplicate.

The mitochondrial activity was determined and expressed as a percentage of the negative control (100% cell viability) by means of the following equation (where Abs = absorbance as read by the spectrophotometer):

$$\%\ \text{Viable Cells} = 100 \times \frac{\text{Abs (sample)} - \text{Abs (positive control)}}{\text{Abs (negative control)} - \text{Abs (positive control)}}$$

Equation 4.1

Where $Abs_{(sample)}$ = absorbance from spectrophotometer of the sample, $Abs_{(positive\ control)}$ = absorbance of the cells treated with 0.3% formic acid (100% cell death), $Abs_{(negative\ control)}$ = absorbance of cells without treatment.

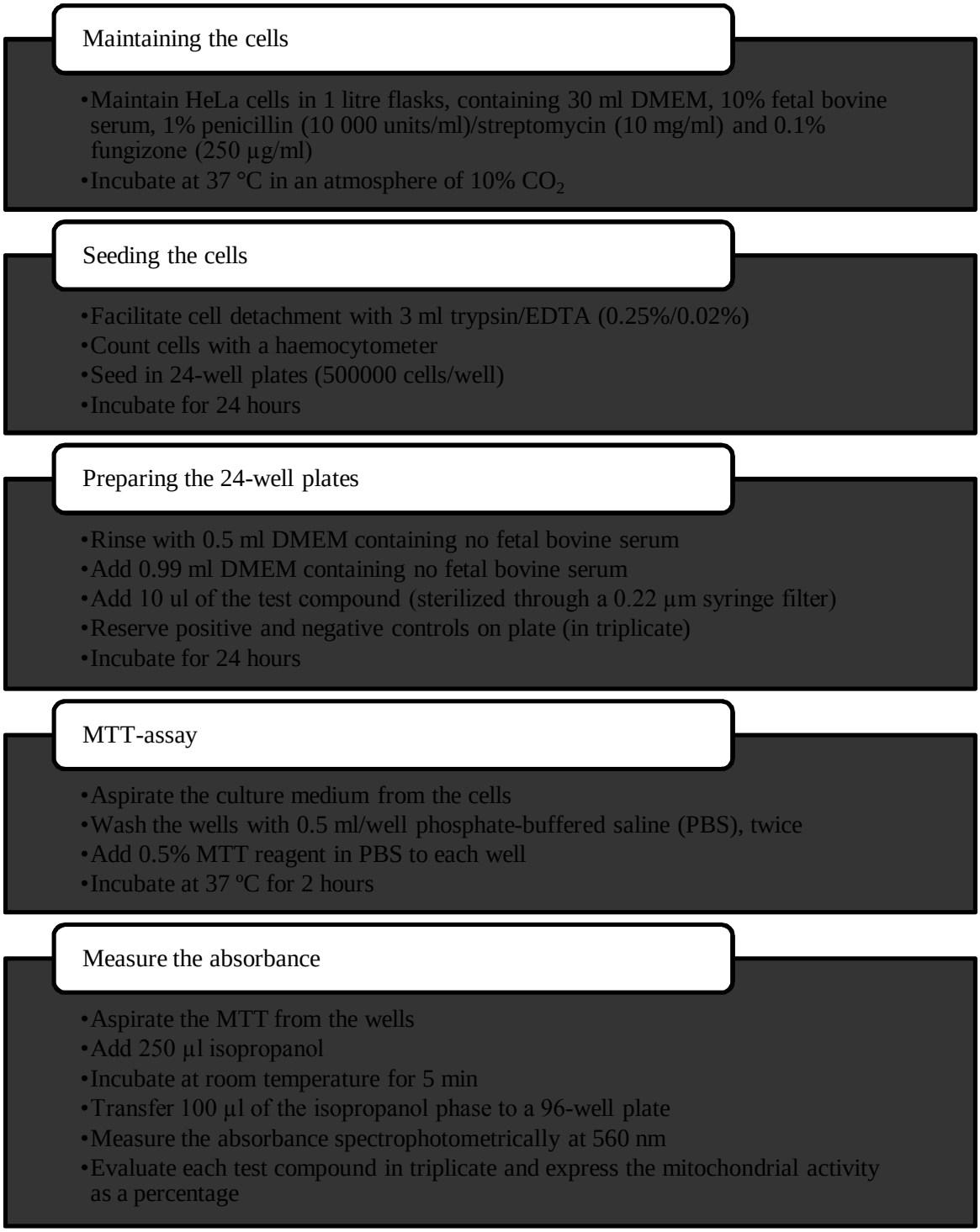

Figure 4.10 Workflow used for the determination of cell viability.

4.7.2 Results - cell viability determination:

The percentage viable cells after treatment with the 3,4-dihydro-2(1*H*)-quinolinone derivatives, **4** and **5**, were calculated as shown by the equation above. The results are shown in Table 4.4. It is evident from the results that at concentrations of 1 μM, that some of the 3,4-dihydro-2(1*H*)-quinolinone derivatives are toxic for the cultured cells. At 1 μM, the cell viability after treatment with the 3,4-dihydro-2(1*H*)-quinolinone derivatives ranged from 55%-105%. At concentrations of 10 μM, the cell viability after treatment with the 3,4-dihydro-2(1*H*)-quinolinone derivatives ranged from 45%-108%. Those compounds that were not toxic to cultured cells, even at 10 μM were **4d** and **5d**. Compounds that exhibited a low degree of cytotoxicity were **4b**, **5a**, **5c** and **5d**. These compounds reduced cell viability to levels >70% at 10 μM. Compounds **4b** and **5a** were found not to be cytotoxic at 1 μM.

Since **5a** was found to be a highly potent MAO-B inhibitor, this compound is an example of a relatively nontoxic high potency MAO-B inhibitor. The most potent MAO-B inhibitors of the series, compounds **5b** and **5c**, unfortunately displayed some degree of cytotoxicity. Compound **5b** reduced cell viability to 64% at 10 μM while **5c** reduced cell viability to 86% at 10 μM. These results suggest that **5c** is less toxic than **5b** and therefore more suitable as a lead for the design of MAO-B inhibitors. While no clear SAR for the cytotoxicity of the 3,4-dihydro-2(1*H*)-quinolinone derivatives are apparent, it is noteworthy that the phenethyl substituted homologues, compounds **4d** and **5d** were not toxic to the cultured cells. This suggests that the phenethyl substitution of the 3,4-dihydro-2(1*H*)-quinolinone moiety yields a lower degree of cytotoxicity than substitution with the other substituents explored in this study.

Table 4.4: The percentage viable cells remaining after treatment with the 3,4-dihydro-2(1*H*)-quinolinone derivatives, **4** and **5**.

	1 μM	**10 μM**
4a	60.5 ± 17.4	45.1 ± 11.2
4b	99.0 ± 8.15	81.9 ± 14.1
4c	68.5 ± 19.3	66.9 ± 5.68
4d	104 ± 37.0	107 ± 18.2
4e	55.3 ± 10.3	45.8 ± 4.49
5a	104 ± 3.96	70.2 ± 15.9
5b	73.4 ± 14.2	64.4 ± 8.27
5c	88.1 ± 9.35	86.1 ± 10.8
5d	105 ± 2.19	108 ± 5.44
5e	88.6 ± 14.9	79.8 ± 7.34

Values are given as mean ± SD of triplicate determinations.

4.8. Conclusion

The present study shows that a series of 3,4-dihydro-2(1*H*)-quinolinone derivatives are highly potent and selective MAO-B inhibitors, even when compared to the previously studied coumarin derivatives (Gnerre *et al.*, 2000). For example, the most potent inhibitor, compound **5c** (IC_{50} = 2.9 nM) is approximately equipotent to coumarin derivative **8**, which represents the most active MAO-B inhibitor among a large series of coumarin derivatives previously studied (Gnerre *et al.*, 2000). It should be noted that **8** was evaluated as an inhibitor of rat brain MAO-B, while in the present study, the human enzymes were employed. Based on its high MAO-B inhibitory potency and selectivity over the MAO-A isoform, **5c** represents a suitable lead for the development of novel therapies for Parkinson's disease. In addition, **5c** interacts reversibly with MAO-B, which is a desirable property when designing antiparkinsonian therapies. The limited SARs derived for the inhibition data show that substitution on the C7 position of the 3,4-dihydro-2(1*H*)-quinolinone moiety, particularly with the benzyloxy substituent, is more favourable for MAO-B inhibition than substitution on the C6 position. In addition, halogen substituents on the benzyloxy phenyl ring further enhances MAO-B inhibition. Although a limited number of derivatives were examined, this study provides "proof of concept" for the proposal that the 3,4-dihydro-2(1*H*)-quinolinone moiety is a promising scaffold for the design of MAO-B inhibitors. A limited examination of the physicochemical properties of 3,4-dihydro-2(1*H*)-quinolinones were carried out to determine if these promising inhibitors may be acceptable as lead compounds for the treatment of CNS disorders. The results show that the 3,4-dihydro-2(1*H*)-quinolinones are highly lipophilic and are expected to readily permeate physiological membranes. These compounds should therefore gain access to the central nervous system. A potential concern is the finding that the LogP values of the 3,4-dihydro-2(1*H*)-quinolinones are >3 which indicates that these compounds may have limited bioavailability due to low solubility. Cytotoxicity studies show that, while the 3,4-dihydro-2(1*H*)-quinolinones are toxic to cultured cells, the concentrations at which they display toxicity are well above the IC_{50} values for the inhibition of MAO-B by the most active inhibitors. For example, compound **5c** exhibits an IC_{50} value of 0.0029 μM while cell viability is reduced to 86% at a concentration of 10 μM. These data suggest that at lower concentrations, the less toxic 3,4-dihydro-2(1*H*)-quinolinones such as **5c** should not reduce cell viability. In this regard, it was interesting to note that the phenethyl substututed homologues, compounds **4d** and **5d** were not toxic to the cultured cells

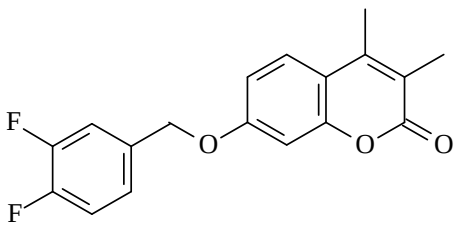

Figure 4.11 The structure of coumarin derivative **8.**

CHAPTER 5
CONCLUSION

In the current study, 3,4-dihydro-2(1*H*)-quinolinone derivatives (**4a-e** and **5a-e**) were synthesized and evaluated as recombinant human MAO-A and MAO-B inhibitors. The structures of the target quinolinone derivatives are shown in table 5.1. The MAOs are mitochondrial bound enzymes which metabolise neurotransmitter and dietary amines in the brain and peripheral tissues. MAO-A is the main form in the placenta and gastrointestinal tract, whilst MAO-B is the main form in the basal ganglia, blood platelets and liver. MAO-A in the intestine, is necessary for the deactivation of catecholamines in circulation as well as vasopressors such as tyramine ingested in the diet. MAO-A inhibitors are used in the treatment of depression since these drugs inhibit the oxidation of serotonin and noradrenaline in the central nervous system. Several side-effects occur with the irreversible inhibition of MAO-A, including the cheese reaction and serotonin syndrome. Since MAO-B is the main enzyme responsible for the catabolism of dopamine in the basal ganglia in the midbrain, inhibitors of this enzyme may be useful in the treatment of PD. MAO-B inhibitors may slow the depletion of dopamine stores and elevate the levels of endogenous dopamine. The combined use of levodopa and MAO-B inhibitors allows for a reduction of the dosage of levodopa that is necessary for a therapeutic response which, in turn, leads to diminished levodopa associated side effects (Fernandez & Chen, 2007).

The lead compounds for the current study was a series of substituted coumarin (1-benzopyran-2-one) derivatives,which have been shown to act as potent MAO-B inhibitors (Gnerre *et al*., 2000). The 3,4-dihydro-2(1*H*)-quinolinone ring system is structurally similar to coumarin and appropriately substituted 3,4-dihydro-2(1*H*)-quinolinone may thus also possess inhibitory activity for MAO-B. Coumarin has previously emerged as a particularly promising scaffold for the design of potent competitive MAO-B inhibitors, with substitution at C7 of the coumarin ring yielding high potency compounds. Based on the structural similarity between the coumarin moiety and 3,4-dihydro-2(1*H*)-quinolinone, the present study examined the possibility that a series of 3,4-dihydro-2(1*H*)-quinolinone derivatives may act as reversible and selective inhibitors of recombinant human MAO-B. Alkyloxy substitutions (benzyloxy, phenylethoxy and phenylpropoxy) were made at C6 and C7 of the 3,4-dihydro-2-(1*H*)-quinolinone moeity. The benzyloxy-substituted 3,4-dihydro-2(1*H*)-quinolinones were further explored by substitution on the benzyloxy phenyl ring with halogens (Cl, Br), since halogen substitution on the benzyloxy ring of 7-substituted benzyloxy-3,4-dimethylcoumarins was previously shown to enhance MAO inhibition potency (Gnerre *et al*., 2000).

Table 5.1: The series of C6- and C7-substituted 3,4-dihydro-2(1*H*)-quinolinones that were synthesised in this study

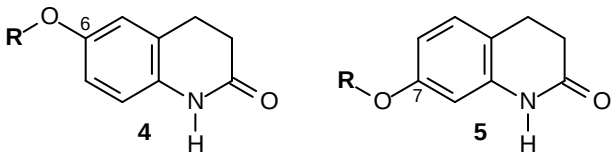

Compound	R
4a	$C_6H_5CH_2$–
4b	3-$ClC_6H_4CH_2$–
4c	3-$BrC_6H_4CH_2$–
4d	$C_6H_5(CH_2)_2$–
4e	$C_6H_5(CH_2)_3$–
5a	$C_6H_5CH_2$–
5b	3-$ClC_6H_4CH_2$–
5c	3-$BrC_6H_4CH_2$–
5d	$C_6H_5(CH_2)_2$–
5e	$C_6H_5(CH_2)_3$–

Ten 3,4-dihydro-2(1*H*)-quinolinone derivatives (**4a-e** and **5a-e**) were synthesized according to the literature procedure (Shigematzu, 1961) (Figure 5.1). Commercially available 6-hydroxy-3,4-dihydro-2(1*H*)-quinolinone (**6**) and 7-hydroxy-3,4-dihydro-2(1*H*)-quinolinone (7), suspended in ethanol, were treated with an appropriately substituted alkyl bromide in the presence of KOH. After heating the mixture at reflux for 5 h, the reaction was poured into aqueous NaOH (1%). The crude thus obtained was purified by recrystallization. The structures of the target inhibitors were verified by ^{1}H NMR, ^{13}C NMR and mass spectrometry (MS). Both ^{1}H NMR and ^{13}C NMR as well as the MS data corresponded with the proposed structures.

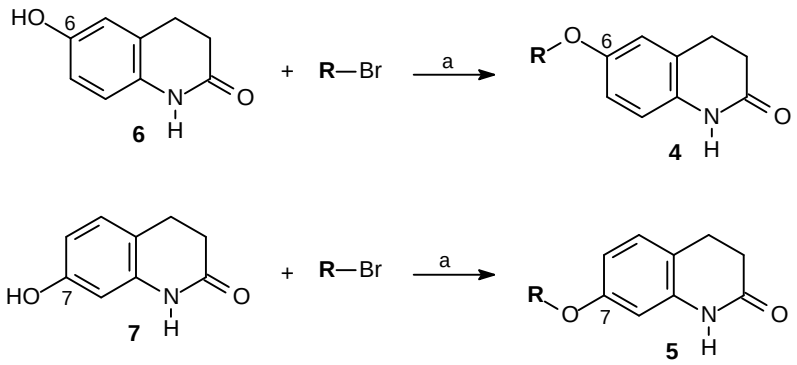

Figure 5.1 Synthetic route to the 3,4-dihydro-2(1*H*)-quinolinone derivatives **4** and **5**. Reagents and conditions: (a) KOH, ethanol, reflux.

The 3,4-dihydro-2(1*H*)-quinolinone derivatives (**4a-e** and **5a-e**) were evaluated as inhibitors of the recombinant human MAO-A and MAO-B enzymes, which are commercially available (Novaroli *et al*., 2005). To measure MAO activities, the MAO-A/B mixed substrate, kynuramine, was employed. Kynuramine is oxidized by the MAO enzymes to yield 4-hydroxyquinoline. Since 4-hydroxyquinoline is fluorescent, the concentrations of the 4-hydroxyquinoline were measured by fluorescence spectrophotometry (λ_{ex} = 310 nm; λ_{em} = 400 nm). From the MAO activity measurements in the presence of the test inhibitors, sigmoidal dose-response curves were constructed and the inhibition potencies, the corresponding IC_{50} values, were calculated. The results showed that the 3,4-dihydro-2(1*H*)-quinolinone derivatives are potent inhibitors of MAO-B with all of the compounds having higher selectivity for MAO-B compared to MAO-A. The most potent MAO-B inhibitor, 7-(3-bromobenzyloxy)-3,4-dihydro-2(1*H*)-quinolinone (**5c**), is an exceptionally potent MAO-B inhibitor with an IC_{50} value of 0.0029 μM. It was shown that substitution on the C7 position of the 3,4-dihydro-2(1*H*)-quinolinone moiety yields compounds which are more potent MAO-B inhibitors compared to substitution on C6. Interestingly benzyloxy substitution on C7 is more favourable than phenylethoxy and phenylpropoxy substitution on this position.

The reversibility of MAO-B inhibition by compound **5c** was evaluated, since this was the most potent MAO-B inhibitor of the series. The results suggested that **5c** acts as a reversible inhibitor of MAO-B. To further determine the mode of inhibition, a set of Lineweaver-Burk plots were constructed. The observation that the lines were linear and intersect on the y-axis suggested that **5c** is a competitive inhibitor of human MAO-B. This was further evidence that the interaction of **5c** with MAO-B is reversible.

LogP, the logarithm of the water/n-octanol partition coefficient was measured to estimate the lipophilicities of the 3,4-dihydro-2(1*H*)-quinolinone derivatives (**4a-e** and **5a-e**). The shake-flask method was employed, using water (hydrophilic phase) and octanol (hydrophobic phase). Hence the partition coefficient is a measure of how hydrophilic or hydrophobic the compounds are. The logP values of the 3,4-dihydro-2(1*H*)-quinolinone derivatives were smaller than 5, but larger than 3. Although within the acceptable range, the relatively high logP values may lead to lower bioavailability. Lipinsky's rules state that compounds with logP values <5 are drug-like and logP values between 1 and 3 are in the ideal range for bioavailability. It may thus be concluded that the 3,4-dihydro-2(1*H*)-quinolinone derivatives are drug-like, but bioavailability may be a problem due to limited solubility of the compounds in aqueous medium.

The toxicity of the 3,4-dihydro-2(1*H*)-quinolinone derivatives were evaluated using the MTT cell viability assay. Human HeLa cells were exposed to the compounds at 1 μM and 10 μM for 24 h and the viability of the cells were subsequently measured. Viable cells reduce MTT to a blue formazan, which may be quantified with a spectrophotometer. The most potent compound, **5c**, was found to be weakly toxic to HeLa cells, with 88.1% viable cells remaining at a concentration of 1 μM of the test compound. This concentration is well above the IC_{50} value for the inhibition of MAO-B by compound **5c**. At the low doses required for MAO-B inhibition, **5c** is thus unlikely to be cytotoxic.

This study has shown that benzyloxy substituted 3,4-dihydro-2(1*H*)-quinolinone derivatives, containing halogens (Cl, Br) on the benzyloxy phenyl ring, are particularly potent MAO-B inhibitors. In this regard, substitution on the C7 position of the 3,4-dihydro-2(1*H*)-quinolinone moiety leads to significantly more potent MAO-B inhibition compared to substitution on C6.

Based on the discussion above, it may be concluded that the objectives given in Chapter 1 has been achieved. In addition, the hypothesis of this study has been proven: 3,4-dihydro-2(1*H*)-quinolinone is a suitable scaffold for the design of MAO-B inhibitors and appropriate substitution yields highly potent MAO-B inhibitors. Such compounds are thus suitable leads for the design of antiparkinsonian therapies.

BIBLIOGRAPHY

Abeles, R.H. & Maycock, A.L. 1976. Suicide enzyme inactivators. *Accounts of chemical research*, 9:313-319

Athanassiadou, A., Voutsinas, G., Psiouri, E., Leroy, E., Polymeropoulos, M.H., Ilias, A., Maniatis, G.M. & Papapetropoulos, T. 1999. Genetic analysis of families with Parkinson disease that carry the Ala53Thr mutation in the gene encoding alpha-synuclein. *The American Journal of Human Genetics*. 65:555-558.

Averill-Bates, D.A., Agostinelli, E., Przybytkowski, E., Mateescu, M.A. & Mondovi, B. 1993. Cytotoxicity and kinetic analysis of purified bovine serum amine oxidase in the presence of spermine in Chinese hamster ovary cells. *Archives of biochemistry and biophysics*, 300:75-79.

Binda, C., Li, M., Hubálek, F., Restelli, N., Edmondson, D.E. & Mattevi, A. 2003. Insights into the mode of inhibition of human mitochondrial monoamine oxidase B from high-resolution crystal structures. *Proceedings of the national academy of sciences of the United States of America*, 100:9750-9755.

Bové, J., Prou, D., Perier, C. & Przedborski, S. 2005. Toxin induced models of Parkinson's disease. *The journal of the American society for experimental neurotherapeutics*, 2:484-494.

Bower, J.H., Maraganore, D.M., McDonnell, S.D.K. & Rocca, W.A. 1999. Incidence and distribution of parkinsonism in Olmsted County, Minnesota, 1976-1990. *Neurology.* 52:1214-20.

Carlsson, A. 1959. The occurrence, distribution and physiological role of catecholamines in the nervous system. *Pharmacological reviews,* 11:490-493.

Chen, J.J. & Swope, D.M. 2005. Clinical pharmacology of rasagiline: a novel, second-generation propargylamine for the treatment of Parkinsons disease. *Journal of clinical pharmacology*. 45:878-94.

Chen, J.F., Steyn, S., Staal, R., Petzer, J.P., Xu, K., Van Der Schyf, C.J., Castagnoli, K., Sonsalla, P.K., Castagnoli Jr., N. & Schwarzschild, M.A. 2002. 8-(3-Chlorostyryl)caffeine may attenuate MPTP neurotoxicity through dual actions of monoamine oxidase inhibition and A_{2A} receptor antagonism. *Journal of biological chemistry,* 277:36040-36044.

Cheng, Y.C. & Prusoff, W.H. 1973. Relationship between the inhibition constant (K_i) and the concentration of inhibitor which causes 50 percent inhibition (I_{50}) of an enzymatic reaction. *Biochemical pharmacology*, 22:3099-3108.

Da Prada, M., Kettler, R., Keller, H.H., Cesura, A.M., Richards, J.G., Saura Marti, J., Muggli-Maniglio, D., Wyss, P.C., Kyburz, E. & Imhof, R. 1990. From moclobemide to ro 19-6327 and ro 41-1049: The development of a new class reversible, selective MAO-A and MAO-B inhibitors. *Journal of neural transmission (suppl.)*, 29:279-292.

Dauer, W. & Przedborski, S. 2003. Parkinson's disease: Mechanisms and models. *Neuron*, 39:889-909.

De Colibus, L., Li, M., Binda, C., Lustig, A., Edmondson, D.E. & Mattevi, A. 2005. Three dimensional structure of human monoamine oxidase A (MAO-A): Relation to the structures of rat MAO-A and human MAO-B. *Proceedings of the national academy of sciences of the United States of America*, 102:12684-12689.

De Rijk, M.C., Breteler, M.M., Graveland, G.A., Ott, A., Grobbee, D.E., van der Meché, F.G. & Hofman, A. 1995. Prevalence of Parkinson's disease in the elderly: the Rotterdam Study. *Neurology*. 45:2143-2146.

Dixon, M. 1953. The determination of enzyme inhibitor constants. *The biochemical journal*, 55:170-171.

Edmondson, D.E., Binda, C. & Mattevi, A. 2004a. The FAD binding sites of human monoamine oxidases A and B. *Neurotoxicology*, 25:63-72.

Edmondson, D.E., Mattevi, A., Binda, C., Li, M. & Hubálek, F. 2004b. Structure and mechanism of monoamine oxidase. *Current medicinal chemistry*, 11:1983-1993.

Edmondson, D.E., Mattevi, A. & Binda, C. 2007. Structural insights into the mechanism of amine oxidation by monoamine oxidases A and B. *Archives of biochemistry and biophysics*, 464:269-276.

Fahn, S., Oakes, D., Shoulson, I., Kieburtz, K., Rudolph, A., Lang, A., Olanow, C.W., Tanner, C., Marek, K. & Parkinson Study Group. 2004. Levodopa and the progression of Parkinson's disease. *The New England journal of medicine*. 351:2498-508.

Fahn, S. & Przedborski, S. 2000. Parkinsonism. (*In* Rowland, L.P., *ed*. Merritt's neurology. 10th ed. New York: Lippincott Williams & Wilkins. p.679-693).

Fernandez, H.H. & Chen, J.J. 2007. Monoamine oxidase B inhibition in the treatment of Parkinson's disease. *Pharmacotherapy*, 27:174S-185S.

Finberg, J.P., Wang, J., Bankiewich, K., Harvey-White, J., Kopin, I.J. & Goldstein, D.S.J. 1998. *Journal of neural transmission*, 52: 279.

Finberg, J.P., Tenne, M. & Youdim, M.B. 1981. Tyramine antagonistic properties of AGN 1135, an irreversible inhibitor of monoamine oxidase type B. *British journal of pharmacology*, 73:65-74.

Finberg, J.P. & Tenne, M. 1982. Relationship between tyramine potentiation and selective inhibition of monoamine oxidase types A and B in the rat vas deferens. *British journal of pharmacology*, 77:13-21.

Fowler, J.S., Volkow, N.D., Logan, J., Wang, G., MacGregor, R.R., Schlyer, D., Wolf, A.P., Pappas, N., Alexoff, D., Shea, C., Dorflinger, E., Kruchowy, L., Yoo, K., Fazzini, E. & Patlak, C. 1994. Synaps, 18:86.

Fowler, J.S., Volkow, N.D., Wang, G., Logan, J., Pappas, N., Shea, C. & MacGregor, R. 1997. Age-related increases in brain monoamine oxidase B in living healthy human subjects. *Neurobiology of aging*, 18:431-435.

Gnerre, C., Catto, M., Leonetti, F., Weber, P., Carrupt, P., Altomare, C., Carotti, A. & Testa, B. 2000. Inhibition of monoamine oxidase by functionalized coumarin derivatives: biological activities, QSAR's, and 3D-QSAR's. *Journal* of *medicinal chemistry,* 43:4747-4758.

David, G., Standaaert & Young, A.B. 2001. Nervous system degenerative disorders. (*In* Hardman, J.G. & Limbird, L.E., *eds.* Goodman & Gilman's the pharmacological basis of therapeutics. 10th ed. New York: McGraw-Hill. p.549-569)

Hasan, F., McCrodden, J.M., Kennedy, N.P. & Tipton, K.F. 1988. The involvement of intestinal monoamine oxidase in the transport and metabolism of tyramine. *Journal of neural transmission (suppl.),* 26:1-9.

Hely, M.A., Reid, W.G., Adena, M.A., Haliday, G.M. & Morris, J.G. 2008. The Sydney multicenter study of Parkinson's disease: The inevitability of dementia at 20 years. *Movement disorders: official journal of the Movement Disorder Society*. 23:837-844.

Hubálek, F., Binda, C., Khalil, A., Li, M., Mattevi, A., Castagnoli, N. & Edmondson, D.E. 2005. Demonstration of isoleucine 199 as a structural determinant for the selective inhibition of human monoamine oxidase B by specific reversible inhibitors. *Journal of biological chemistry*, 280:15761-15766.

Jenner, P. 1998. Oxidative mechanisms in nigral cell death in Parkinson's disease. *Movement disorders (suppl.)*, 1:24-34.

Katzenschlager, R., Head, J., Schraq, A., Ben-Shlomo, Y., Evans, A. & Lees, A.J. 2008. Fourteen-year final report of the randomized PDRG-UK trial comparing three initial treatments in PD. *Neurology*. 71:474-480.

Kerns, E. & Di, L. 2008. Drug-like properties: concepts, structure design and methods: from ADME to toxicity optimization. New Jersey: Academic Press.

Khalil, A.A., Davies, B. & Castagnoli, N. 2006. Isolation and characterization of a monoamine oxidase B selective inhibitor from tobacco smoke. *Bioorganic & medicinal chemistry*, 14:3392-3398.

Kirkinezos, I.G. & Moraes, C.T. 2001. Reactive oxygen species and mitochondrial diseases. *Cell & developmental biology*, 12:449–457.

Korrell, M. & Tanner, C.M. 2005. Epidemiology of Parkinson's disease: an overview. (*In* Ebadi, M. & Pfeiffer, R., *eds*. Parkinson's disease. Florida: CRC Press. p.39-50).

Kruger, R., Kuhn, W., Muller, T., Woitalla, D., Graeber, M., Kosel, S., Przuntek, H., Epplen, J.T., Schols, L. & Riess, O. 1998. Ala30Pro mutation in the gene encoding alpha-synuclein in Parkinson's disease, *Nature genetics*. 18:106-108.

Lees, A.J., Hardy, J. & Revesz, T. 2009. Parkinson's disease. *The lancet*, 373:2055-2066.

LeWitt, P.A. & Taylor, D.C. 2008. Protection against Parkinson's disease progression: clinical experience. *Neurotherapeutics*. 5:210-225.

Lineweaver, H. & Burk, D. 1934. The determination of enzyme dissociation constants. *Journal of the American chemical society*, 56:658-666.

Miller, J.R. & Edmondson, D.E. 1999. Influence of flavin analogue structure on the catalytic activities and flavinylation reactions of recombinant human liver monoamine oxidase A and B. *The journal of biological chemistry*, 274:23515-23525.

Miyasaki, J.M. 2006. New practice parameters in Parkinson's disease. *Nature reviews neurology.* 2:638-639.

Morpurgo, L., Agostinelli, E., Muccigrosso, J., Martini, F., Mondovi, B. & Avigliano, L. 1989. Benzylhydrazine as a pseudo-substrate of bovine serum amine oxidase. *Biochemical jounal*, 260:19-25.

Mosmann, T. 1983. Rapid colorimetric assay for cellular growth and survival: application to proliferation and cytotoxicity assays. *Journal of immunological methods,* 65:55-63.

Murray, R.K., Granner, D.K., Mayes, P.A. & Rodwell, V.W. 2003. Enzymes: kinetics. *Harper's illustrated biochemistry*. 26th ed. s.l.:McGraw-Hill. p60-71.

Novaroli, L., Reist, M., Favre, E., Carotti, A., Catto, M. & Carrupt, P.A. 2005. Human recombinant monoamine oxidase B as reliable and efficient enzyme source for inhibitor screening. *Bioorganic and medicinal chemistry*, 13:6212.

Nicotra, A. & Parvez, S.H. 1999. Methods for assaying monoamine oxidase A and B activities: Recent developments. *Biogenic amines*, 15:307-320.

Nicotra, A., Pierucci, F., Parvez, H. & Santori, O. 2004. Monoamine Oxidase Expression During Development and Aging. *Neurotoxicology,* 25:155.

Parkinson, J. An essay on the shaking palsy. 2002. (Republished) *Journal of neuropsychiatry and clinical neuroscience,* 14:223-236.

Petzer, A., Pienaar, A. & Petzer, J.P. 2013. *Arzneimittel-Forsch*, 63:462.

Petzer, A., Harvey, B.H., Wegener, G. & Petzer, J.P. 2012. Azure B, a metabolite of methylene blue, is a high-potency, reversible inhibitor of monoamine oxidase**.** *Toxicology and Applied Pharmacology*, 258:403.

Polymeropoulos, M.H., Lavedan, C., Leroy, E., Ide, S.E., Dehejia, A., Dutra, A., Pike, B., Root, H., Rubenstein, J., Boyer, R., Stenroos, E.S., Chandrasekharappa, S., Athanassiadou, A., Papapetropoulos, T., Johnson, W.G., Lazzarini, A.M., Duvoisin, R.C., Di lorio, G., Golbe, L.I. & Nussbaum, R.L. 1997. Mutation in the alpha-synuclein gene identified in families with Parkinson's disease, *Science,* 276:2045-2047.

Rahbari, R., Sheahan, T., Modes, V., Collier, P., Macfarlane, C. & Badge, R.M. 2009. A novel L1 retrotransposon marker for HeLa cell line identification. *Biotechniques*, 46: 277-84.

Ramsay, R.R. 1991. Kinetic mechanism of monoamine oxidase A. *Biochemistry*, 30:4624-4629.

Rascol, O., Goetz, C.G., Koller, W.C. & Poewe, W. 2002a. Physical and occupational therapy in Parkinson's disease. *Movement disorders*, 4:156-159.

Rascol, O., Goetz, C.G., Koller, W.C. & Poewe, W. & Sampaio, C. 2002b. Treatment interventions for Parkinson's disease: an evidence based assessment. *Lancet,* 359:1589-98.

Riederer, P., Danielczyk, W. & Grunblatt, E. 2004. Monoamine oxidase-B inhibition in Alzheimer's disease. *Neurotoxicology*, 25:271-277.

Shigematsu, N. 1961. *Chemical and pharmaceutical bulletin,* 9:970.

Shih, J.C., Chen, K. & Ridd, M.J. 1999. Monoamine oxidase: From genes to behaviour. *Annual Review of Neuroscience.* 22:197-217.

Silverman, R.B., Hoffman, S.J. & Catus III, W.B. 1980. A mechanism for mitochondrial monoamine oxidase catalyzed amine oxidation. *Journal of the American chemical society*, 102:7126-7128.

Stevanato, R., Vianello, F. & Rigo, A. 1995. Thermodynamic analysis of the oxidative deamination of polyamines by bovine serum amine oxidase. *Archives of biochemistry and biophysics*, 324:374-378.

Tipton, K.F., Boyce, S., O'Sullivan, J., Davey, G.P. & Healy, J. 2004. Monoamine oxidases: Certainties and uncertainties. *Current medicinal chemistry*, 11:1965-1982.

Weissbach, H., Smith, T.E., Daly, J.W., Witkop, B. & Udenfriend, S. 1960. A rapid spectrophotometric assay of monoamine oxidase based on the rate of disappearance of kynuramine. *The jounal of biological chemistry*, 235:1160-1163.

Yacoubian, T.A. & Standaert, D.G. 2009. Targets for neuroprotection in Parkinson's disease. *Biochimica et biophysica acta*, 1792:676-687.

Youdim, M.B.H. & Bakhle, Y.S. 2006. Monoamine oxidase: Isoforms and inhibitors in Parkinson's disease and depressive illness. *British journal of pharmacology*, 147(Suppl 1):S287-S296.

Youdim, M.B.H., Edmondson, D. & Tipton, K.F. 2006. The therapeutic potential of monoamine oxidase inhibitors. *Nature reviews. Neuroscience*, 7:295-309.

Youdim, M.B.H., Finberg, J.P.M. & Tipton, K.F. 1988. Monoamine oxidase. (*In* Trendelenburg, U. & Weiner, N., *eds*. Catecholamine II. Handbook of experimental pharmacology. Berlin: Springer. p.119-192).

Youdim, M.B.H. & Weinstock, M. 2004. Therapeutic applications of selective and non-selective inhibitors of monoamine oxidase A and B that do not cause significant tyramine potentiation. *Neurotoxicology*, 25:243-250.

Zarranz, J.J., Alegre, J., Gomez-Esteban, J.C., Lezcano, E., Ros, R., Ampuero, I., Vidal, L., Hoenicka, J., Rodriguez, O., Atares, B., Llorens, V., Gomez Tortosa, E., del Ser, T., Munoz, D.G. & de Yebenes, J.G. 2004. The new mutation, E46K, of alpha-synuclein causes Parkinson and Lewy body dementia, *Annals of neurology*. 55:164-173.

Zhou, J.J.P., Zhong, B. & Silverman, R.B. 1996. Direct continuous fluorometric assay for monoamine oxidase B. *Analytical biochemistry*, 234:9-12.

Zhou, M. & Panchuk-Voloshina, N. 1997. A one-step fluorometric method for the continuous measurement of monoamine oxidase activity. *Analytical biochemistry*, 253:169-174.

APPENDIX A

6-(Benzyloxy)-3,4-dihydro-2(1*H*)-quinolinone (4a)

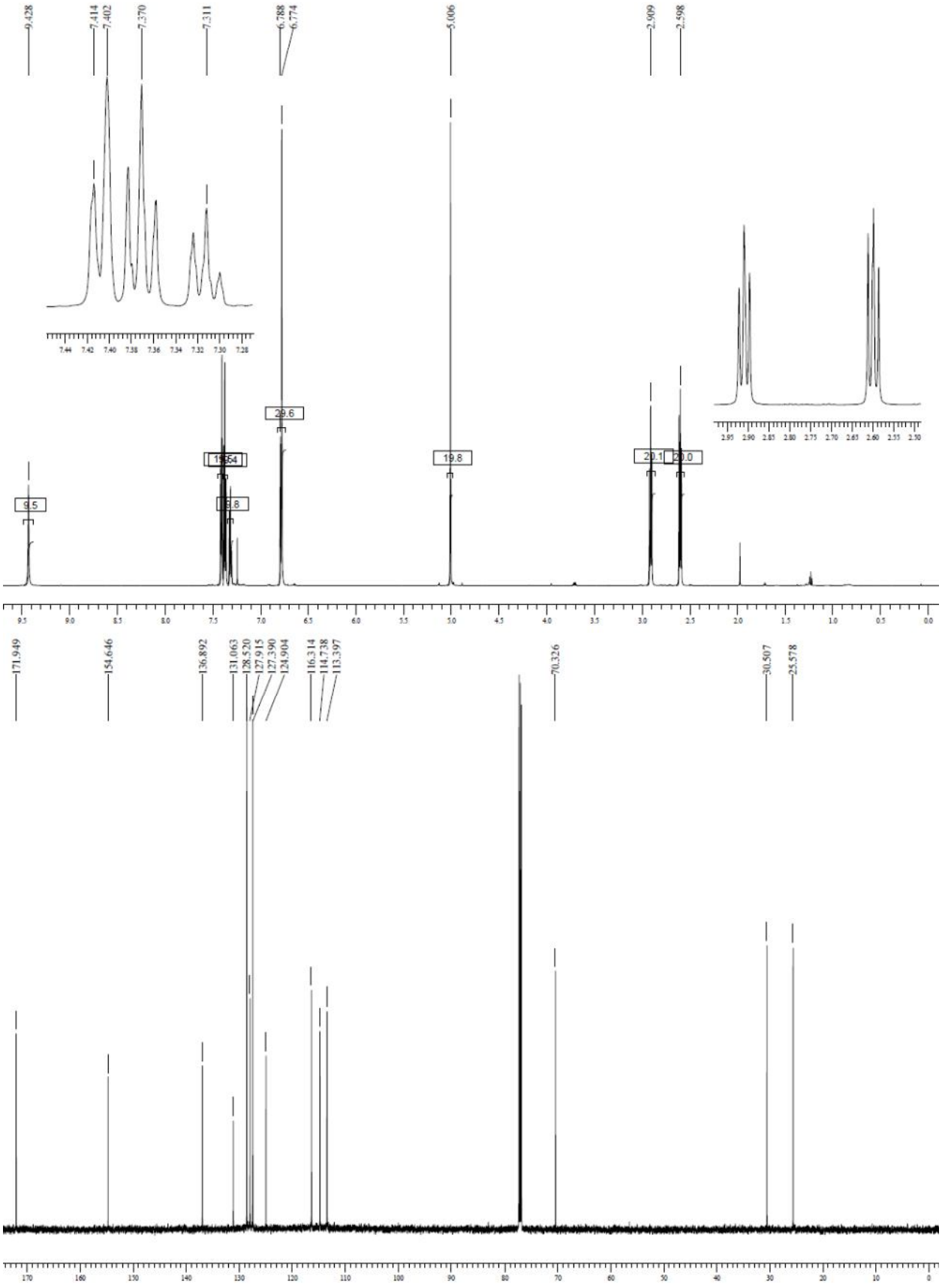

6-(3-Chlorobenzyloxy)-3,4-dihydro-2(1*H*)-quinolinone (4b)

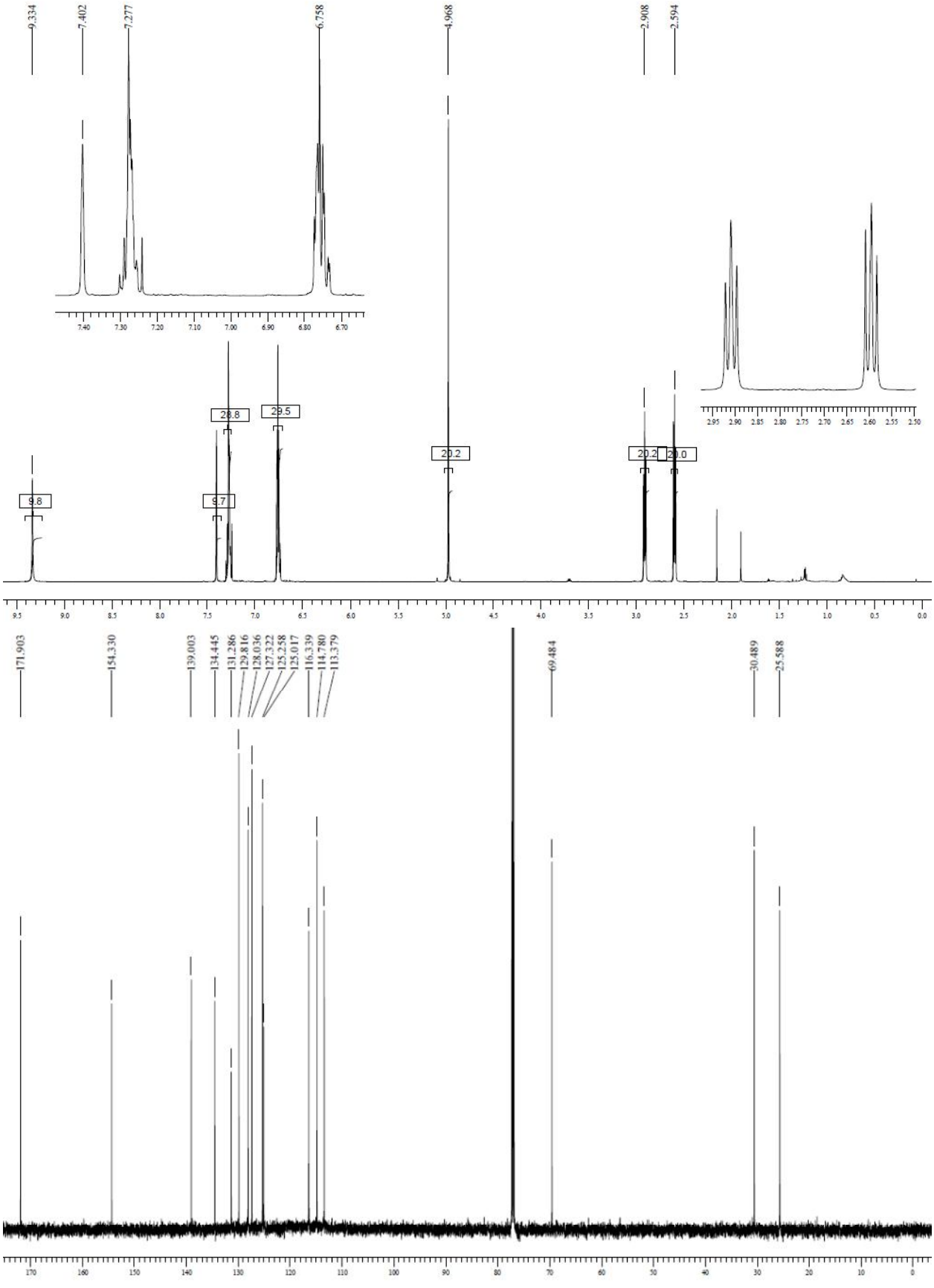

6-(3-Bromobenzyloxy)-3,4-dihydro-2(1*H*)-quinolinone (4c)

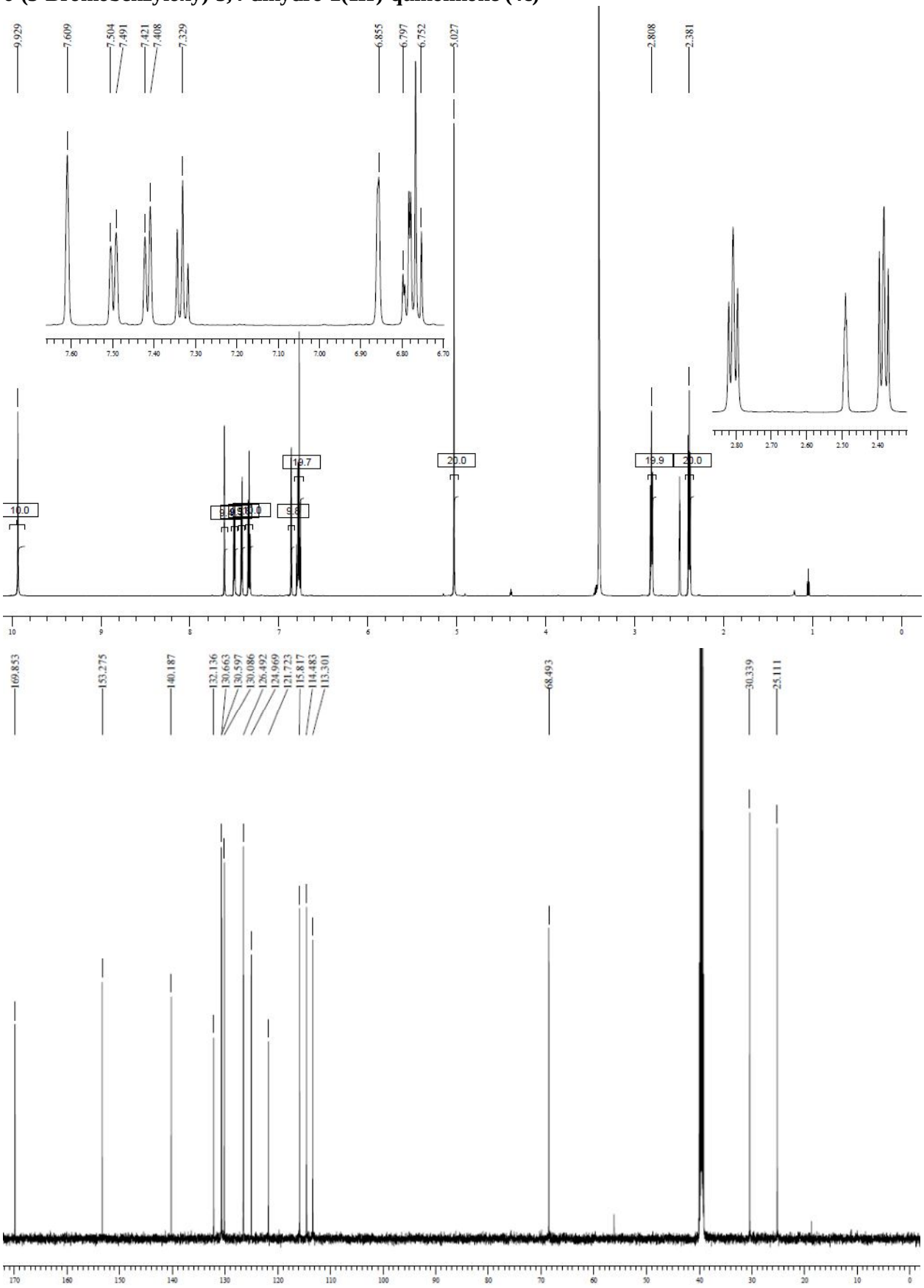

6-(2-Phenylethoxy)-3,4-dihydro-2(1*H*)-quinolinone (4d)

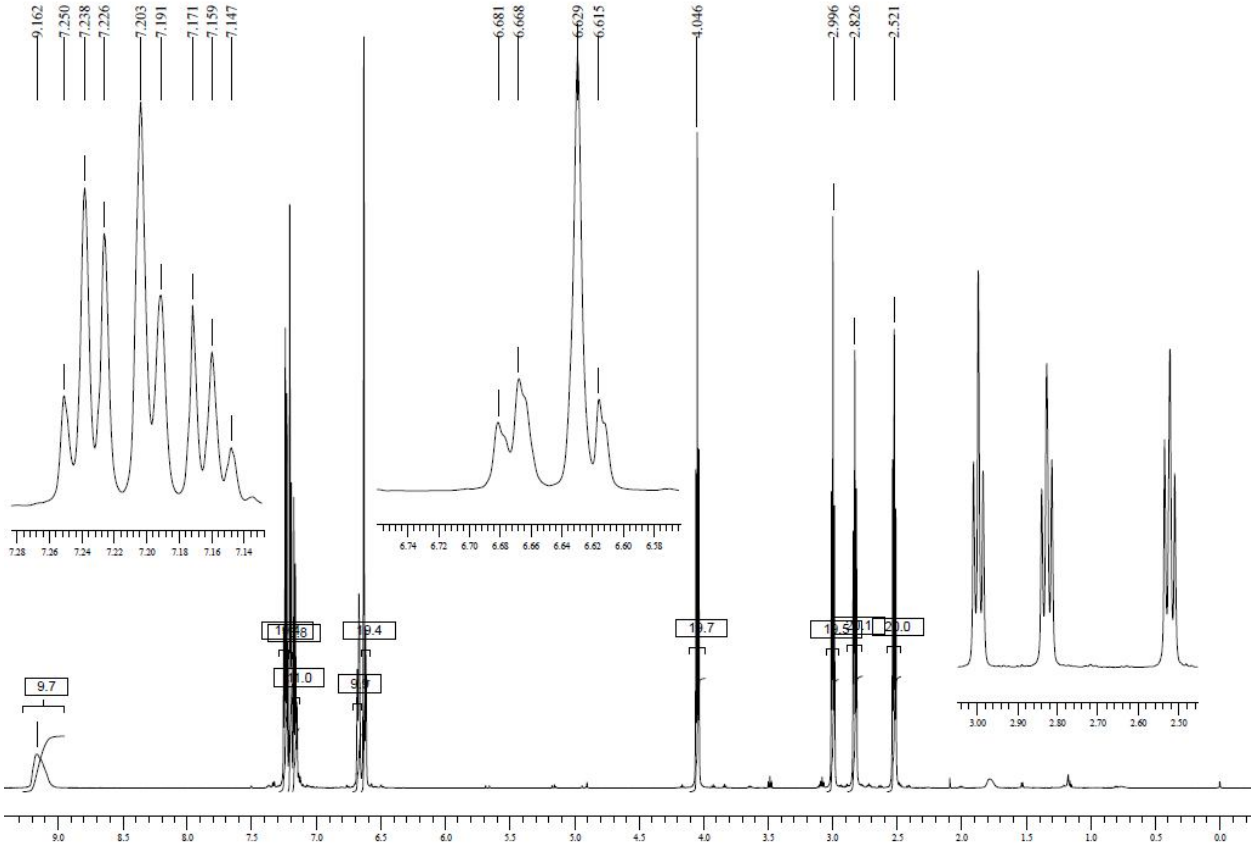

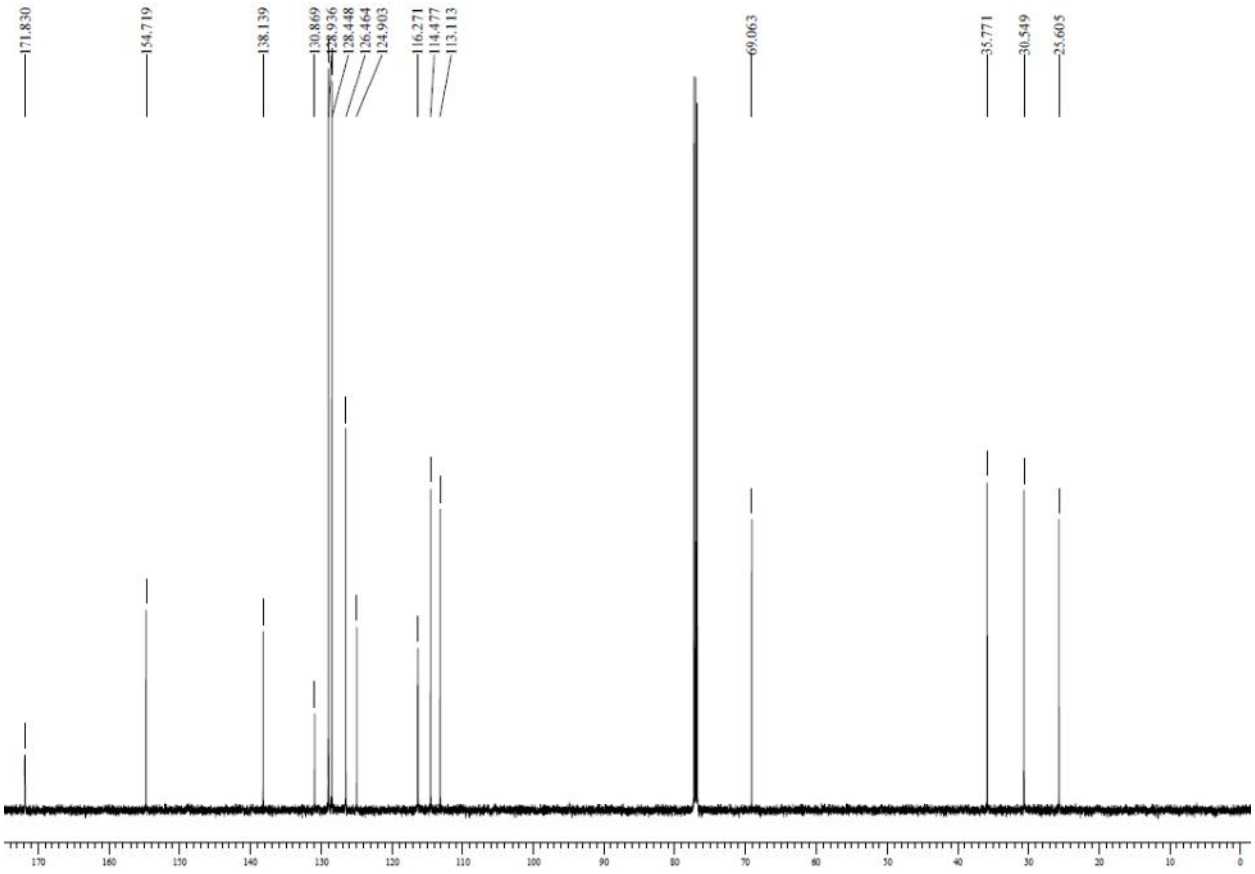

6-(3-Phenylpropoxy)-3,4-dihydro-2(1*H*)-quinolinone (4e)

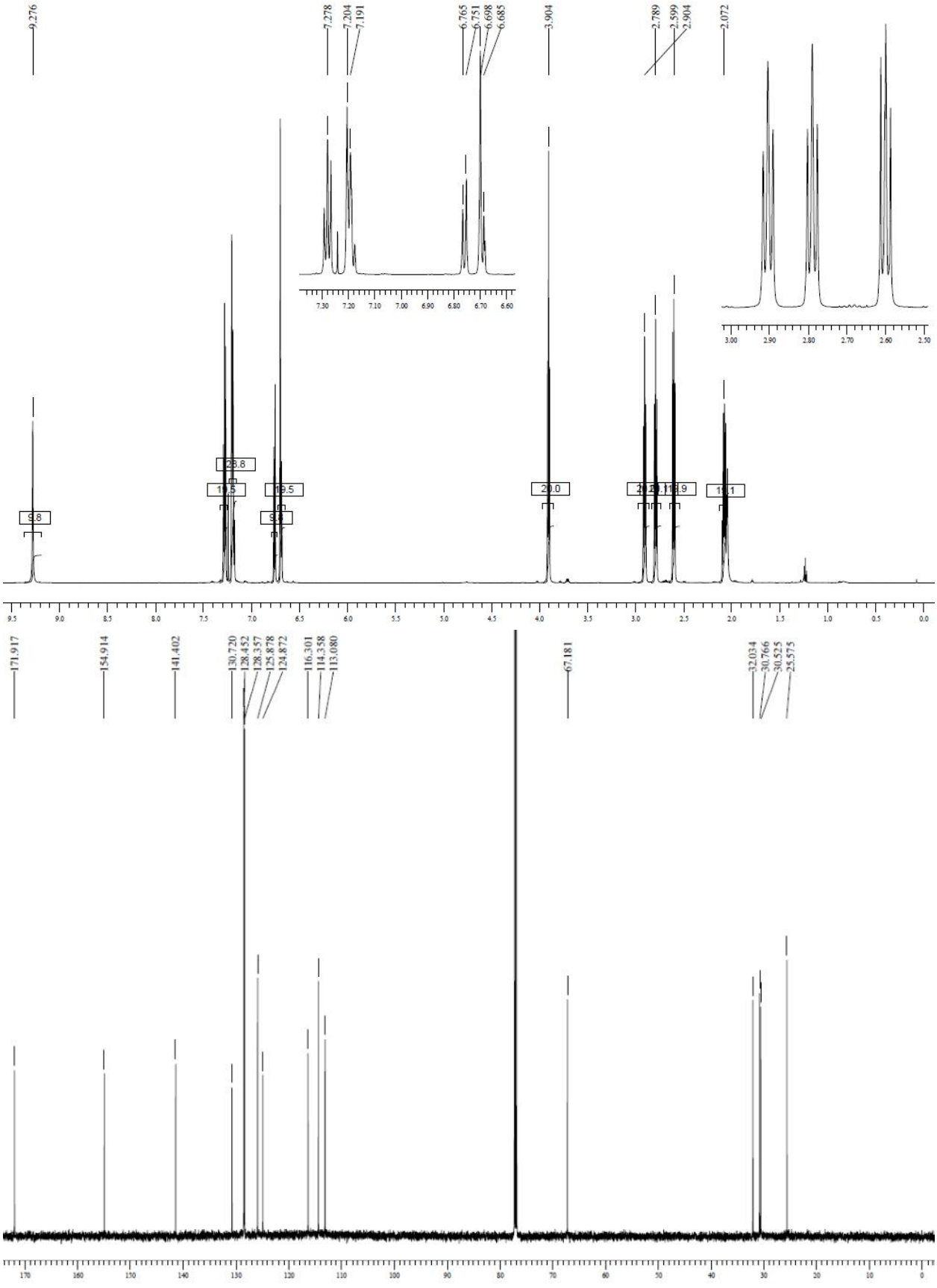

7-(Benzyloxy)-3,4-dihydro-2(1*H*)-quinolinone (5a)

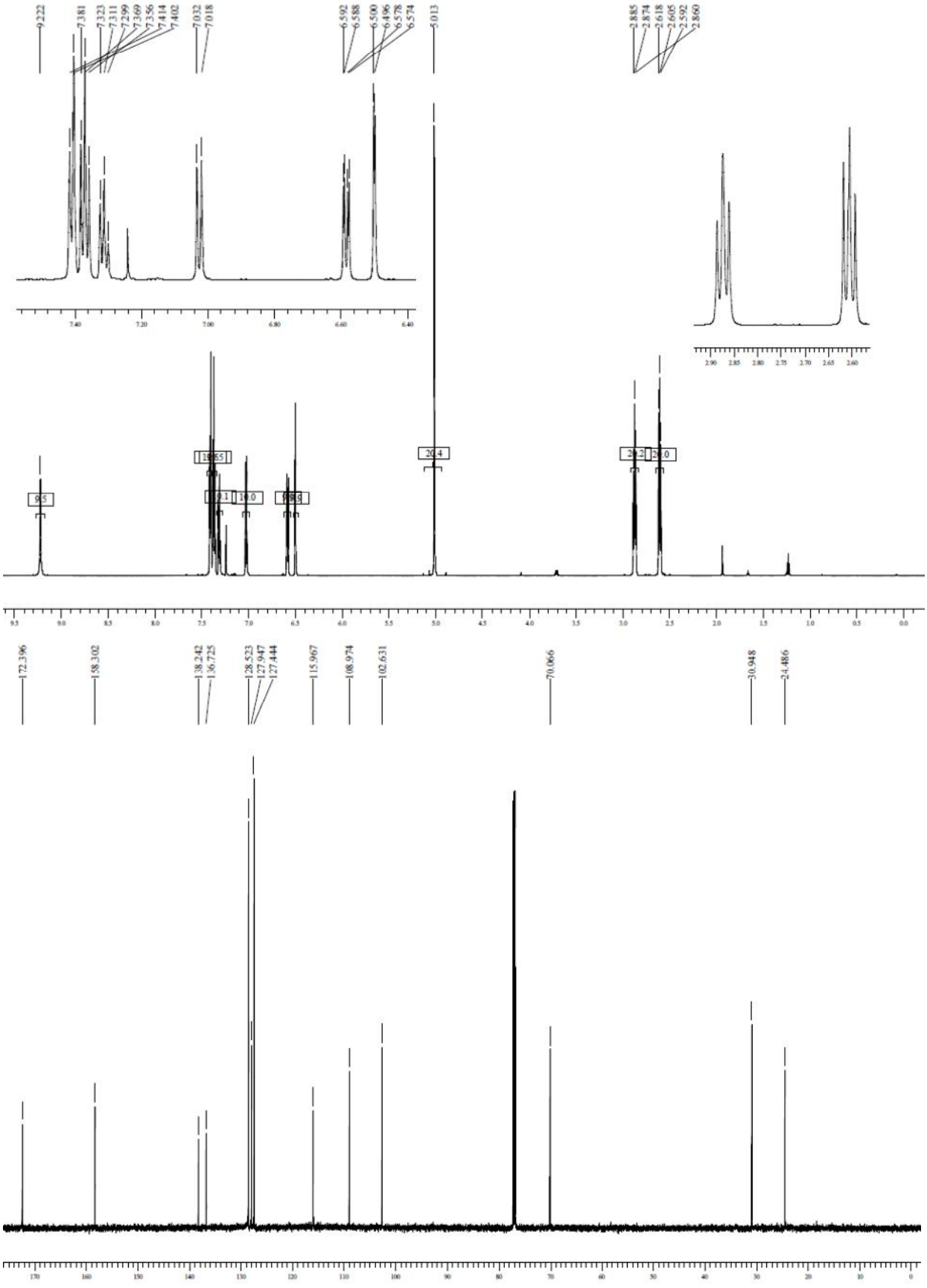

7-(3-Chlorobenzyloxy)-3,4-dihydro-2(1*H*)-quinolinone (5b)

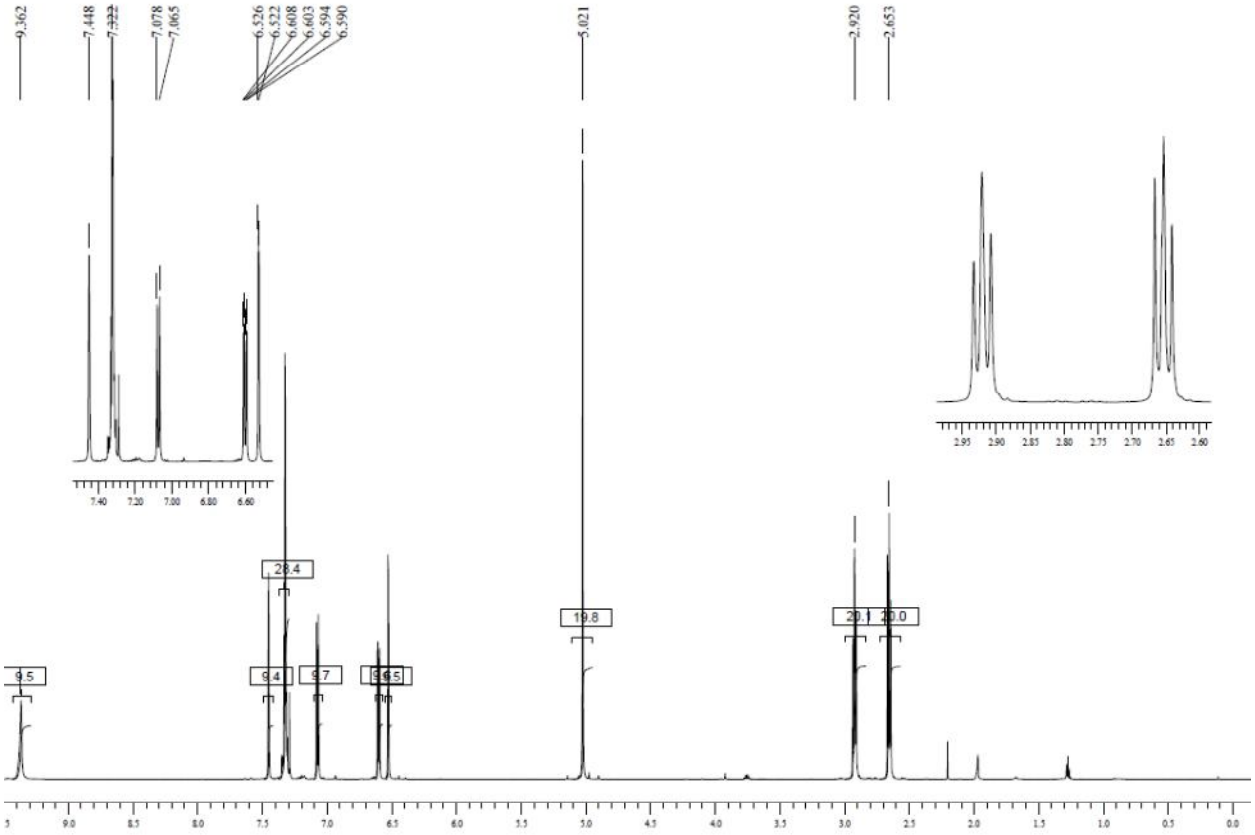

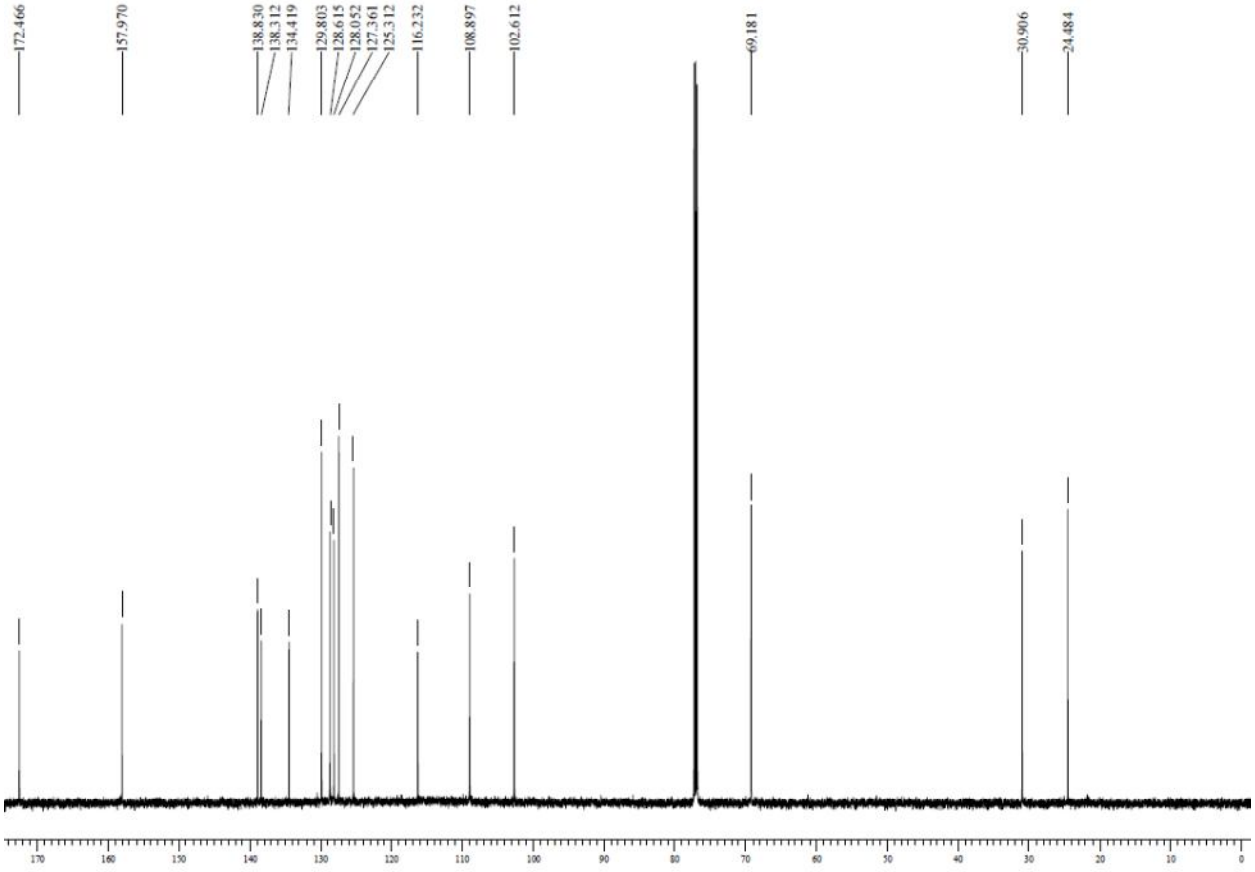

7-(3-Bromobenzyloxy)-3,4-dihydro-2(1*H*)-quinolinone (5c)

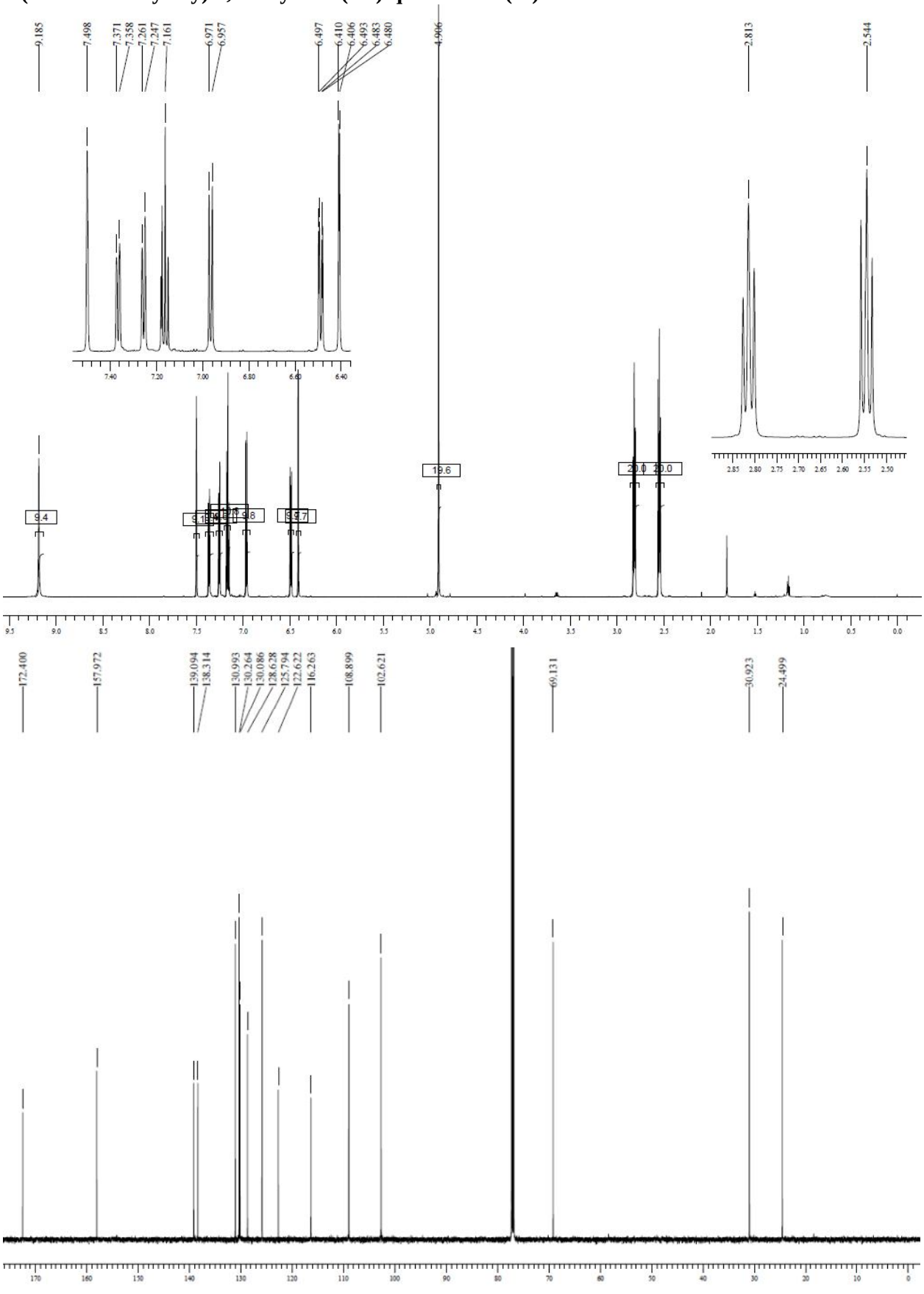

7-(2-Phenylethoxy)-3,4-dihydro-2(1*H*)-quinolinone (5d)

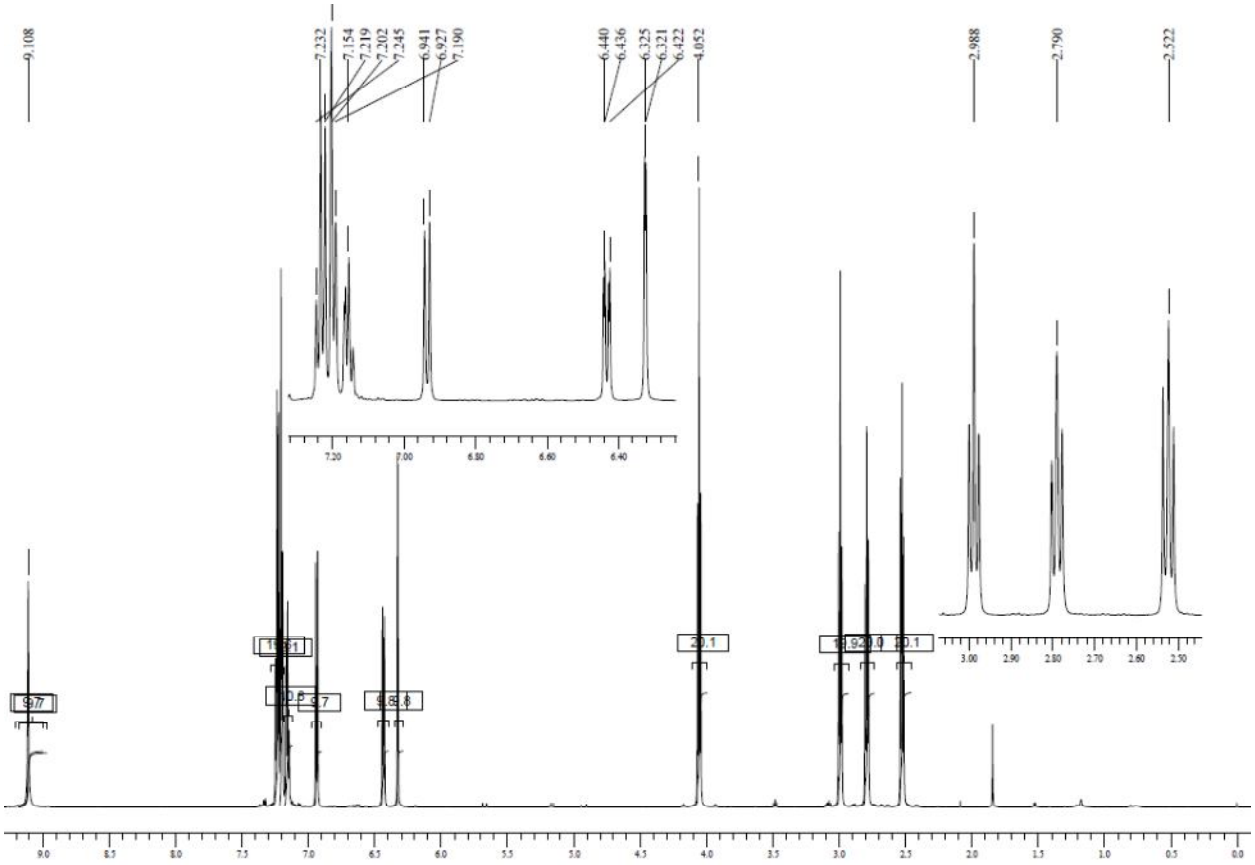

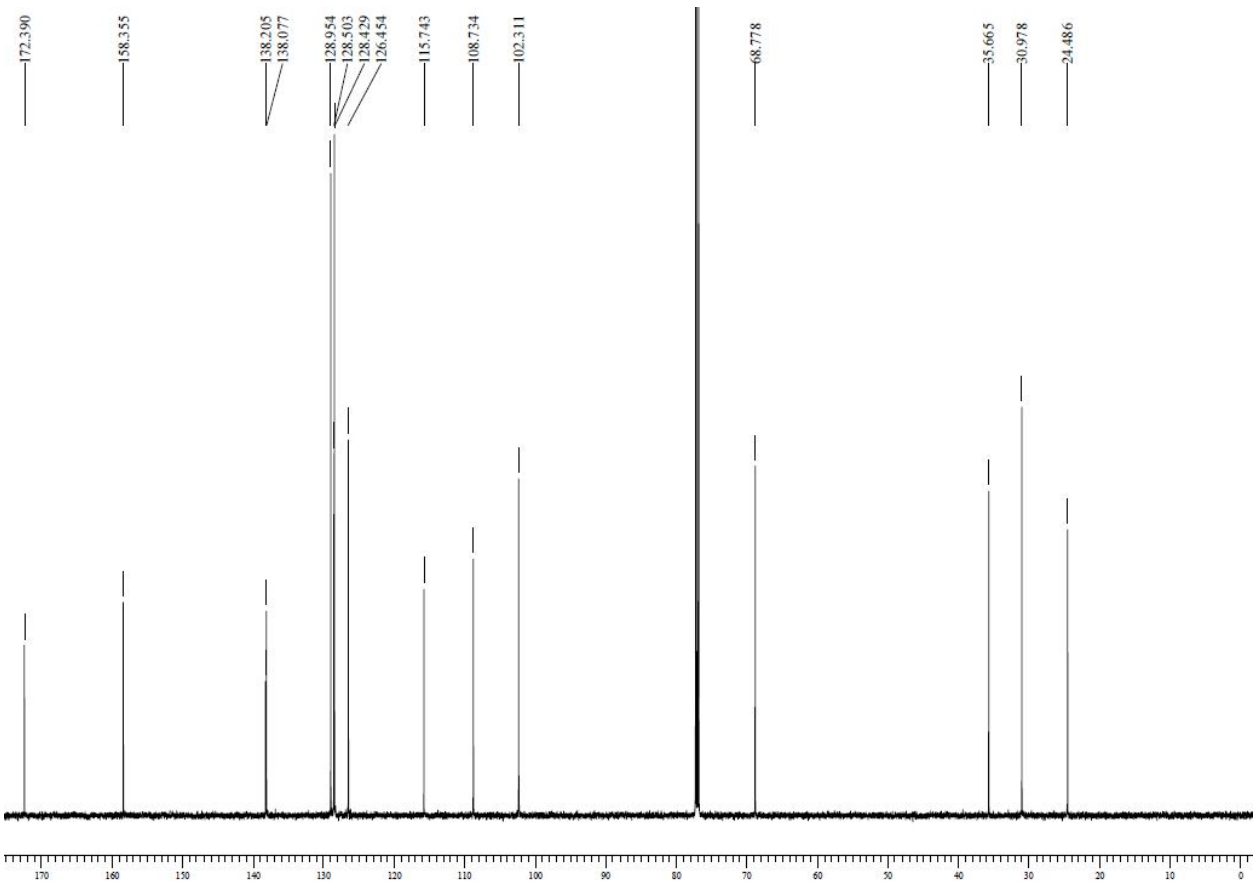

7-(3-Phenylpropoxy)-3,4-dihydro-2(1*H*)-quinolinone (5e)

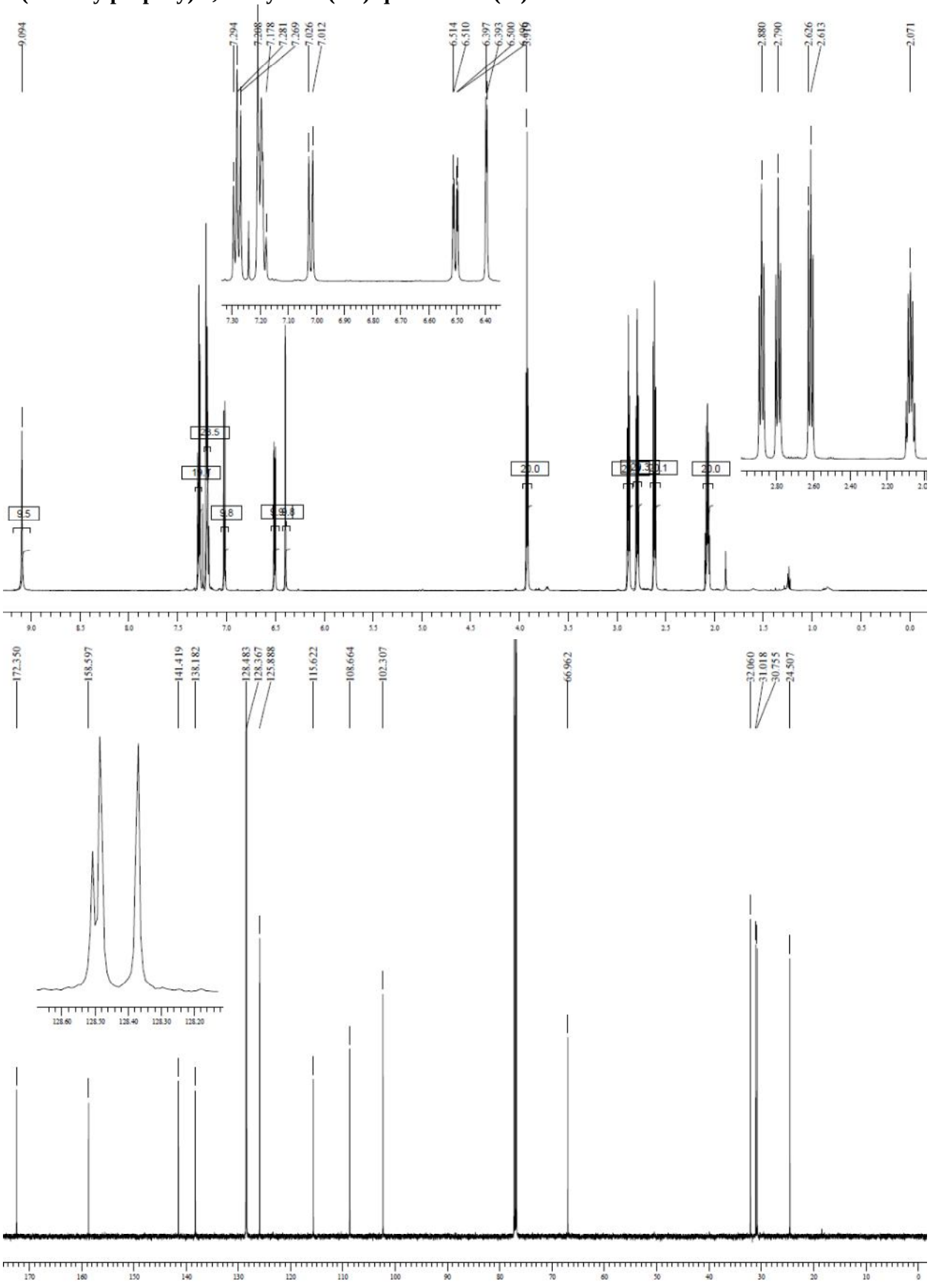

APPENDIX B
PUBLISHED ARTICLE

Bioorganic & Medicinal Chemistry Letters 23 (2013) 5498–5502

Contents lists available at ScienceDirect

Bioorganic & Medicinal Chemistry Letters

journal homepage: www.elsevier.com/locate/bmcl

Inhibition of monoamine oxidase by 3,4-dihydro-2(1*H*)-quinolinone derivatives

Letitia Meiring [a], Jacobus P. Petzer [a], Anél Petzer [b,*]

[a] Pharmaceutical Chemistry, School of Pharmacy, North-West University, Private Bag X6001, Potchefstroom 2520, South Africa
[b] Centre of Excellence for Pharmaceutical Sciences, School of Pharmacy, North-West University, Private Bag X6001, Potchefstroom 2520, South Africa

ARTICLE INFO

Article history:
Received 28 June 2013
Revised 12 August 2013
Accepted 15 August 2013
Available online 22 August 2013

Keywords:
Monoamine oxidase
Reversible inhibition
Selectivity
3,4-Dihydro-2(1*H*)-quinolinone
Structure–activity relationship

ABSTRACT

In the present study, a series of 3,4-dihydro-2(1*H*)-quinolinone derivatives were synthesized and evaluated as inhibitors of recombinant human monoamine oxidase (MAO) A and B. The 3,4-dihydro-2(1*H*)-quinolinone derivatives are structurally related to a series of coumarin (1-benzopyran-2-one) derivatives which have been reported to act as MAO-B inhibitors. The results document that the quinolinones are highly potent and selective MAO-B inhibitors with most homologues exhibiting IC_{50} values in the nanomolar range. The most potent MAO-B inhibitor, 7-(3-bromobenzyloxy)-3,4-dihydro-2(1*H*)-quinolinone, exhibits an IC_{50} value of 2.9 nM with a 2750-fold selectivity for MAO-B over the MAO-A isoform. An analysis of the structure–activity relationships for MAO-B inhibition shows that substitution on the C7 position of the 3,4-dihydro-2(1*H*)-quinolinone scaffold leads to significantly more potent inhibition compared to substitution on C6. In this regard, a benzyloxy substituent on C7 is more favourable than phenylethoxy and phenylpropoxy substitution on this position. It may be concluded that C7-substituted 3,4-dihydro-2(1*H*)-quinolinones are promising leads for the therapy of Parkinson's disease.

The monoamine oxidases (MAOs) are mitochondrial bound enzymes which metabolize neurotransmitter and dietary amines in the brain and peripheral tissues. The MAOs have been drug targets for numerous decades and inhibitors of these enzymes are used primarily to treat neuropsychiatric syndromes.[1,2] MAO-B inhibitors, in particular, are considered useful in the therapy of Parkinson's disease since oxidation by MAO-B represents a major catabolic pathway of dopamine in the central nervous system. MAO-B inhibitors conserve the depleted dopamine stores in the parkinsonian brain and enhance the elevation of dopamine levels after administration of levodopa, the metabolic precursor of dopamine.[3,4] The combined use of levodopa and MAO-B inhibitors allows for a reduction of the dosage of levodopa that is necessary for a therapeutic response which, in turn, leads to diminished levodopa associated side effects.[5] MAO-B may also indirectly increase extracellular dopamine concentrations by blocking the metabolism of β-phenethylamine. β-Phenethylamine is a false neurotransmitter that mediates the release of neuronal dopamine and inhibits its active uptake.[6,7] Also of interest are reports that MAO-B inhibitors may exert neuroprotective effects in Parkinson's disease by reducing the formation of potentially harmful metabolic by-products of MAO catalysis.[1,8] For example, aldehydes derived from the MAO catalytic cycle has been implicated in the aggregation of α-synuclein, a process which is associated with the pathogenesis of Parkinson's disease.[9] Hydrogen peroxide formed during MAO catalysis may lead to oxidative damage and promotes apoptotic signaling events.[9,10] Considering that MAO-B activity increases in the brain with age, the concomitant increase of these metabolic by-products may be especially relevant to the pathogenesis of Parkinson's disease.[11,12]

It should be noted that MAO-A also metabolizes dopamine in the primate and possibly human brain and, similar to MAO-B inhibitors, MAO-A inhibitors also enhance the elevation of dopamine levels derived from levodopa.[4] The clinical use of MAO-A inhibitors have, however, declined in recent years because of side effects that may arise from the combination of MAO-A inhibitors with the dietary amine, tyramine. MAO-A inhibitors block the peripheral metabolism of tyramine, and the subsequent increase in systemic tyramine concentrations leads to the release of norepinephrine from peripheral neurons, which results in a potentially severe hypertensive response.[13] Another adverse effect of MAO-A inhibitors which limits their clinical use is serotonin toxicity, a potentially fatal syndrome which develops when serotonergic agents and MAO-A inhibitors are combined.[14,15] The combination of MAO-A inhibitors, which block the MAO-A-catalyzed metabolism of serotonin, with selective serotonin reuptake inhibitors (SSRIs) and serotonin-releasing agents leads to excessive extracellular serotonin concentrations in the central nervous system and hence serotonin toxicity. Based on these considerations, inhibitors with a high degree of selectivity for MAO-B over the MAO-A isoform are generally more suitable for Parkinson's disease therapy.

* Corresponding author. Tel.: +27 18 2994464; fax: +27 18 2994243.
E-mail address: 12264954@nwu.ac.za (A. Petzer).

0960-894X/$ - see front matter © 2013 Elsevier Ltd. All rights reserved.
http://dx.doi.org/10.1016/j.bmcl.2013.08.071

In addition, MAO-B inhibitors with a reversible mode of action may possess certain advantages over irreversible MAO-B inhibitors, which are currently used in Parkinson's disease therapy. The most notable advantage is an immediate recovery of enzyme activity when the inhibitor has been eliminated from the tissues. In contrast, after termination of treatment with irreversible inhibitors, the rates of recovery of enzyme activity are slow and variable, in part because the turnover rate for the biosynthesis of MAO-B in the human brain may be as much as 40 days.[16,17]

In the search for improved antiparkinsonian therapies, the design of new MAO-B inhibitors is pursued by several research groups. Based on the above analyses these inhibitors should be reversible and selective for the MAO-B isoform. In this regard, coumarin (1-benzopyran-2-one) (**1**) has emerged as a particularly promising scaffold (Fig. 1).[18] Substituted coumarins have been shown to act as competitive MAO inhibitors, with substitution on C7 of the coumarin ring yielding particularly potent MAO-B inhibitors. For example, 7-(3,4-difluorobenzyloxy)-3,4-dimethylcoumarin (**2**) was shown to inhibit rat brain MAO-B with an IC_{50} value of 1.14 nM and a 108-fold selectivity for MAO-B over the MAO-A isoform.[18] Based on the structural similarity between the coumarin moiety and 3,4-dihydro-2(1*H*)-quinolinone (**3**), the present study examines the possibility that a series of 3,4-dihydro-2(1*H*)-quinolinone derivatives (**4** and **5**) may act as reversible and selective inhibitors of recombinant human MAO-B. For this purpose substitution on the C6 and C7 positions of the 3,4-dihydro-2(1*H*)-quinolinone moiety was considered. Since alkyloxy substituents on C6 and C7 of the coumarin moiety yields compounds with good MAO-B inhibitory potencies,[18] in the present study alkyloxy substituents (benzyloxy, phenylethoxy and phenylpropoxy) were also selected for substitution on C6 and C7 of 3,4-dihydro-2(1*H*)-quinolinone ring system (Table 1). Among these, the benzyloxy side chain has been shown to be particularly suited for enhancing the MAO inhibition potencies of coumarin.[18] Furthermore, the proposal that benzyloxy-substituted 3,4-dihydro-2(1*H*)-quinolinones may act as MAO inhibitors is supported by a report, demonstrating that 7-(benzyloxy)-3,4-dihydro-2(1*H*)-quinolinone (**5a**) inhibits rat MAO-A and MAO-B with IC_{50} values of 102 μM and 1.05 μM, respectively.[18] We have therefore further explored the MAO inhibitory properties of the benzyloxy-substituted 3,4-dihydro-2(1*H*)-quinolinones by substitution on the benzyloxy phenyl ring with halogens (Cl, Br). Halogen substitution on the benzyloxy ring has previously been shown to significantly enhance the MAO-B inhibitory properties of 7-substituted benzyloxy-3,4-dimethylcoumarins as exemplified by structure **2**.[18] The aim of this study is therefore to discover novel highly potent and selective MAO-B inhibitors which may act as leads for the design of antiparkinsonian therapies.

The C6- and C7-substituted 3,4-dihydro-2(1*H*)-quinolinone derivatives **4** and **5** were synthesized according to the literature procedure (Scheme 1).[19] Commercially available 6-hydroxy-3,4-dihydro-2(1*H*)-quinolinone (**6**) and 7-hydroxy-3,4-dihydro-2(1*H*)-quinolinone (**7**), suspended in ethanol, were treated with an appropriately substituted alkyl bromide in the presence of KOH. After heating the mixture at reflux for 5 h, the reaction was poured into aqueous NaOH (1%). The crude thus obtained was purified by recrystallization and the structures of the target compounds were verified by ^{1}H NMR, ^{13}C NMR and mass spectrometry as cited in the Supplementary data.

To evaluate the MAO inhibitory properties of the 3,4-dihydro-2(1*H*)-quinolinone derivatives (**4** and **5**), the recombinant human MAO-A and MAO-B enzymes were used.[20] To measure MAO activities, the MAO-A/B mixed substrate, kynuramine, was employed. Kynuramine is oxidized by the MAOs to ultimately yield 6-hydroxyquinoline, a metabolite which fluoresces (λ_{ex} = 310 nm; λ_{em} = 400 nm) in alkaline media.[21] Using fluorescence spectrophotometry, the formation of 6-hydroxyquinoline can be readily measured in the presence of the test inhibitors since the 3,4-dihydro-2(1*H*)-quinolinone derivatives do not fluoresce under these assay conditions. From the MAO activity measurements in the presence of the test inhibitors, sigmoidal concentration–inhibition curves were constructed and the inhibition potencies, the corresponding IC_{50} values, were calculated (Fig. 2).

The IC_{50} values for the inhibition of human MAO-A and MAO-B by the 3,4-dihydro-2(1*H*)-quinolinone derivatives, **4** and **5**, are given in Table 1. The results show that the 3,4-dihydro-2(1*H*)-

Table 1
The IC_{50} values for the inhibition of recombinant human MAO-A and MAO-B by compounds **4** and **5**

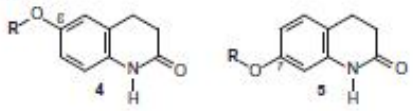

	R	IC_{50} (μM)[a]		SI[b]
		MAO-A	MAO-B	
4a	$C_6H_5CH_2$–	25.3 ± 15.2	4.01 ± 1.196	6
4b	3-$ClC_6H_4CH_2$–	50.6 ± 10.3	0.620 ± 0.148	82
4c	3-$BrC_6H_4CH_2$–	12.4 ± 1.93	0.086 ± 0.029	144
4d	$C_6H_5(CH_2)_2$–	22.5 ± 9.69	2.33 ± 1.33	10
4e	$C_6H_5(CH_2)_3$–	19.7 ± 12.8	0.284 ± 0.049	69
5a	$C_6H_5CH_2$–	90.4 ± 47.1	0.038 ± 0.013	2379
5b	3-$ClC_6H_4CH_2$–	No Inh[c]	0.0062 ± 0.00063	–
5c	3-$BrC_6H_4CH_2$–	7.98 ± 1.09	0.0029 ± 0.0009	2751
5d	$C_6H_5(CH_2)_2$–	53.7 ± 12.0	0.191 ± 0.041	281
5e	$C_6H_5(CH_2)_3$–	22.5 ± 4.08	0.130 ± 0.010	173

[a] All values are expressed as the mean ± SD of triplicate determinations.
[b] The selectivity index is the selectivity for the MAO-B isoform and is given as the ratio of IC_{50}(MAO-A)/IC_{50}(MAO-B).
[c] No inhibition at a maximum tested concentration of 100 μM.

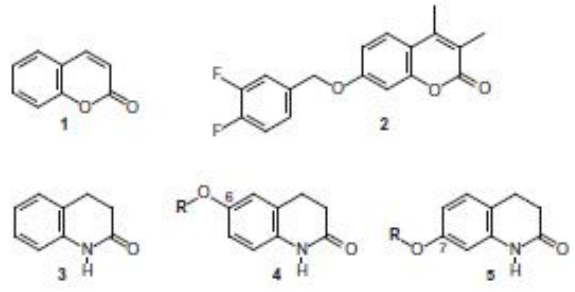

Figure 1. The structures of coumarin (**1**), 7-(3,4-difluorobenzyloxy)-3,4-dimethylcoumarin (**2**), 3,4-dihydro-2(1*H*)-quinolinone (**3**) and the 3,4-dihydro-2(1*H*)-quinolinone derivatives **4** and **5**.

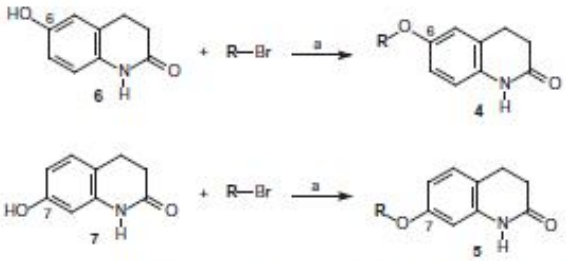

Scheme 1. Synthetic route to the 3,4-dihydro-2(1*H*)-quinolinone derivatives **4** and **5**. Reagents: (a) KOH, ethanol, reflux.

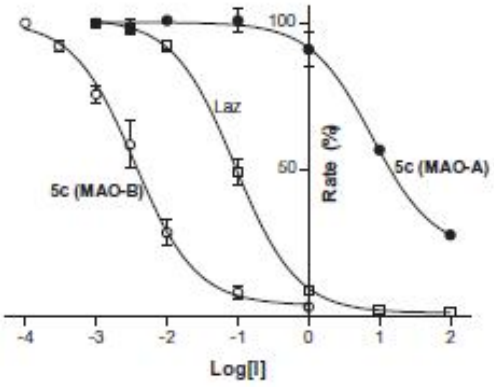

Figure 2. The sigmoidal concentration–inhibition curves for the inhibition of recombinant human MAO-A (filled circles) and MAO-B (open circles) by various concentrations of **5c**. For comparison, the sigmoidal concentration–inhibition curve (squares) for the inhibition of MAO-B by lazabemide (Laz) is also provided.

quinolinone derivatives are potent inhibitors of MAO-B with most homologues (8 of 10) exhibiting IC_{50} values in the nanomolar range. The results further demonstrate that all of the 3,4-dihydro-2(1*H*)-quinolinone derivatives are selective MAO-B inhibitors. The most potent MAO-B inhibitor, 7-(3-bromobenzyloxy)-3,4-dihydro-2(1*H*)-quinolinone (**5c**), is an exceptionally potent MAO-B inhibitor with an IC_{50} value of 0.0029 μM. Even though **5c** (IC_{50} = 7.98 μM) also was the most potent MAO-A inhibitor of the series, this compound is a highly selective inhibitor with a ~2750-fold selectivity for MAO-B over the MAO-A isoform. Another highly potent MAO-B inhibitor among the compounds evaluated is compound **5b** (IC_{50} = 0.0062 μM). Since compound **5b** did not exhibit any inhibitory activity towards MAO-A (up to a maximal tested concentration of 100 μM) it may also be considered as highly selective for MAO-B. Compared to the reversible MAO-B selective inhibitor, lazabemide (IC_{50} = 0.091 μM), compounds **5b** and **5c** are approximately 14- and 31-fold, respectively, more potent as MAO-B inhibitors under identical conditions.[22] It is interesting to note that **5a** is a relatively potent MAO-B inhibitor with an IC_{50} value of 0.038 μM. This IC_{50} value is 27-fold more potent than the previously reported value of 1.05 μM for the inhibition of rat brain MAO-B.[18] This result suggests that relatively large differences may exist between the inhibition potencies obtained with rat MAO-B and those obtained with the human isoform. The potencies by which **5a** inhibits human (IC_{50} = 90.4 μM) and rat (IC_{50} = 102 μM) MAO-A are, however, similar.

An analysis of the structure–activity relationships (SARs) for MAO-B inhibition reveals interesting trends. Substitution on the C7 position of the 3,4-dihydro-2(1*H*)-quinolinone moiety leads to significantly more potent MAO-B inhibition compared to substitution on C6. For example **5a** (IC_{50} = 0.038 μM), substituted with the benzyloxy moiety on C7, is approximately 100-fold more potent than **4a** (IC_{50} = 4.01 μM), the homologue bearing the benzyloxy moiety at C6. In fact compounds **5a–e** were in each instance more potent MAO-B inhibitors than their corresponding C6 substituted homologues **4a–e**. It may thus be concluded that C7-substituted 3,4-dihydro-2(1*H*)-quinolinones are, in general, more suitable for the design of exceptionally potent MAO-B inhibitors than C6-substituted 3,4-dihydro-2(1*H*)-quinolinones. In spite of this, with the appropriate substitution certain C6-substituted 3,4-dihydro-2(1*H*)-quinolinones such as **4c** (IC_{50} = 0.086 μM) may still be viewed as potent MAO-B inhibitors. Another interesting SAR is the finding that a benzyloxy substituent on C7 of the 3,4-dihydro-2(1*H*)-quinolinone moiety is more favourable for MAO-B inhibition than phenylethoxy and phenylpropoxy substitution on this position. For example, the C7 benzyloxy substituted homologue **5a** (IC_{50} = 0.038 μM) is at least threefold more potent than the phenylethoxy [(**5d**); IC_{50} = 0.191 μM] and phenylpropoxy [(**5e**); IC_{50} = 0.130 μM] substituted homologues. Interestingly, for the C6-substituted 3,4-dihydro-2(1*H*)-quinolinones, the benzyloxy substituted homologue **4a** (IC_{50} = 4.01 μM) was a weaker MAO-B inhibitor than the C6 phenylethoxy (**4d**) and phenylpropoxy (**4e**) substituted homologues. Reasons for the different trends observed with the C7- and C6-substituted 3,4-dihydro-2(1*H*)-quinolinones are not apparent. From a design point of view, it is noteworthy that, for the C7 benzyloxy substituted 3,4-dihydro-2(1*H*)-quinolinones, halogen (Cl, Br) substitution on the benzyloxy phenyl ring further enhances MAO-B inhibition potency. In this regard, the chlorine and bromine substituted homologues **5b** (IC_{50} = 0.0062 μM) and **5c** (IC_{50} = 0.0029 μM) are 6- to 13-fold more potent than the unsubstituted compound **5a** (IC_{50} = 0.038 μM). For those compounds with benzyloxy substituents on C6 of the 3,4-dihydro-2(1*H*)-quinolinone moiety, a similar trend was observed with the chlorine and bromine substituted homologues **4b** (IC_{50} = 0.620 μM) and **4c** (IC_{50} = 0.086 μM) exhibiting more potent MAO-B inhibition than the unsubstituted 6-benzyloxy-3,4-dihydro-2(1*H*)-quinolinone **4a** (IC_{50} = 4.01 μM). From these data it is apparent that bromine substitution yields more potent MAO-B inhibitors compared to chlorine substitution. Further investigation is necessary to evaluate the effects on MAO-B inhibition of other halogen and alkyl substituents on the benzyloxy phenyl ring. For the inhibition of MAO-A, no clear SARs are apparent. As noted above, the most potent MAO-B inhibitor of the series **5c** also was the most potent MAO-A inhibitor. Also, since **5c** as well as **4c**, the second most potent MAO-A inhibitor of the series, contain bromine on the benzyloxy phenyl ring, substitution with this halogen also enhances MAO-A inhibitory potency. To evaluate the importance of the C6 and C7 substituent for the inhibition of the MAOs by the the 3,4-dihydro-2(1*H*)-quinolinone derivatives, 6-hydroxy-3,4-dihydro-2(1*H*)-quinolinone (**6**) and 7-hydroxy-3,4-dihydro-2(1*H*)-quinolinone (**7**) were also evaluated as human MAO inhibitors. The results are given in Table 2 and show that **6** and **7** are weak MAO inhibitors with IC_{50} values >161 μM. This result demonstrates that appropriate C6 and C7 substitution is a requirement for the MAO inhibitory activities of 3,4-dihydro-2(1*H*)-quinolinone derivatives.

The reversibility of MAO-B inhibition by the most potent compound of the series **5c** was evaluated by examining the recovery of enzyme activity after the dilution of the enzyme–inhibitor complexes.[23] None of the 3,4-dihydro-2(1*H*)-quinolinone derivatives were potent MAO-A inhibitors. For this purpose, MAO-B and **5c** were combined and preincubated for 30 min at inhibitor concentrations equal to 10 × IC_{50} and 100 × IC_{50}. The reactions were sub-

Table 2
The IC_{50} values for the inhibition of recombinant human MAO-A and MAO-B by 6-hydroxy-3,4-dihydro-2(1*H*)-quinolinone (**6**) and 7-hydroxy-3,4-dihydro-2(1*H*)-quinolinone (**7**)

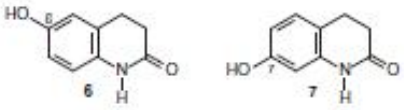

	IC_{50} (μM)[a]		SI[b]
	MAO-A	MAO-B	
6	161 ± 16.1	201 ± 31.3	0.8
7	183 ± 2.48	No inh[c]	–

[a–c] See Table 1 for footnotes.

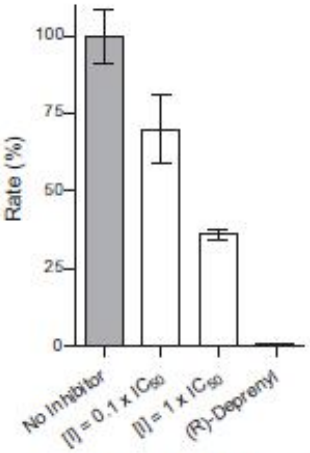

Figure 3. The reversibility of inhibition of MAO-B by compound **5c**. MAO-B was preincubated with **5c** at $10 \times IC_{50}$ and $100 \times IC_{50}$ for 30 min and then diluted to $0.1 \times IC_{50}$ and $1 \times IC_{50}$, respectively. For comparison, the irreversible MAO-B inhibitor, (*R*)-deprenyl, at $10 \times IC_{50}$, was similarly incubated with MAO-B and diluted to $0.1 \times IC_{50}$. The residual activity of MAO-B was subsequently measured.

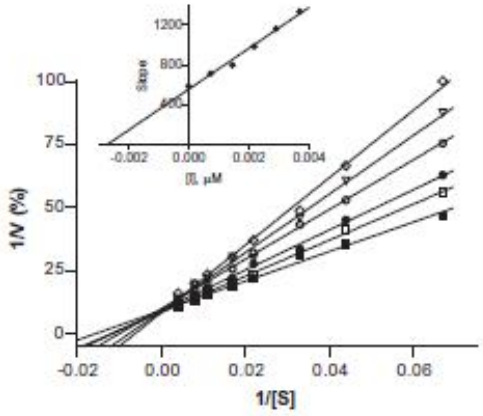

Figure 4. Lineweaver–Burk plots for the inhibition of human MAO-B by **5c**. The plots were constructed in the absence (filled squares) and presence of various concentrations of **5c**. The inset is a plot of the slopes of the Lineweaver–Burk plots versus inhibitor concentration.

sequently diluted 100-fold to yield concentrations of **5c** of $0.1 \times IC_{50}$ and $1 \times IC_{50}$, and the residual enzyme activities were measured. Control reactions conducted in the absence of inhibitor were also included in the study. The results are given in Figure 3 and show that, after dilution of **5c** to concentrations of $0.1 \times IC_{50}$ and $1 \times IC_{50}$, the catalytic activities of MAO-B are recovered to levels of 70% and 36% of the control levels, respectively. This result suggests that **5c** acts as a reversible MAO-B inhibitor since, after similar treatment of MAO-B with the irreversible inhibitor (*R*)-deprenyl at concentrations equal to $10 \times IC_{50}$, and dilution of the resulting reactions to $0.1 \times IC_{50}$, the MAO-B activities are not recovered (0.7% of control). Interestingly, after dilution of **5c** to concentrations of $0.1 \times IC_{50}$ and $1 \times IC_{50}$, the MAO-B catalytic activities are not recovered to 90% and 50%, respectively, as would be expected for reversible inhibition. This result suggests that **5c** may possess a quasi-reversible interaction or tight-binding component.

To further examine the mode of MAO-B inhibition by the 3,4-dihydro-2(1*H*)-quinolinone derivatives, a set of Lineweaver–Burk plots for the inhibition of MAO-B by **5c** was constructed. For this purpose, the MAO-B catalytic rates were recorded at eight different kynuramine concentrations (15–250 μM) in the absence of inhibitor, and presence of five different concentrations (¼ × IC_{50}, ½ × IC_{50}, ¾ × IC_{50}, 1 × IC_{50} and 1¼ × IC_{50}) of **5c**. The set of Lineweaver–Burk plots is given in Figure 4. The observation that the lines are linear and intersect on the *y*-axis suggests that **5c** is a competitive inhibitor of human MAO-B. This is further evidence that the interaction of **5c** with MAO-B is reversible. From a replot of the slopes of the Lineweaver–Burk plots versus the concentration of **5c**, a K_i value of 0.0027 μM for the inhibition of MAO-B is estimated.

In conclusion, the present study shows that a series of 3,4-dihydro-2(1*H*)-quinolinone derivatives are highly potent and selective MAO-B inhibitors, even when compared to the previously studied coumarin derivatives.[18] For example, the most potent inhibitor, compound **5c** (IC_{50} = 2.9 nM) is approximately equipotent to coumarin derivative **2**, which represents the most active MAO-B inhibitor among a large series of coumarin derivatives previously studied.[18] It should be noted that **2** was evaluated as an inhibitor of rat brain MAO while in the present study, the human enzymes were employed. Based on its high MAO-B inhibitory potency and selectivity over the MAO-A isoform, **5c** represents a suitable lead for the development of novel therapies for Parkinson's disease. In addition, **5c** interacts reversibly with MAO-B, which is a desirable property when designing antiparkinsonian therapies. The limited SARs derived for the inhibition data show that substitution on the C7 position of the 3,4-dihydro-2(1*H*)-quinolinone moiety, particularly with the benzyloxy substituent, is more favourable for MAO-B inhibition than substitution on the C6 position. In addition, halogen substituents on the benzyloxy phenyl ring further enhances MAO-B inhibition. Although a limited number of derivatives were examined, this study provides 'proof of concept' for the proposal that the 3,4-dihydro-2(1*H*)-quinolinone moiety is a promising scaffold for the design of MAO-B inhibitors. Further examination of the physicochemical properties of 3,4-dihydro-2(1*H*)-quinolinones is necessary to determine if these promising inhibitors may be acceptable as lead compounds for the treatment of central nervous system disorders.

Acknowledgments

The NMR and MS spectra were recorded by André Joubert and Johan Jordaan of the SASOL Centre for Chemistry, North-West University. This work is based on the research supported in part by the Medical Research Council and National Research Foundation of South Africa (Grant specific unique reference numbers (UID) 85642 and 80647). The Grantholders acknowledge that opinions, findings and conclusions or recommendations expressed in any publication generated by the NRF supported research are that of the authors, and that the NRF accepts no liability whatsoever in this regard.

Supplementary data

Supplementary data associated with this article can be found, in the online version, at http://dx.doi.org/10.1016/j.bmcl.2013.08.071.

References and notes

1. Youdim, M. B. H.; Bakhle, Y. S. *Br. J. Pharmacol.* **2006**, *147*, S287.
2. Ramsay, R. R. *Curr. Top. Med. Chem.* **2012**, *12*, 2189.

3. Di Monte, D. A.; DeLanney, L. E.; Irwin, I.; Royland, J. E.; Chan, P.; Jacowec, M. W.; Langston, J. W. *Brain Res.* **1996**, *738*, 53.
4. Finberg, J. P.; Wang, J.; Bankiewich, K.; Harvey-White, J.; Kopin, I. J.; Goldstein, D. S. *J. Neural Transm.* **1998**, *52*, 279.
5. Fernandez, H. H.; Chen, J. J. *Pharmacotherapy* **2007**, *27*, 174S.
6. Iasbennes, F.; Sercombe, R.; Seylaz, J. *J. Cereb. Blood Flow. Metab.* **1983**, *3*, 521.
7. Finberg, J. P.; Lamensdorf, I.; Armoni, T. *Neurobiology (Bp)* **2000**, *8*, 137.
8. Marchitti, S. A.; Deitrich, R. A.; Vasiliou, V. *Pharmacol. Rev.* **2007**, *59*, 125.
9. Burke, W. J.; Kumar, V. B.; Pandey, N.; Panneton, W. M.; Gan, Q.; Franko, M. W.; O'Dell, M.; Li, S. W.; Pan, Y.; Chung, H. D.; Galvin, J. E. *Acta Neuropathol.* **2008**, *115*, 193.
10. Mallajosyula, J. K.; Kaur, D.; Chinta, S. J.; Rajagopalan, S.; Rane, A.; Nicholls, D. G.; Di Monte, D. A.; Macarthur, H.; Andersen, J. K. *PLoS One* **2008**, *3*, e1616.
11. Nicotra, A.; Pierucci, F.; Parvez, H.; Santori, O. *Neurotoxicology* **2004**, *25*, 155.
12. Fowler, J. S.; Volkow, N. D.; Wang, G. J.; Logan, J.; Pappas, N.; Shea, C.; MacGregor, R. *Neurobiol. Aging* **1997**, *18*, 431.
13. Da Prada, M.; Zürcher, G.; Wüthrich, I.; Haefely, W. E. *J. Neural Transm.* **1988**, *26*, 31.
14. Ramsay, R. R.; Dunford, C.; Gillman, P. K. *Br. J. Pharmacol.* **2007**, *152*, 946.
15. Stanford, S. C.; Stanford, B. J.; Gillman, P. K. *J. Psychopharmacol.* **2010**, *24*, 1433.
16. Tipton, K. F.; Boyce, S.; O'Sullivan, J.; Davey, G. P.; Healy, J. *Curr. Med. Chem.* **2004**, *11*, 1965.
17. Fowler, J. S.; Volkow, N. D.; Logan, J.; Wang, G.; MacGregor, R. R.; Schlyer, D.; Wolf, A. P.; Pappas, N.; Alexoff, D.; Shea, C.; Dorflinger, E.; Kruchowy, L.; Yoo, K.; Fazzini, E.; Patlak, C. *Synaps* **1994**, *18*, 86.
18. Gnerre, C.; Catto, M.; Leonetti, F.; Weber, P.; Carrupt, P. A.; Altomare, C.; Carotti, A.; Testa, B. *J. Med. Chem.* **2000**, *43*, 4747.
19. Shigematsu, N. *Chem. Pharm. Bull.* **1961**, *9*, 970.
20. Novaroli, L.; Reist, M.; Favre, E.; Carotti, A.; Catto, M.; Carrupt, P. A. *Bioorg. Med. Chem.* **2005**, *13*, 6212.
21. Strydom, B.; Malan, S. F.; Castagnoli, N., Jr.; Bergh, J. J.; Petzer, J. P. *Bioorg. Med. Chem.* **2010**, *18*, 1018.
22. Petzer, A.; Pienaar, A.; Petzer, J. P. *Arzneimittel-Forsch.* **2013**, *63*, 462.
23. Petzer, A.; Harvey, B. H.; Wegener, G.; Petzer, J. P. *Toxicol. Appl. Pharm.* **2012**, *258*, 403.